THE UNIVERSITY *of* EDINBURGH

Exploring Distributed Neural Network Connections in a Rat Model of *SYNGAP1* Haploinsufficiency

Faith Colaguori

A thesis presented for the degree of Master of Science by Research

Centre for Discovery Brain Sciences

University of Edinburgh

Scotland

United Kingdom

October 2023

1 Abstract

Neurodevelopmental disorders (NDDs), such as autism spectrum disorder (ASD), intellectual disability (ID), and childhood epilepsy, have been attributed to *SYNGAP1* haploinsufficiency – a genetic condition characterized by alterations in the *SYNGAP1* gene. This gene plays a pivotal role in the proper development and functioning of neural circuits associated with cognitive processes and emotional responses. Fear conditioning, a vital aspect of adaptive behaviour, involves learning to associate specific stimuli with threat and is a fundamental model for exploring the neural basis of fear memory.

This study explores the behavioural and neural manifestations of fear conditioning in wildtype (WT) and *Syngap*$^{+/\Delta GAP}$ (SG) rats. Fear extinction, a process where learned fear responses diminish when the conditioned stimulus (CS) no longer predicts the unconditioned stimulus (US), was investigated in both genotypes. As with previous laboratory findings, SG rats exhibited sustained freezing behaviour during extinction, indicative of difficulty in unlearning the CS-US association compared to their WT counterparts.

To investigate the neural basis of these differences, we employed *in vivo* electrophysiological techniques combined with sophisticated neural data analysis. While rats underwent surgical procedures to implant six local field potential (LFP) and three electroencephalogram (EEG) electrodes across relevant brain structures, our analysis focuses on key brain regions including the infralimbic cortex, amygdala, and olfactory bulb – regions implicated in fear memory and extinction. To extract insights from data, a custom software analysis package was developed in MATLAB, and power and coherence analyses were conducted to identify potential electrophysiological biomarkers that differentiate the genotypes and predict their variations in behaviour.

While no definitive biomarkers for freezing behaviour emerged, intriguing patterns requiring further investigation surfaced in the gamma and delta frequency bands across multiple brain regions. Notably, the olfactory bulb's power showed a significant correlation with prolonged freezing, suggesting a potential neural driver or result of this behaviour. These findings emphasize the complex interplay between neural circuits and behaviour, indicating that SG rats might possess an elevated baseline anxiety level compared to WT rats, possibly contributing to their propensity for freezing.

In summary, this thesis explores the connection between *SYNGAP1* haploinsufficiency and fear-related behaviours. By employing fear conditioning as a model, we reveal how altered neural dynamics in SG rats could underlie their impaired fear extinction. Understanding these mechanisms not only advances our knowledge of NDDs but also provides insights into the broader mechanisms governing fear learning and memory.

1.1 Lay Abstract

Female mammals have two copies of all genes, one inherited from the mother and one from the father. Male mammals have two copies of all genes except those located on the X and Y chromosomes, for which only a single copy is present. For genes located on autosomal chromosomes (i.e., not the X and Y chromosomes that determine the sex of the animal), if the loss of function of a single copy leads to differences in behaviour, the gene is said to be haploinsufficient. More formally, haploinsufficiency is the requirement for two functional copies of a gene to preserve normal function; when one copy of a haploinsufficient gene is inactivated or otherwise destroyed, the dosage of normal product generated by the single functional gene is not enough to preserve normal activity. The *SYNGAP1* gene is critical for normal brain development; *SYNGAP1* haploinsufficiency causes a severe neurodevelopmental disorder with commonly overlapping diagnoses of intellectual disability (ID), autism spectrum disorder (ASD), and epilepsy. This condition is commonly diagnosed as *SYNGAP1*-related intellectual disability (*SYNGAP1*-ID).

In the laboratory environment, we can replicate these genetic alterations in rats and study the behaviour and brain function that results. We can then compare these modified rats ($Syngap^{+/\Delta GAP}$ rats, abbreviated as 'SG') with 'neurotypical,' or wildtype (WT) rats to study differences between normal and disturbed neural function. These differences are often studied through a variety of behaviour tests, each with a known behavioural output related to normal function.

One of these common behaviour tests, known as fear conditioning, taps into the brain circuits underlying fear and anxiety. In this experiment, an innocuous stimulus, like a flashing light (known as the conditioned stimulus; CS), is paired with a naturally fearful stimulus, like a mild electric foot shock (unconditioned stimulus; US) so the CS predicts the US. When a WT rat learns the association between the CS and US, the rat will engage in an innate fear response, which presents as total body freezing. Later in the protocol, when the CS (light) is presented multiple times without the US (foot shock), the rats learn there is no longer an association between the two, and the freezing behaviour will quickly cease – this is called extinction learning.

SG rats show impaired extinction learning and continue to freeze much longer than WT rats; they need many more light presentations without shocks to learn the former no longer predicts the latter.

To understand the brain areas involved in this phenomenon, we surgically implanted rats with electrodes that let us record neural activity during the fear conditioning paradigm. Using these neural traces, we can calculate the strength of the brain activity in these brain regions (also known as power) and whether the brain regions are working together (also known as coherence). We wanted to look for a clear neural signature of what caused the SG rats to be unable to learn their conditioned fear response.

While no definitive neural signatures of freezing behaviour emerged, interesting patterns requiring further investigation were found in multiple brain regions. In particular, abnormal neural signatures were found in the infralimbic cortex, the part of the brain that controls relationship between cues and behaviour; the amygdala, the part of the brain that controls fear; and the olfactory bulb, the part of the brain that detects and understands scent, which is

the main sensory way rats navigate the world. These findings suggest that SG rats experience heightened anxiety, and that this anxiety can interfere with learning pathways in the brain. It is our hope that future work will identify more neural signatures of *SYNGAP1*-ID, which can ultimately be used for non-invasive diagnosis, prognosis, and clinical studies.

Contents

List of Figures

2 Declaration

I declare that this thesis has been composed solely by myself and that it has not been submitted, in whole or in part, in any previous application for a degree. Except where stated otherwise by reference or acknowledgement, the work presented

X

Faith Colaguori
MScR Candidate

Acknowledgements

This work was conducted at the Centre of Discovery Brain Sciences at the University of Edinburgh (2021 – 2023). My work was funded by the Simons Initiative for the Developing Brain – to all my funders, administrators, and international support staff, I cannot thank you enough for your financial and logistical assistance. Without you, this project never would have happened!

To begin, I would like to thank my supervisors, Dr Peter Kind and Dr Thomas Watson, for their invaluable expertise and knowledge as I have embarked upon this project. My time at the University of Edinburgh has been full of tremendous hardships in my personal life, and I would not have been able to successfully navigate throughout the thesis production process without their constant support. I would also like to thank other members of the lab and broader department who have provided steadfast help throughout this journey, namely Dr Sally Till, Dr Martin Simmen, Dr Catherine Abbott, and Jane Wright; I know my MSc experience has deviated greatly from the norm, and I cannot thank them enough for their support and guidance during my time at the university.

To my fellow lab members, especially Vanesa Salazar-Sanchez and Chloe Henley: thank you for making this American feel right at home in the UK! My life has been greatly enriched by their friendship, and I cannot express my gratitude enough for all of their support and encouragement.

Finally, I would like to dedicate this thesis to: my family, especially my mom and dad, who have always supported me from all the way across the Atlantic Ocean; my friends back home in the US, especially those who flew halfway around the world to cheer me on (Grace, Sam, and Arianna), to celebrate their own milestones and graduations (Rose and Teresa), and to help me move flats during a very difficult time (Kristen); and finally, all the new friends I have made in the UK (especially Anna and Connie). My life is so much richer for having had this experience, and I could not have done it without all those named here!

4 Introduction

4.1 Introduction to Neurodevelopmental Disorders (NDDs)

Neurodevelopmental disorders (NDDs) encompass a wide variety of conditions that profoundly impact an individual's cognitive, social, and behavioural functioning. These disorders manifest as variations in how individuals interact with others, communicate, process information, and behave [1]. NDDs collectively represent a spectrum of impaired social and cognitive behaviours, which can manifest with varying degrees of severity across the diagnosed patient population. In previous decades, NDDs, including autism spectrum disorder (ASD), were often categorized under the broader diagnostic umbrella of 'pervasive developmental disorders' (PDDs) [2]. However, due to a lack of clear boundaries between PDDs and difficulty distinguishing between subtypes of these disorders, recent diagnostic criteria such as the International Classification of Diseases, Eleventh Edition (ICD-11) and the American Psychiatric Association's Diagnostic and Statistical Manual, Fifth Edition (DSM-5), have adopted the term ASD as an overarching construct [2-4]. Additional diagnostic classifiers are then used to differentiate between specific subtypes and various clinical presentations within the realm of NDDs. In this thesis, the term 'autism' will be employed to refer to ASD in a general sense, with additional classifications or subtypes clearly specified.

The diagnostic criteria for ASD, as outlined in the DSM-5, require individuals to exhibit persistent deficits in each of three key areas of social communication and interaction, along with at least two of four types of restricted, repetitive behaviours [2, 4-5]. **Figure 1** provides a simplified outline of the criteria for diagnosing ASD according to the DSM-5.

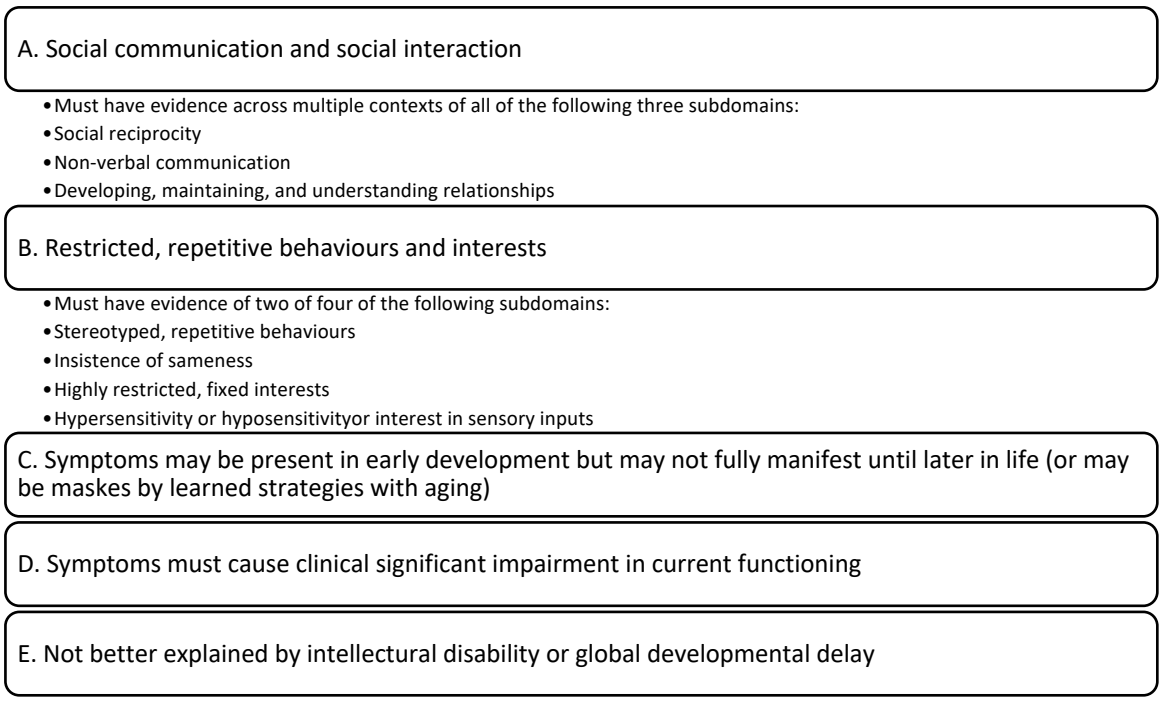

Figure 1 - Simplified Diagnostic Criteria for ASD Adapted from the DSM-5:

ASD diagnostic criteria compromises of five symptom clusters (A-E), two of which have additional sub-criteria (A-B).

Traditionally, research has indicated a higher prevalence of ASD in males compared to females, with a reported sex ratio of 4:1 in the 2010 Global Burden of Disease study [2, 6-8]. However, recent critiques of these ratios have highlighted non-inclusive diagnostic criteria for female patients, who are better at "masking" non-social and repetitive behaviours than their male counterparts [7]. Additionally, the reported ratios of autism tend to be higher in high-income countries, although this trend is largely attributed to improved access to parental and caregiver education and healthcare [7,8]. On a global scale, rates of autism do not appear to differ significantly based on ethnicity, nationality, or socioeconomic status [2].

NDDs, including ASD, have been associated with various environmental risk factors. These factors include advanced parental age (maternal age >40, paternal age >50) [9], neonatal hypoxia, gestational diabetes mellitus, valproate use during pregnancy, <12-month interpregnancy interval, preterm birth, and maternal obesity [10]. These factors cannot be considered causal, they may play reactive or independent roles in autism diagnosis. Several hypotheses of environmental risk factors of ASD have been clearly disproven by the scientific literature, including causation linked to early membrane rupture, caesarean section, assisted vaginal delivery, prolonged labour, and vaccinations [2,11].

Understanding the broader mechanisms and pathophysiology of NDDs, including autism, remains an ongoing challenge [1,2]. Unlike some medial conditions characterised by gross brain pathophysiology, NDDs typically do not exhibit such overt anatomical abnormalities. However, subtle differences in brain anatomy and function have been observed through post-mortem and electrophysiological studies [2]. Importantly, autism is thought to have a significant genetic component, with heritability estimates ranging from 40% to 90% [12-13]. To date, over 200 genes and genomic regions have been associated with ASD, encompassing variations from single-base changes to segments of DNA spanning thousands to millions of bases [14-15].

Among individuals diagnosed with autism, a subset of cases, estimated at 10% to 30%, can be attributed to monogenetic (single gene) variations [2, 16]. These de novo genetic variations, though less common, are often employed in laboratory animal research due to their feasibility for replication. This project focuses on *SYNGAP1*-related intellectual disability (*SYNGAP1*-ID), a monogenic NDD that often includes a co-diagnosis of ASD.

4.2 *SYNGAP1* Haploinsufficiency: A Genetic Link to NDDs

Genetics have emerged as a pivotal factor in our understanding of NDDs. Recent advancements in genomic sequencing have unveiled a multitude of genetic loci that are implicated in the aetiology of developmental brain disorders.

Among these genetic players, *SYNGAP1 (Syngap1)* stands out as a gene with profound implications for NDDs. De novo nonsense mutations in SYNGAP1 have been identified as causative factors in a spectrum of NDDs, encompassing intellectual disability (ID), ASD, epileptic encephalopathy (EE), and schizophrenia (SCZ) [17]. These disorders arise from genetic haploinsufficiency, a condition where the presence of two wildtype copies of a gene is necessary for the expression of a normal phenotype. When one copy of a haploinsufficient gene is deleted or undergoes a loss-of-function mutation, the residual expression of the single wild-type gene is not sufficient for normal function [18].

SYNGAP1 haploinsufficiency reduces the expression of SynGAP protein, which causes a severe comorbid syndrome that frequently includes overlapping diagnoses of ID, ASD, and epilepsy [19]. Clinically, this condition is diagnosed as *SYNGAP1*-related intellectual disability (*SYNGAP1*-ID), and it is characterized by many behavioural abnormalities that mirror those associated with ASD. These can include stereotypic behaviours (such as hand flapping or obsessions with specific objects), impaired social development, problems with feeding and food, inattention, aggressive behaviour, and sleep disorders [17].

Of the existing patient population, the following clinical characteristics of *SYNGAP1*-ID emerge: 100% of affected individuals have developmental delay (DD) or ID, ~84% have generalized epilepsy, and ~50% present with ASD or similar behaviour abnormalities [17]. While no formal diagnostic criteria have been published for *SYNGAP1*-ID, it is generally diagnosed in individuals with DD or ID for whom molecular genetic testing identifies either a heterozygous pathogenic variant in *SYNGAP1*(~89% of affected individuals) or a deletion of 6p21.3 (~11% of affected individuals) [17].

SYNGAP1-ID was only recently described in the scientific literature, with the first description of three affected individuals being presented by Hamdan et al in 2009 [20]. It is highly plausible that many *SYNGAP1*-ID patients may have previously received broader NSS diagnoses, including general ID and ASD. This misclassification often occurs due to the necessity of genetic testing to arrive at a definitive *SYNGAP1*-ID diagnosis, a step that many individuals with disabilities do not undergo. Nonetheless, existing data from the *SYNGAP1*-ID patient population demonstrates that life expectancy can last into adulthood [21]. This population also demonstrates that penetrance of *SYNGAP1*-ID is 100%, with all individuals with pathogenic variants in *SYNGAP1* having DD, ID, cognitive dysfunction, and/or epilepsy [17], although with varying severity of presentation.

Due to its behaviour phenotype resembling ASD and its suitability for replication in laboratory rodents, *SYNGAP1* haploinsufficiency has become a valuable genetic model in neuroscience research. This thesis will delve into research focusing on prediction impairment and fear learning, conducted in $Syngap^{+/\Delta GAP}$ animals, which serve as a phenotypic model for studying ASD-related behaviours.

4.3 Fear Conditioning as a Model for Exploring Neural Circuits

Introduction to Fear and Its Neural Basis

According to the American Psychological Association, fear is “a basic, intense emotion aroused by the detection of an imminent threat, involving an immediate alarm reaction that mobilizes the organism by triggering a set of physiological changes” [22]. Evolutionarily, fear is understood to have evolved as a defence mechanism to protect animals from danger. While fear can be hardwired to certain kinds of stimuli (e.g., humans are naturally afraid of sudden, loud noises), fear can also be acquired rapidly via the pairing of various stimuli and learning from past experiences. In the laboratory, this can be achieved through classical fear conditioning, which has become the gold standard task for studying the anatomical, cellular, and circuitry bases of fear memory formation in the brain [23].

Fear Learning and Memory

In the classical fear conditioning paradigm [24], an initially innocuous conditioned stimulus (CS) is paired with a naturally aversive unconditioned stimulus (US) to elicit a reflexive unconditioned fear response (UR). Through CS-US association formation and learning, the CS comes to produce a conditioned response (CR) that is similar to the instinctive, innate fear response (UR) [23]. In the fear conditioning paradigm employed here, a flashing light is the CS paired with a mild electric shock (rodent foot shock) as a US. A small number of CS-US pairings produce a robust fear response, typically exhibited as a CR of freezing [25-28]. Freezing in the fear conditioning context is defined as the cessation of all movements except those related to respiration [25]. This paradigm is illustrated in **Figure 2** below.

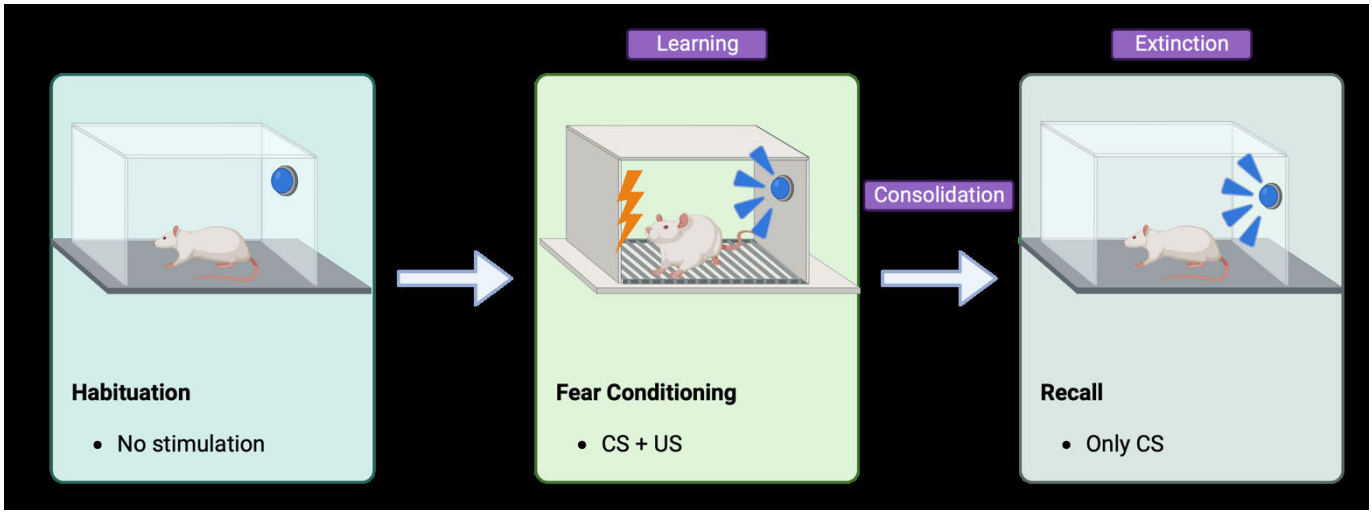

Figure 2 – Classical Fear Conditioning Schematic:

A graphic depiction of the three steps of the classical fear conditioning paradigm (habituation, fear conditioning, and recall) and the three neural processes that are associated with fear acquisition and eventual decline (learning, consolidation, and extinction). The detailed protocol of this process relating to this thesis is outlined in Figure 4.

As illustrated in the figure above, the acquisition of fear memory happens in three broad stages: **learning**, which occurs during the conditioning stage of the paradigm (the CS-US association), **consolidation**, which is the neural process by which fear memories are created and stored, and **extinction**, which occurs during the recall stage of the paradigm. During extinction learning, the CS is no longer paired with the US; once this association has been unlearned, the subject should cease the UR. This thesis will focus on the recall stage of the fear conditioning paradigm, as this is where the behaviour between the genotypes differs the most.

This classical fear conditioning paradigm is robust and reliable, and has been used in the study of fear and learning for over a century – the technique was first published for rodents by Watson and Rayner in 1920 [24], but the premise can be traced to Pavlov and his salivating dogs in the 1897 [29]. In addition, because this response is taught quickly (often with just a single CS-US pairing) and has a lasting effect until extinction learning begins, fear conditioning has become a popular behavioural tool for analysing learning and memory [23].

The Neural Circuity of Fear

At the core of fear conditioning lies a complex neural circuity involving various brain regions. Key players in this circuitry include:

1. **Amygdala (AMY):** The amygdala, especially the lateral nucleus (LA) and central nucleus (CeA), is widely recognized as a hub for processing and integrating fear-related information [30-31]. It receives input from sensory pathways conveying information about the CS and US, enabling the formation and storage of fear memories.
2. **Infralimbic Cortex (IRL) and Prelimbic Cortex (PRL):** The prefrontal cortex, compromising the infralimbic and prelimbic regions, plays a crucial role in regulating and modulating fear responses. These regions are involved in fear extinction [23, 32-33].
3. **Olfactory Bulb (OFB):** The olfactory bulb increases odour discrimination through inhibitory synaptic mechanisms [34] and is emerging as a region of interest in fear-related research. It is thought the emphasize the sensory-specific aspects of fear learning [35].

This research presented in this thesis will focus on neural analysis conducted in the infralimbic cortex, the amygdala, and the olfactory bulb.

Fear Conditioning in Research

Fear conditioning is not only a fundamental model for understanding the neural basis of fear, but also a powerful tool in neuroscience research [23]. By utilizing this model, researchers can manipulate and investigate the neural circuits that underly fear, test hypotheses related to neural plasticity, and explore the effects of genetic or pharmacological interventions on fear-related behaviours.

In this thesis, fear conditioning serves as a pivotal framework for exploring the behavioural and neural manifestations of fear in both wildtype (WT) and *Syngap*$^{+/\Delta GAP}$ (SG) rats. By analysing the neural circuity involved in fear conditioning and fear extinction, we aim to uncover insights into the altered neural dynamics in SG rats and their potential contribution to impaired fear extinction. This research not only advances our understanding of *SYNGAP1* haploinsufficiency but also contributes to the broader understanding of how neural circuits mediate fear learning and memory, with implications for NDDs and beyond.

4.4 Significance of Neural Analysis in Understanding Behaviour

The brain is a highly complex system, wherein parallel processing coexists and contradicts across various regions and interconnected networks, but without a centralised coordination centre [36]. Despite this complexity, the brain then integrates these neural processes that occur in different times and locations into a single perceptual experience.

Neural Oscillations and Behaviour

This remarkable feat of neural integration relies on neural oscillations – a rhythmic and synchronised pattern of neural activity that extends across different brain structures. Neural oscillations, when synchronised and concurrently active across various brain regions, play a critical role in shaping an individual's cognitive and behavioural experiences [37]. They serve as a fundamental mechanism by which the brain communicates and coordinates its activities to support behaviour.

Measuring Neural Oscillations in Awake and Behaving Animals

To gain insights into the role of neural oscillations in behaviour, researchers employ electrophysiological recordings, including techniques such as electroencephalography (EEG), magnetoencephalography (MEG), and local field potential recordings (LFP). These methods allow for the direct measurement of neural oscillations in awake and behaving animals, providing a unique window into the brain's activity during real-life experiences [37].

Coherence: Uncovering Interactions in Behaviour-Related Neural Circuits

One powerful mathematical tool for understanding the relationship between neural oscillations and behaviour is coherence. Coherence quantifies the degree of synchronisation and similarity between neural oscillations recorded in two distinct brain regions [37]. It serves as a means to assess how strongly these regions interact with each other during specific behaviours, scenarios, or stimulus presentations.

To calculate coherence, electrophysiological recordings undergo pre-processing to eliminate background noise, such as baseline wandering drift or power-line interference. Mathematical algorithms like Welch's method are then employed to compute the coherence function. This function allows researchers to gauge the statistical similarity and strength of interaction between two neural signals in different brain regions, shedding light on the coordination of neural activity underlying behaviour [38-39].

Power: Unveiling the Energetic Aspect of Behaviour-Related Activity

Another valuable mathematical application of neural oscillations is power. Power measures the strength of neural signals by summing the absolute squares of the time-domain samples and dividing by the signal's length. In essence, it quantifies the energy expended by neural circuits in generating specific behaviours [40]. The exact mathematical processes for calculating both coherence and power employed by this thesis are outlined in Section 5.5.3: Coherence, Power, and Spectrogram Calculations.

Coherence and Power in Fear Learning and Prediction Impairment

In alignment with the growing significance of coherence and power analysis, this thesis leverages these tools as primary instruments for dissecting the differences between WT and

SG fear learning and prediction impairment. By analysing coherence and power patterns, we aim to uncover the neural circuitry alterations underlying aberrant fear-related behaviours in *SYNGAP1* haploinsufficiency. This approach not only contributes to our understanding of *SYNGAP1*-related neurodevelopmental disorders but also highlights the pivotal role of neural analysis in unravelling the intricate relationship between neural activity and behaviour.

4.5 Research Rationale

Previous research in our laboratory has revealed an impaired extinction response in SG rats during the fear conditioning paradigm [41]. In this study, we aim to investigate the extinction of fear learning in both SG and WT rats using the standard fear conditioning protocol, which includes a flashing light conditioned stimulus (CS) paired with a foot shock unconditioned stimulus (US). Notably, neither SG nor WT rats displayed significant freezing behaviour (conditioned response, CR) before the initial CS presentation, and both groups exhibited similar levels of freezing during the six CS-US presentations during conditioning [41].

However, a significant divergence emerged during the recall stage of the experiment, with SG rats exhibiting significantly higher freezing behaviour. This discrepancy in fear extinction between the two genotypes serves as the central question driving this thesis. We aim to leverage *in vivo* recording techniques and advanced neural data analysis to explore potential circuit- and system-level explanations for this observed phenomenon. Unlike earlier studies in the lab, this current work features several key distinctions.

4.6 Aims and Hypotheses

Aim 1: To determine whether the implementation of LFP electrodes and EEG screws, accompanied by anaesthesia and changes in housing conditions, influences the previously reported extinction deficit phenotype observed in SG animals following fear conditioning.

Hypothesis: Despite the variations in surgical and housing conditions, we anticipate that the extinction deficit behaviour will persist in SG rats. The difference is likely attributable to neural mechanisms, such as distinctions in neural connectivity between WT and SG rats, rather than being influenced by the external variables under investigation.

Aim 2: To investigate whether the altered extinction behaviour correlates with changes in coherence across specific brain regions, including the infralimbic cortex (IRL), amygdala (AMY), and olfactory bulb (OFB), and whether these changes directly relate to both CS presentations and scored rat behaviour.

Aim 3: To investigate whether the altered extinction behaviour is associated with variations in power within the same target brain regions (IRL, AMY, and OFB) and whether these power differences also correlate with CS presentations and observed rat behaviour.

5 Methods and Optimisation of Protocols

5.1 Animals

All procedures performed on animals were conducted in compliance with the national Animals (Scientific Procedure) Act, 1986, United Kingdom.

All subjects used in this study were in-facility bred male Long Evans-*SG*$^{em2/PWC}$, hereafter referred to *Syngap*$^{+/\Delta GAP}$ (SG) rats and wildtype (WT) littermate rats. Colony founders were produced by Sigma Advanced Genetic Engineering (SAGE) Labs (St. Louis, MO, US) using zinc finger nuclease (ZFN)-mediated deletion [41] of the GAP domain of *Syngap.* Pups were weaned from their dams at postnatal-day 22 (P22) and housed in mixed genotype cages with littermates, 2-4 animals per cage. Animals were kept in a 12h/12h light/dark cycle with ad libitum access to water and food. After surgery, performed around 3 months of age, animals were moved into a larger cage to accommodate the implanted head stage, and they shared the cage with a single littermate that had also undergone surgery. Animals were re-genotyped by PCR at the end of the experiment.

5.2 Surgical Methods

All of the surgeries and fear conditioning tasks included in this thesis were completed by Dr Thomas Watson. The surgical methods and fear conditioning protocol are included here for clarity, although my involvement with this project began with the development of the electrophysiological pipeline and subsequent analysis of the data (Section 5.4).

Rats were anesthetised and prepared for stereotaxic surgery, craniotomies were drilled and an LFP electrode (140 µm diameter Teflon coated stainless-steel, A-M systems, USA) or single recording screw (1 x 3 mm Cheese Head Stainless steel, Screws and More, Germany) were positioned at each of the following coordinates relative to bregma (**Figure 3**):

- IRL: AP +3.24; ML +0.5; DV +4 mm
- AMY: AP -2.4; ML +4.7; DV +7.5 mm
- OFB: AP +7; ML +1 mm
- Superior Colliculus: AP -6.72; ML +1.5; DV +3 mm

A screw positioned over the cerebellum served as a reference/ground. Recording implants were placed unilaterally and then connected to an electronic interface board (EIB 16, Neuralynx). The implant was covered with dental cement, and the incision was then closed using surgical sutures (Ethicon, Henry Schein, UK) and rats were left to recover for a minimum of two weeks post-surgery. During recovery, analgesia was administered as needed.

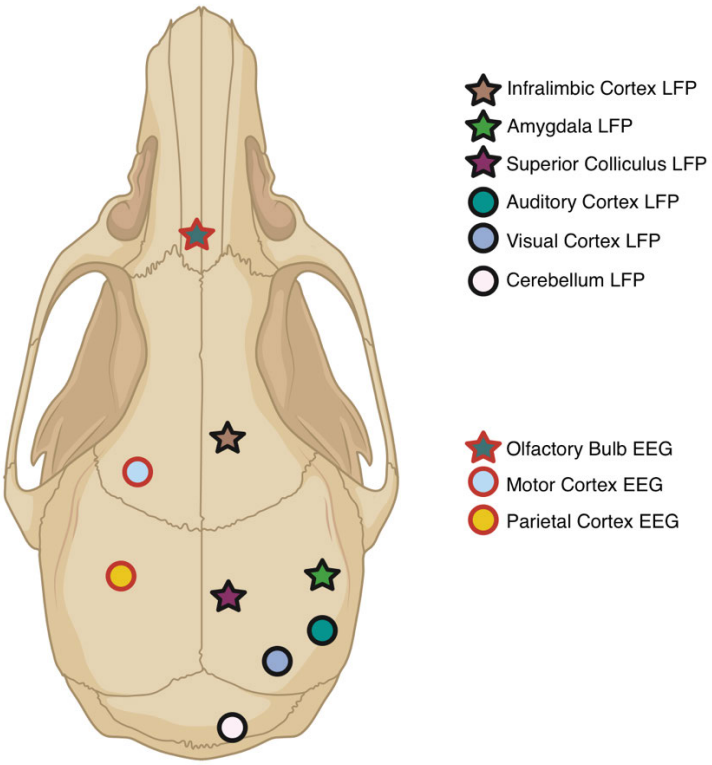

Figure 3 – LFP Electrode and Single Recording Screw (EEG) Implant Locations:

A simplified diagram of a rat skull outlining the locations where LFP electrodes or single recording screws were placed during the surgery. The locations marked by stars are the structures that were analysed in this thesis; the data was collected for the locations marked by circles, but not analysed here due to time and analysis constraints. The symbols outlined in black are LFP electrodes, and the symbols outlined in red are single recording screws. A key is provided to the right, and the exact coordinates of the analysed structures are in the Section 5.2.

5.3 Fear Conditioning and Extinction Task

5.3.1 Fear Conditioning Protocol

The fear conditioning protocol is a moderate severity procedure that was approved by the University of Edinburgh animal welfare committee and was performed under a United Kingdom Home Office project license.

The protocol involves two contexts and is conducted over a period of five consecutive days. A day-by-day breakdown of the protocol is included below, and this workflow is presented graphically in **Figure 4**:

- **Day 1 (Habituation):** The implanted rat is placed in the recall chamber and tethered to the neural recording acquisition head stage. The rat is allowed to explore the chamber for five minutes, and the neural recordings are collected with the OpenEphys acquisition software. The trial is recorded from a video camera mounted in front of the testing context, and a microphone is running to collect ultrasonic

vocalisations. Between rats, the recall chamber is cleaned with 70% ethyl alcohol (EtOH).

- **Day 2 (Rest):** The rat remains in their home cage, and no procedures are conducted.
- **Day 3 (Habituation):** The Day 1 Habituation protocol is replicated in the recall chamber under the same conditions.
- **Day 4 (Pre-Conditioning Light Exposure and Fear Learning):** The implanted rat is placed in the fear conditioning chamber. Prior to conditioning, the CS (flashing blue light) is presented to the rat for 10 sec as a pre-conditioning CS baseline. Conditioning occurred over a 21-minute period, and CS and US events are controlled by a custom protocol in the Freeze Frame software. This protocol consists of a 3-minute period to allow for exploration of the chamber, followed by 6 pairings of a conditioned stimulus (CS) co-terminating with the unconditioned stimulus (US). The CS is a flashing blue light (5 Hz 110 lux flashes, 50/50 duty cycle) and the US is a 1 sec, 0.8 mA scrambled foot shock delivered through the bars of the floor. CS presentations start at the following times of the protocol: 180 sec, 360 sec, 490 sec, 770 sec, 980 sec, and 1280 sec. The CS presentation lasts for 10 sec, with the final 1 sec also containing the US. The trial is recorded from a video camera mounted in front of the testing context, and a microphone is running to collect ultrasonic vocalisations. Between rats, the fear chamber is cleaned with 1:100 diluted Distel in water.
- **Day 5 (Recall):** The implanted rat is placed in the recall chamber and tethered to the neural recording acquisition head stage. Retention and extinction of the conditioned response is tested over a period of 24 minutes. The rat has 4 minutes to explore the recall context, then the CS is presented in twelve 30 sec long presentations, each followed by 30 sec with no CS presentation. Rat freezing behaviour is observed and timed via subsequent video analysis. The trial is recorded from a video camera mounted in front of the testing context, and a microphone is running to collect ultrasonic vocalisations. Between rats, the recall chamber is cleaned with 70% EtOH.

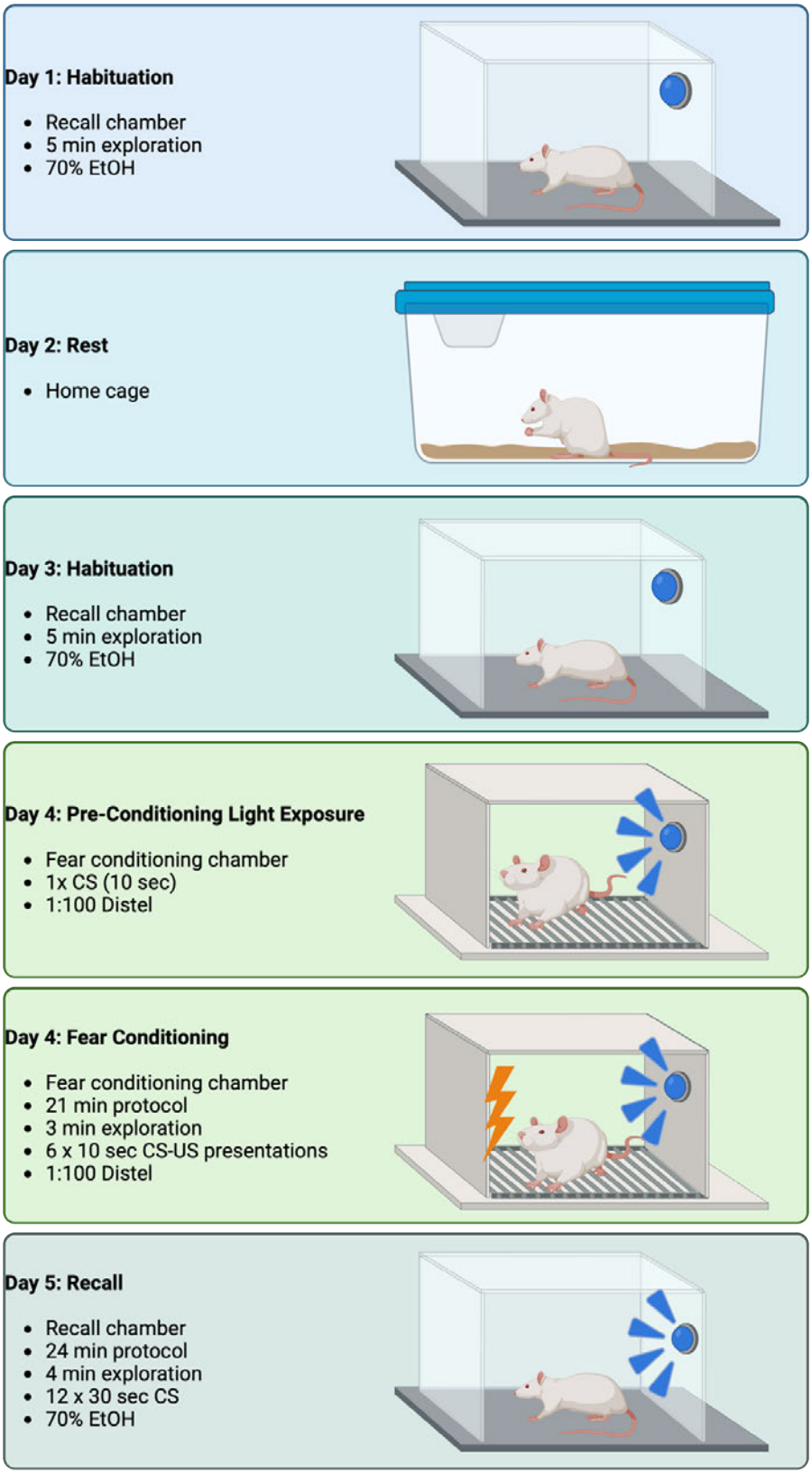

Figure 4 – Fear Conditioning Protocol:

A graphic protocol outlining the fear conditioning paradigm employed in this thesis.

5.3.2 Fear Conditioning Apparatus

The fear conditioning protocol consists of two chambers, varying in design, construction, and even scent. The recall chamber (a modified Coulbourne Instruments rat Habitest box) is used for the habituation and recall steps of the fear conditioning protocol; it measures 30 cm x 25 cm x 32 cm, and has a solid, plastic floor that is painted black. Three of the walls are painted in alternating black and white stripes, and the final wall consists of a clear plastic door on a hinge through which the rat can be placed in the chamber and observed during the session. The top of the chamber is also clear plastic and contains holes through which the microphone and neural acquisition probe can be tethered. Prior to habituation and recall sessions, the chamber is sprayed with 70% EtOH; this disinfects the chamber from the scents of previous rats and distinguishes the chamber in scent from the fear conditioning chamber. Finally, the top sides of the chamber have two strips of LED lights, which flash blue when triggered with the external control software, FreezeFrame (ActiMetrics, IL, USA).

By contrast, the fear conditioning chamber has a drastically different design. This is to assure the recall behaviour is due to the rat's acquisition of the CS, rather than a response to the rat's external environment.

The fear conditioning chamber is an unmodified Habitest rat box with aluminium wall inserts and an electrified shock floor (Colbourne H10-11R-TC-SF) that is constructed of the same clear plastic material. The floor is a metal grating of bars that are connected to an electrical control box (Colbourne) to control the flow of the current for the foot shock. Three sides walls have been covered with a plain black backdrop, and the roof contains the same holes for the microphone and neural acquisition tethered probe. The chamber is sprayed with Distel (diluted 1:100) to differentiate it in scent from the recall chamber, and the same blue LED lights are arranged in the chamber.

For both chambers, the entire apparatus is controlled by an external computer with FreezeFrame. The software allows for the development of a custom protocol, and can simultaneously control stimuli timings such as when the LED lights flash and when the foot shocks are administered.

There were many limitations with regards to the apparatus design and the quality of neural data, mainly due to electrical noise from the foot shock grid. While this did not impact the findings presented here (as analysis was only completed in the non-electric recall chamber), I did modify the fear conditioning chamber to correct this drawback. The optimised conditioning apparatus is outlined in Section 7.4: Future Work.

5.3.3 Neural Recording Acquisition System

On recording days of the fear conditioning protocol, neural recordings were acquired with an OpenEphys acquisition system (OEPS, Portugal), through a 16 channel digitising head stage (C3334, Intan Technologies, USA). LFP signals were bandpass-filtered from 0.1 – 600 Hz and sampled at 2 kHz in OpenEphys software. Video recordings were made using FreezeFrame software (15 frame per sec; ActiMetrics) synchronised with electrophysiological signals via pre-programmed TTL pulses.

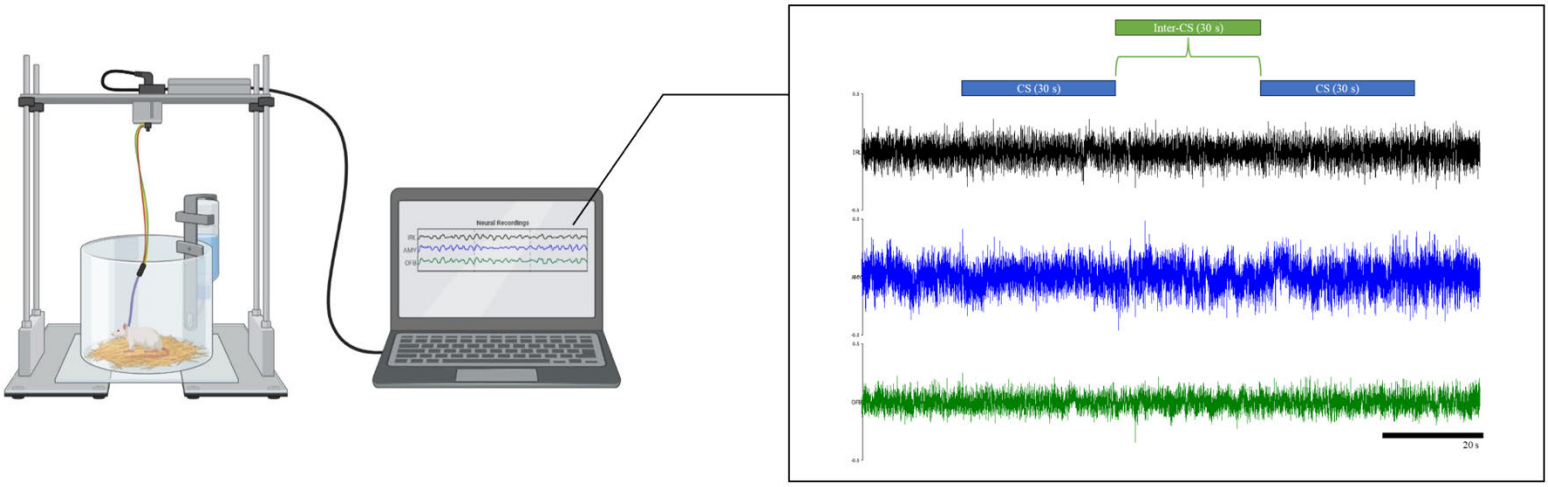

Figure 5 – Neural Recording Acquisition Schematic:

A graphic representation of the neural recording acquisition system employed by this thesis. The headstage was connected to a wired probe, which transmitted neural data via the OpenEphys acquisition system. LFP signals were bandpass-filtered from 0.1 – 600 Hz and sampled at 2 kHz. The close-up on the right shows real neural signals collected from this thesis, prior to signal cleaning and calculations in MATLAB.

5.4 Behavioural Analysis Methods

5.4.1 Behaviour Scoring via MATLAB

To analyse the differences between the *Syngap*$^{+/\Delta GAP}$ and wildtype animals in the fear conditioning paradigm, behaviour must first be scored manually. The purpose of this is three-fold; firstly, scoring behaviour allows us to determine differences purely between the behaviour of the two groups, such as differences in time spent frozen, probability of freezing during any point in the paradigm, etc. Secondly, scoring behaviour allows us to properly "bin" or "segment" neural recording data to align neural output with behaviour; via this grouping of data, we can make conclusions about mathematical properties such as coherence and power defined by behaviour (such as coherence during freezing vs. motion) rather than strictly by time in the paradigm (such as coherence during CS presentation vs. normal conditions). Finally, scoring behaviour allows us to validate the lab's previously reported *Syngap*$^{+/\Delta GAP}$ extinction deficit [41] in animals under these varying conditions, including undergoing surgery and being tethered during the fear conditioning protocol.

Prior to the start of this project, the laboratory scored videos using a custom MATLAB App that used MATLAB's built-in video player to mark two behaviours while playing back a recorded trial. These two behaviours were as follows: 1) Start of CS Presentation 1, and 2) Freezing. Behaviours were marked by selecting the number of the behaviour being recorded, 1 or 2, and holding down the spacebar while the behaviour was being displayed. The MATLAB App did not allow the scorer to move forwards or backwards in the video. After going through the video, the times of the marked behaviours were exported to a MATLAB

table, and all periods of freezing less than 2 sec were removed from the final table. This app was developed by a former postdoctoral student in the lab, Dr Adam Jackson.

There are many drawbacks to this approach, all of which result in the inaccurate reporting of scored behaviour. Most prominently, the inability to move forwards or backwards in the media player meant the beginnings of freezes were often not recorded, and extra time was often recorded after freezing behaviour stopped. Furthermore, these scored behaviours could not be edited; they were controlled by holding down the spacebar, and they could not be extended or shortened once the spacebar was released. In addition, CS timings were often marked incorrectly in neural data; after finding the frame of the first CS presentation, the script merely added 30 sec to this time, then determined the start time of each subsequent CS presentation from that data. However, this approach failed to account for the compression of the video, and how compressed frame rates can cause misalignment with true timings.

After using this MATLAB app to begin the analysis for this thesis, I realised that a new approach would need to be developed for more accurate behaviour scoring. That new approach, which would later form the first step of the entire electrophysiology analysis pipeline, is outlined in the following section.

5.4.2 Optimised Behaviour Scoring via ELAN

ELAN (Version 6.6 for Windows, 2023) is a linguistic annotation software that was developed by the Language Archive at the Max Planck Institute for Psycholinguistics (The Language Archive, Nijmegen, the Netherlands). It enables the manual and semi-automatic annotation of audio and video recordings simultaneously by using a tier-based data model that supports multi-level annotation [42].

ELAN improved the accuracy of the behavioural scoring. Not only does ELAN allow methodical annotations via moving forwards or backwards in the video, but annotations can be amended, combined, or deleted if a mistake is made. In addition, ELAN's tiered design enables multiple annotations to be made and tracked at all times; rather than just scoring CS presentations and freezing behaviours, with ELAN scoring behaviours were expanded to include jumping, US presentation, and non-fear freezing. Finally, ELAN's multi-media platform enables video and audio recordings to be scored simultaneously; while not utilised in this thesis, this feature will allow the alignment of ultrasonic vocalisations and scored behaviours in future studies.

To score behaviour in ELAN, videos were first covered from .AVI to .MP4 using VLC Media Player (VideoLAN, Version 3.0.18 for Windows). The .MP4 videos were uploaded to ELAN, along with the corresponding .WAV audio recording. A custom template was then applied with the following tiers: CS Presentation, US Presentation, Freeze, Jump, Non-Fear Freeze, and USV. Videos were scored manually by dragging the cursor over the tier of the corresponding behaviour during the correct time. Once scoring was completed, the table of times for each behaviour and rat was exported to Excel (Microsoft Office Suite, 2016) and then uploaded to MATLAB and converted to a .mat table. Freezing times were verified for a sample of rats by cross-checking with times where the accelerometer on the head stage was equal to zero.

5.4.3 Development of Behaviour Analysis MATLAB Scripts

All behavioural analysis functions and scripts were written by the author of this thesis in MATLAB R2022b (The MathWorks Inc., Version 9.13.0 for Windows). This interconnected set of scripts used the outputted .mat table to generate vectors of CS presentation start and end times and freeze start and end times, and used these vectors to quantify and compare behavioural data between individual subjects and groups. The outputs of these scripts quantified total freezing, percent of freezing between vs. during CS presentations, quantity of freezing episodes, average freezing bout lengths, and the probability of freezing onset during vs. between CS presentation. These were represented both quantitatively and graphically via the output of the MATLAB scripts, and further statistical analysis and graphical juxtaposition was completed using GraphPad Prism (GraphPad Software, Version 9 for Windows).

5.5 Neural Recording Analysis Methods

5.5.1 Development of Electrophysiology Analysis Pipeline

The 'Electrophysiology Analysis Pipeline' is the assortment of MATLAB applications (.mlapp), scripts, and functions that load, score, sort, and calculate parameters of interest from the raw electrophysiological data. The pipeline was developed by the author of this thesis, although one of the initial applications (OeP_loader_Tom.mlapp) was developed by Dr Adam Jackson, a former postdoctoral researcher in the laboratory. Dr Jackson had his own analysis pipeline, which informed some of the coding decisions that went into the development of this pipeline.

Figure 6 shows the flow of data through this pipeline in a simplified schematic. It is important to note that user-inputted behaviour data (freeze scoring) is incorporated into the processed electrophysiology structure; in subsequent scripts, the incorporation of both streams of data allows the user calculate parameters of interest, like coherence and power, during various parts of the recall protocol (i.e., during CS presentations as indicated by TTL pulse, during freezing behaviour as indicated by scored videos, etc.)

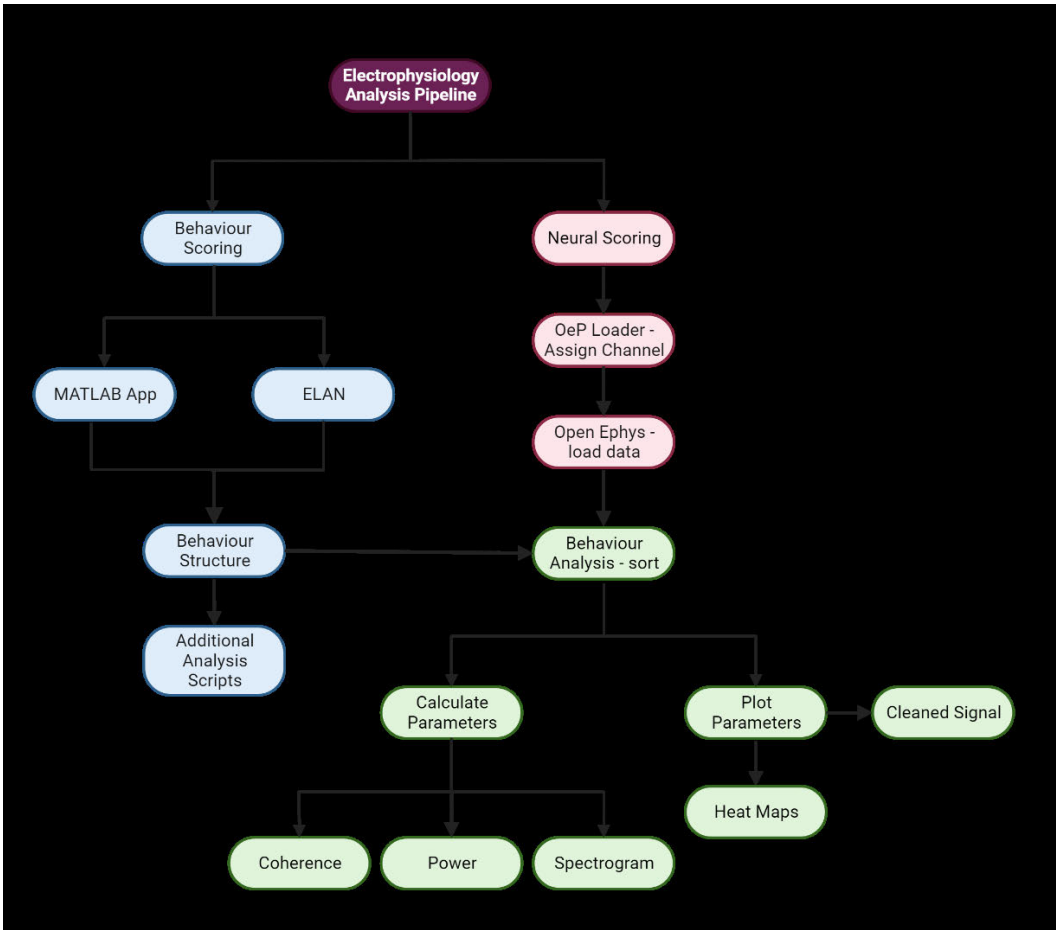

Figure 6 – Electrophysiological Analysis Pipeline Flowchart:

A simple flowchart outlining the custom-created electrophysiology analysis pipeline. The blue bubbles indicate behavioural analysis, the red bubbles indicate the initial neural data loading, and the green bubbles indicate the possible outputs when combining behavioural and neural data.

Subsequent sections will break down this pipeline in further detail, as well as discuss the signal processing and methodology for calculating key parameters. The pipeline in its entirety consists of two applications and over a dozen functions and scripts; a link to these scripts is provided in Appendix III: Access to the Electrophysiology Analysis Pipeline.

5.5.2 Channel Assignment and Neural Data Conversion

The MATLAB App **'OeP_loader_Tom'** is used to load raw electrophysiological data, assign channels, and create the initial structure with the electrophysiological data in a form that MATLAB can understand and manipulate.

The app uses a function developed by Open Ephys [43] called **'load_open_ephys_data_faster**.' This function is a MATLAB utility that is designed to open and load electrophysiology (ephys) data filed into MATLAB. It provides a convenient way to access continuous, event, or spike data recorded using the Open Ephys data format. The function takes a file path as input and returns the loaded data, timestamps, and additional

information contained in this file – in this case, the TTL pulses that signal the start of the CS presentations. By using this function, the app can easily access and analyse ephys data in the MATLAB workflow.

In this instance, the app constrains the Open Ephys function to only access **.continuous** files in the selected directory. The app then separates the audio files and stores them in a separate part of the structure ('AUXfilelist') and stores the remaining loaded data in a 'rawData' list. A pop-up then asks the user to assign the channels to the correct brain region (this changes based on how the EIB was wired during surgery); if there are duplicate channels, the app then prompts the user to scroll through the waveforms for both channels and select the one with the least amount of noise. These final channels, which will be used for subsequent analysis, are saved in the structure under 'keepRawData' and 'keepChannelList.' TTL channels are then manually labelled, and the 'fileInfo' structure is saved for analysis in the following scripts.

5.5.3 Coherence, Power, and Spectrogram Calculations

In preparation for coherence and power analysis, the ephys signals undergo a cleaning process to enhance the reliability and interpretability of the subsequent calculations. First, any obvious seizures are manually removed from the neural recordings. Prior to the Fourier Transform, a Hann windowing function is applied to minimize spectral leakage and mitigate edge effects. This windowing technique ensures a smooth transition at the signal boundaries, preventing artifacts that could distort the frequency content during the analysis.

Next, a Gaussian smoothing operation is employed to reduce high-frequency noise and enhance the signal-to-noise ratio, contributing to the robustness of the subsequent coherence and power calculations. It is important to note that no additional window pre-processing is performed before the Fourier Transform, preserving the integrity of the signal during frequency domain analysis.

These pre-processing steps collectively contribute to the refinement of the ephys signals, paving the way for accurate coherence and power analyses.

The coherence, power, and spectrogram calculations are best explained within the context of the **'behaviour_analysis_v4_faith.m'** script, which performs coherence and power analysis on selected files during specified behaviour epochs and saves these outputs in an updated 'fileInfo' structure. The user enters the following inputs:

- **'epoch':** The name of the behaviour of interest. This can be 'Freeze' from the scored behaviour, or 'visual' or 'nonvisual' for during or between CS presentations, respectfully.
- **'savename':** The name under which the output will be saved in 'fileInfo'.
- **'minDuration':** The minimum duration of a behaviour bout to be included in the analysis. For this thesis, the minimum duration was 2 seconds, meaning that freezing episodes less than 2 seconds in duration were not included in the analysis.
- **'analysisPeriod':** The duration of the analysis window for each behaviour bout. For this thesis, the analysis window for freezing was five seconds. For the CS presentations, the entire 30 second CS was the analysis window.

After selecting the data files that the user wants to analyse, the script calls on the **'Epoch_coh_power'** function to perform coherence and power analysis on the specified behaviour epoch. The results are assigned to variables and stored in the structure 'fileInfo' under 'savename'. In addition, the function determines the alignment between the behaviour data and the ephys data by matching the CS start time in both. This is a vital step, to ensure the calculations are performed on the correct portion of data.

Signal processing is a complicated area of analysis, but a brief overview of how the **'Epoch_coh_power'** function performs coherence and power analysis is included below:

1. **Coherence:**
   The 'mscohere' function in the MATLAB Signal Processing Toolbox is used to estimate the magnitude-squared coherence between two signals. Coherence is a measure of the linear relationship between two signals in the frequency domain. It quantifies the degree to which the signals share common frequency components, and it is not impacted by offset between signals. 'Mscohere' calculates the coherence using Welch's averaged modified periodogram method.

   The coherence estimate, $C_{xy}(f)$, for each frequency bin, f, is computed as the squared magnitude of the cross-spectral density (CSD) between the input signals X and Y, divided by the product of their individual power spectral densities (PSD). The CSD represents the Fourier transform, or the frequency content, of the cross-correlation function.

   Mathematically, coherence is calculated as:

$$C_{xy}(f) = \frac{\left|P_{xy}(f)\right|^2}{\left(P_{xx}(f) \cdot p_{yy}(f)\right)}$$

   Where:
   - $C_{xy}(f)$ is the coherence between signals X and Y at frequency *f*.
   - $P_{xy}(f)$ is the cross-spectral density between X and Y at frequency *f*.
   - $P_{xx}(f)$ is the power spectral density of X at frequency *f*.
   - $P_{yy}(f)$ is the power spectral density of Y at frequency *f*.

2. **Power:**
   The 'pwelch' function in the MATLAB Signal Processing Toolbox is used to estimate the power spectral density (PSD) of a signal using Welch's method. The PSD represents the distribution of signal power over different frequencies.

   Welch's method divides the input signal into overlapping segments, applies a windowing function to each segment, computes the Fourier transform of each segment, and averages the resulting periodograms to obtain the final power spectral density estimate. This approach reduces spectral leakage and provides a smoother estimate of the PSD compared to the standard periodogram method.

The PSD estimate, $P_{xx}(f)$ at each frequency bin, *f*, is calculated by averaging the squared magnitude of the Fourier transforms of the individual segments.

Mathematically, the PSD estimate using Welch's method is given by:

$$P_{xx} = \left(\frac{1}{M \cdot L}\right) \Sigma(|xk(f)|^2)$$

Where:

- $P_{xx}(f)$ is the power spectral density estimate at frequency *f*.
- M is the number of segments.
- L is the length of each segment.
- $Xk(f)$ is the Fourier transform of the kth segment at frequency *f*.

3. **Spectrograms:**
The 'cohgramc' function is from the Chronux Analysis Software, an open-source software package for the analysis of neural data developed at the Mitra Lab in Cold Spring Harbor Laboratory. In this thesis, Chronux version 2.102 v03 (latest release, 2018) was used by the function. Chronux analysis software can be retrieved from: http://chronux.org/

The 'cohgramc' function is used to compute a coherence spectrogram, also known as a coherogram. A coherogram provides a time-frequency representation of the coherence between two signals over time.

The 'cohgramc' function calculates the coherogram by dividing the input signals into overlapping segments, applying a windowing function to each segment, and computing the coherence using the cross-spectral density (CSD) estimate between signals. The resulting coherence values are then plotted as a function of time and frequency.

This is a high-level overview of a complicated multitaper spectral estimation method employed by the function. Mathematically, the resulting coherence spectrogram is represented as a matrix of coherence values $C_{xy}(t, f)$, where *t* represents the time index and *f* represents the frequency index. Each element in the matrix represents the coherence between the signals at a specific time and frequency.

The 'cohgramc' function provides a visual representation of how the coherence between two signals varies over time and frequency, allowing for the analysis of changes in relationships between the two signals.

5.5.4 Additional Analysis Scripts of Importance

As explained above, the entire electrophysiology analysis pipeline consists of too many scripts to include them all here. These scripts do everything from calculating additional parameters of behaviour (percent time freezing in different parts of the protocol, freezing probability, etc.), to creating heatmaps of genotypic differences in coherence and power, to

plotting acceleration against freeze times to confirm the correct alignment of neural and scoring data.

It is important to note that all scripts in the electrophysiology pipeline follow the methodology outlined above for the computation of power and coherence. Access to the scripts and functions that constitute the electrophysiology pipeline are provided in Appendix III. The full pipeline and all scripts will eventually be made available on GitHub for public use.

5.6 Statistical Analysis

While in-depth statistical analyses are included for the data presented throughout the results of this thesis, this section describes the general methodology for the statistical methods employed in this study. The quantity of groups and comparisons complicates this analysis, but the general methodology remains consistent.

The primary aim was to assess the impact of electrode implantation and conditioned stimulus (CS) presentation on freezing behaviour in both non-implanted and implanted rats. Prior to conducting statistical tests, the normality of data distributions was evaluated to determine the appropriateness of parametric or non-parametric tests.

Normality Assessment

Normality of the data distributions was assessed using the Shapiro-Wilk test. These tests were conducted separately for each experimental group (non-implanted and implanted rats) and each CS presentation modality to ensure the validity of subsequent statistical analyses.

The Shapiro-Wilk test was chosen as it is adequate for small sample sizes (n <50) and has more power to detect nonnormality than other small sample size normality tests [44]. The test statistic, W, is calculated as follows:

$$W = \frac{\left(\sum_{i=1}^{n} a_i x_{(i)}\right)^2}{\sum_{i=1}^{n}(x_i - \bar{x})^2}$$

Where:

- $x_{(i)}$ is the ith order statistic
- $\bar{x} = (x_1 + \cdots + x_n)/n$ is the sample mean.

The null-hypothesis of this test is that the population is normally distributed. Therefore, if the p-value is less than the chosen alpha level (in this instance, $\alpha = 0.05$), the null hypothesis is rejected and the data is considered nonnormally distributed. The normality of the distribution influences the subsequent analytical tests, as outlined below.

Behaviour, Power, or Coherence Comparison

For each modality of comparison (behaviour, power, and coherence), the data was analysed using a two-way analysis of variance (ANOVA). This analysis aimed to investigate the effects of two independent variables: electrode implantation and CS presentation. The results of this analysis were used to assess whether differences in these outputs were statistically significant between groups (SG vs. WT, implanted vs. non-implanted, etc.)

Unless otherwise stated, all results met the conditions for normality defined by the Shapiro-Wilk Normality test. When populations were found to be non-parametric, the two-way ANOVA was replaced by an appropriate non-parametric test (in most instances, this was a Mann-Whitney U Test/Wilcoxon rank-sum test for independent comparisons, or a Wilcoxon signed-rank test for matched comparisons. Matched comparisons were necessary when analysing differences within a single genotype during various timepoints of the paradigm.) Significant comparisons are outlined in Section 6: Results, and all additional statistical analyses can be found in Appendix I: Supplementary Statistics.

Post-hoc Analysis

In cases where significant main effects or interactions were detected in the ANOVA, post-hoc analyses were conducted to further investigate specific group differences. Bonferroni's multiple comparisons test was used to identify pairwise differences between groups at individual CS presentations.

Sample Size

This study was compromised of 41 rats; 23 rats were non-implanted subjects (WT, n = 12; SG, n = 11) and 18 were implanted (WT, n = 10; SG, n = 8). An a priori analysis was conducted to determine the ideal sample sizes of each group; using a large effect size (d = 0.8) due to a previously-recorded effect [41] and common values for α error probability and power ($\alpha = 0.05$; $(1-\beta) = 0.8$), a sample size of 26 was found for each group.

This would equate to a necessary 104 rats for the study (26 rats per group x 4 groups); while the following results do not meet these exact requirements for significance, it is important to note the results of the a priori analysis both for context and as a guideline for future studies.

6 Results

6.1 Behavioural Variances Between Groups

Aim 1 sought to validate the lab's previously reported extinction learning deficit in *Syngap*$^{+/\Delta GAP}$ animals [41]. While the extraneous variables in this repetition were altered (i.e., rats were implanted with LFP electrodes and EEG screws; housing conditions were variant; an additional pre-conditioning light exposure was included), I hypothesized that the extinction deficit was regulated by an underlying neural difference between wildtype and *Syngap*$^{+/\Delta GAP}$ rats, resulting in a similar behavioural phenotype even when the surgical, housing, and protocol conditions are modified.

Figures 7 and **8** illustrates that this hypothesis is correct; even under the varying conditions of this protocol, the implanted *Syngap*$^{+/\Delta GAP}$ rats displayed a similar diminished fear extinction phenotype when compared to their non-implanted counterparts in the lab's previous study [41]. While this does not verify our hypothesis about underlying neural variances, it does signify that a mechanism other than extraneous factors such as housing, diet, or socialisation is behind the disparity.

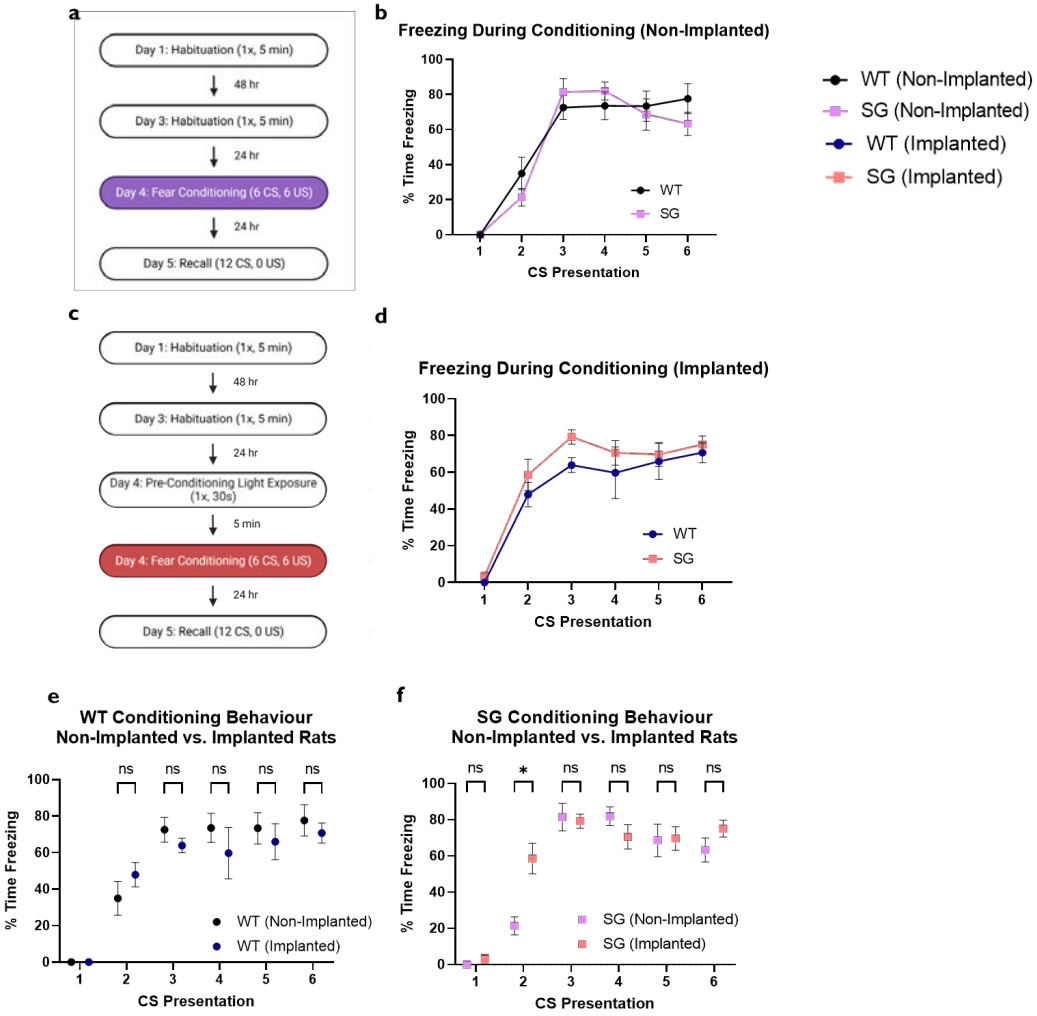

Figure 7 – Overview of Behaviour during Conditioning, Non-Implanted versus Implanted Rats:

Behaviour comparison for non-implanted (WT, n = 12; SG, n = 11) and implanted (WT, n = 10; SG n = 8) rats during the conditioning stage of the fear conditioning protocol.

(a) Experimental protocol for non-implanted rats. *Behaviour outlined here is from protocol Day 4, Fear Conditioning. CS, conditioned stimulus; US, unconditioned stimulus.*

(b) Freezing during conditioning, non-implanted rats. *Percent time freezing during each CS presentation. Error bars: mean ± SEM.*

(c) Experimental protocol for implanted rats. *Behaviour outlined here is from protocol Day 4, Fear Conditioning. Pre-conditioning light exposure is included in Figure 9. CS, conditioned stimulus; US, unconditioned stimulus.*

(d) Freezing during conditioning, implanted rats. *Percent time freezing during each CS presentation. Error bars: mean ± SEM.*

(e) WT conditioning behaviour comparison. *A two-way ANOVA was performed to analyze the effect of electrode implantation and CS presentation on freezing behaviour. An interaction between electrode presence and CS presentation was found to not have statistical significance (F(DFn, DFd) = 0.8257, p = 0.5347). CS presentation had a highly significant effect on behaviour (p < 0.0001****), while electrode presence did not (p = 0.5344). Bonferroni's multiple comparisons test revealed no significant differences between implant groups.*

(f) SG conditioning behaviour comparison. *A two-way ANOVA was performed to analyze the effect of electrode implantation and CS presentation on freezing behaviour. An interaction between electrode presence and CS presentation was found to have statistical significance (F(DFn, DFd) = 4.469, p = 0.0012). CS presentation had a highly significant effect on behaviour (p < 0.0001****), while electrode presence did not (p = 0.2089). Bonferroni's multiple comparisons test revealed a significant difference in freezing behaviour between the implanted SG and non-implanted SG rats at CS 2 (p = 0.0160*), although no significant differences were found across the other CS presentations.*

It is important to note that, during conditioning, the SG rats displayed a significant difference in freezing behaviour during CS 2 (Figure 7f). As the first foot shock (US) is administered at the end of CS 1, it is normal to see an increase in freezing behaviour during CS 2. However, the statistically significant increase in SG implanted freezing behaviour is most likely due to increased baseline anxiety associated with surgery and single housing, as illustrated in Figure 9a (increased freezing in SG rats during pre-conditioning light exposure). During recall, both the implanted and non-implanted groups exhibited similar behaviour across the genotypes, with no significant differences in freezing identified across any of the CS presentations.

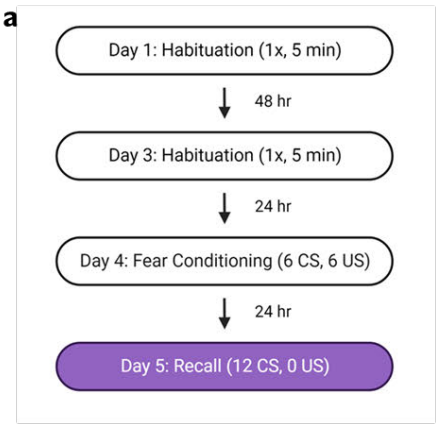
a
Day 1: Habituation (1x, 5 min)
48 hr
Day 3: Habituation (1x, 5 min)
24 hr
Day 4: Fear Conditioning (6 CS, 6 US)
24 hr
Day 5: Recall (12 CS, 0 US)

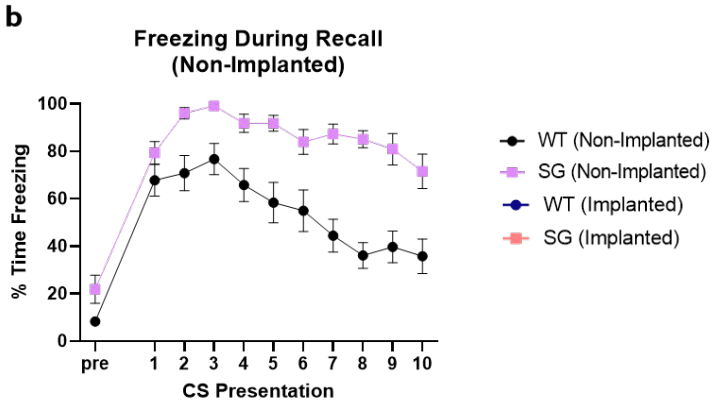
b
Freezing During Recall
(Non-Implanted)
% Time Freezing
CS Presentation
pre
WT (Non-Implanted)
SG (Non-Implanted)
WT (Implanted)
SG (Implanted)

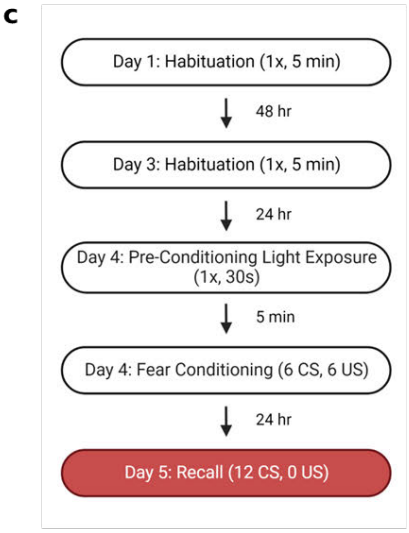
c
Day 1: Habituation (1x, 5 min)
48 hr
Day 3: Habituation (1x, 5 min)
24 hr
Day 4: Pre-Conditioning Light Exposure
(1x, 30s)
5 min
Day 4: Fear Conditioning (6 CS, 6 US)
24 hr
Day 5: Recall (12 CS, 0 US)

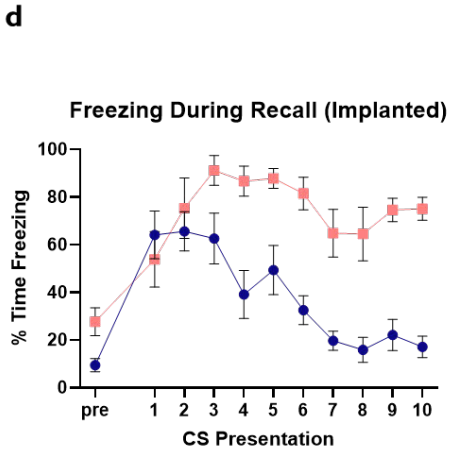
d
Freezing During Recall (Implanted)
% Time Freezing
CS Presentation
pre

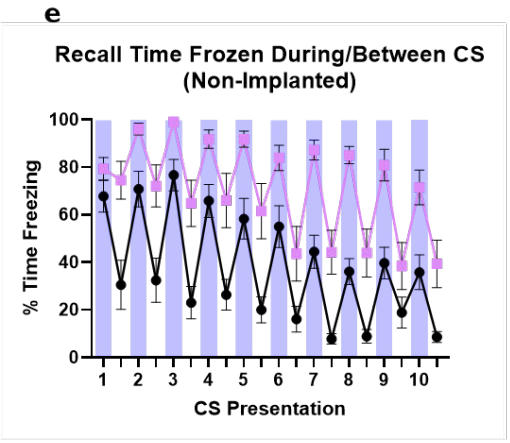
e
Recall Time Frozen During/Between CS
(Non-Implanted)
% Time Freezing
CS Presentation

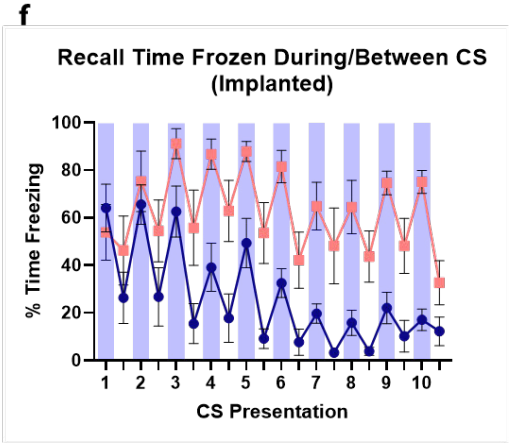
f
Recall Time Frozen During/Between CS
(Implanted)
% Time Freezing
CS Presentation

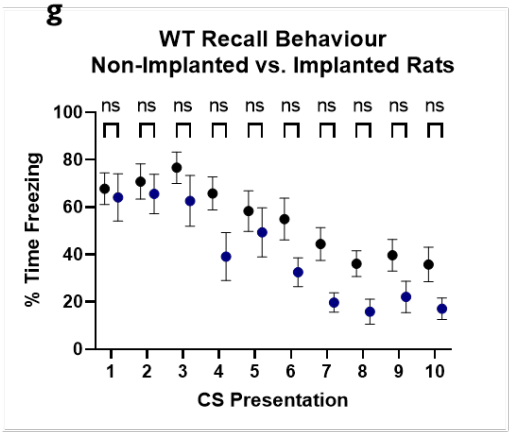
g
WT Recall Behaviour
Non-Implanted vs. Implanted Rats
ns
% Time Freezing
CS Presentation

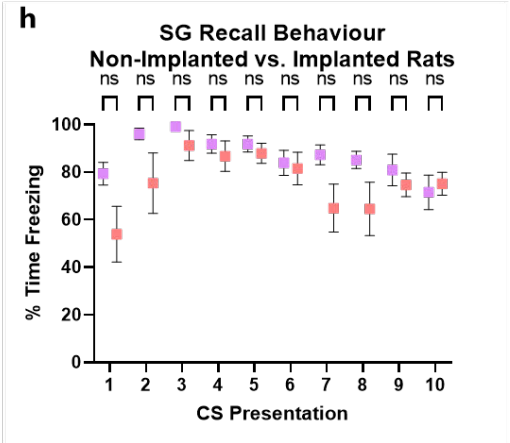
h
SG Recall Behaviour
Non-Implanted vs. Implanted Rats
ns
% Time Freezing
CS Presentation

Figure 8 - Overview of Behaviour during Recall, Non-Implanted versus Implanted Rats:

Behaviour comparison for non-implanted (WT, n = 12; SG, n = 11) and implanted (WT, n = 10, SG, n = 8) rats during the recall stage of the fear conditioning protocol.

(a) Experimental protocol for non-implanted rats. *Behaviour outlined here is from protocol Day 5, Recall. CS, conditioned stimulus; US, unconditioned stimulus.*

(b) Freezing during recall, non-implanted rats. *Percent time freezing during each CS presentation. Error bars: mean ± SEM.*

(c) Experimental protocol for implanted rats. *Behaviour outlined here is from protocol Day 5, Recall. CS, conditioned stimulus; US, unconditioned stimulus.*

(d) Freezing during recall, implanted rats. *Percent time freezing during each CS presentation. Error bars: mean ± SEM.*

(e-f) Freezing during recall, non-implanted and implanted rats, during versus between CS presentations. *Percent time freezing during and between each CS presentation. Blue regions on graph correspond to presence of blue LED light (CS). Error bars: mean ± SEM.*

(g) WT recall behaviour comparison*. A two-way ANOVA was performed to analyse the effect of electrode implantation and CS presentation on freezing behaviour. An interaction between electrode presence and CS presentation was found to not have statistical significance (F(DFn, DFd) = 0.8314, p = 0.5882). CS presentation had a highly significant effect on behaviour (p < 0.0001****), while electrode presence did not (p = 0.3484). Bonferroni's multiple comparisons test revealed no significant differences between implant groups.*

(h) SG conditioning behaviour comparison. *A two-way ANOVA was performed to analyse the effect of electrode implantation and CS presentation on freezing behaviour. An interaction between electrode presence and CS presentation was found to not have statistical significance (F(DFn, DFd) = 1.657, p = 0.1040). CS presentation had a highly significant effect on behaviour (p < 0.0008***), while electrode presence did not (p = 0.3789). Bonferroni's multiple comparisons test revealed no significant differences between implant groups.*

Figure 9 further explores these differences in behaviour between the implanted *Syngap*$^{+/\Delta GAP}$ and wildtype rats during the recall stage of the fear conditioning paradigm; in all other stages, no significant difference in freezing behaviour is observed. It is worth noting that there is a significant difference between total freezing duration and average freezing bout length between the two genotypes; however, there is no significant difference between the quantity of freezing bouts, nor between freezing behaviour during the pre-conditioning light exposure (an additional measure used as a baseline for the electrophysiological recordings). Furthermore, *Syngap*$^{+/\Delta GAP}$ rats spend a significantly greater percent of time freezing before the first CS presentation during the recall protocol than the wildtype rats, indicating higher baseline levels of anxiety in the SG genotype. Finally, there is a significant difference in the extinction index and overall modulation index between the genotypes; for the modulation index, this significant difference is present during the early CS presentations (CS 1-3) but has diminished during the late CS presentations (CS 8-10). This replicates the modulation index disparity found between the non-implanted SG and WT animals in our lab's previous studies [41].

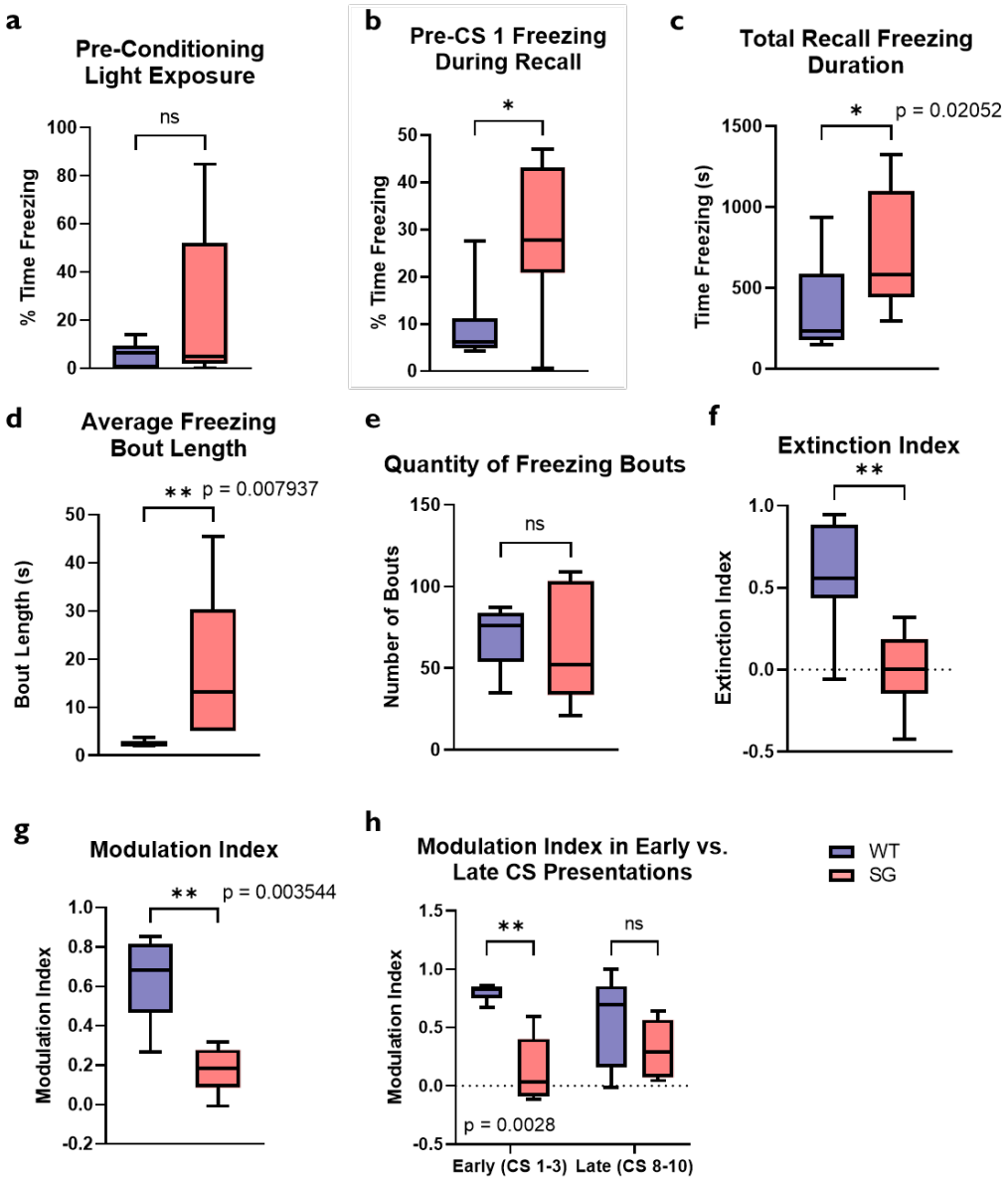

Figure 9 - Overview of Differences in Freezing Behaviour between Implanted SG and WT Rats during the Recall Stage of Fear Conditioning:

Detailed behaviour comparison for implanted (WT, n = 10, SG, n = 8) rats during the recall stage of the fear conditioning protocol. ***Detailed statistical analysis, including tests for normality and full T test/Mann-Whitney test results, can be found in Appendix I: Supplementary Statistics.***

(a) Pre-Conditioning Exposure Baseline: *Percentage of time freezing during CS exposure prior to conditioning. No significant difference (p = 0.7944) was found between the genotypes.*

(b) Pre-CS 1 Freezing: *SG rats exhibited significantly greater freezing (p = 0.0401*) that the WT littermates before the first CS presentation.*

(c) Total Freezing Duration: *SG rats exhibited significantly greater total freezing time (p = 0.0205*) compared to WT rats.*

(d) Average Freezing Bout Duration: *SG rats had significantly longer freezing bout durations (p = 0.0079**) than WT rats.*

(e) Quantity of Freezing Bouts: *No significant difference (p = 0.8002) in the number of freezing bouts between genotypes.*

(f) Overall Extinction Index: *The extinction index [(total time freezing during CS 8-10 – total time freezing during CS 1-3)/(total time freezing during CS 8-10 + total time freezing during CS 1-3)] was calculated for each rat. WT rats had significantly higher extinction indexes (p = 0.0012**, t = 4.062, df = 16) than SG rats.*

(g) Overall Modulation Index: *The modulation index [(total time freezing during CS presentations – total time freezing between CS presentations)/(total time freezing)] was calculated for each rat across all CS presentations. SG rats had significantly different modulation indexes (p = 0.0035**, t = 4.078, df = 16) compared to WT rats.*

(h) Early vs. Late Modulation Indexes: *The modulation index was calculated for each rat across early (CS 1-3) and late (CS 8-10) CS presentations Genotype had a significant effect on modulation index (p = 0.0030**) during early CS presentations.*

See 'Appendix I: Supplementary Statistics' for the full statistical analysis of this figure.

Figure 10 compares the extinction and modulation indexes between the non-implanted and implanted rats of each genotype. There were no significant differences between any of the pairings, further confirming that the behavioural phenotype is consistent despite the varying conditions of this experiment due to the surgical interventions and necessary amendments to the protocol.

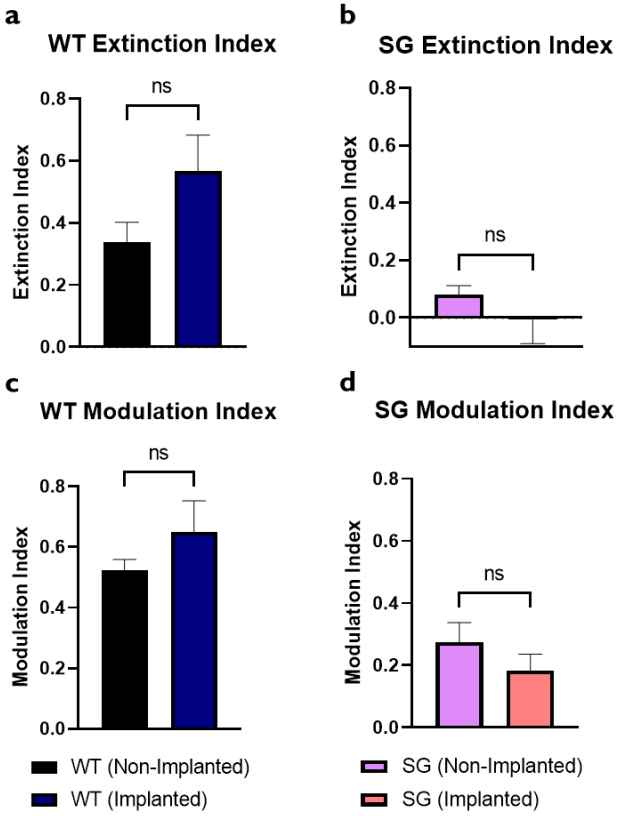

Figure 10 - Overview of Extinction and Modulation during Recall, Non-Implanted versus Implanted Rats:

(a-b) WT and SG Extinction Indexes, Non-Implanted versus Implanted Rats. *Both comparisons passed a Shapiro-Wilk test for normality. An unpaired, two-tailed T test was conducted for both comparisons, and no significant differences (WT: p = 0.0761, t = 1.882, df = 20; SG: p = 0.2711, t = 1.137, df = 17) were found.*

(c-d) WT and SG Overall Modulation Indexes, Non-Implanted versus Implanted Rats. *Both comparisons passed a Shapiro-Wilk test for normality. An unpaired, two-tailed T test was conducted for both comparisons, and no significant differences (WT: p = 0.1515, t = 1.511, df = 20; SG: p = 0.3745, t = 0.9174, df = 17) were found.*

6.2 Verification of Electrophysiological Recordings and Analysis

6.2.1 Raw Traces and Spectrograms

An example of a raw trace is depicted in Figure 5, but for verification of the quality of the electrophysiological recordings, additional representative traces and spectrograms are shown for both a wildtype and *Syngap*$^{+/\Delta GAP}$ rat in **Figure 11**. These traces and spectrograms were generated from the raw electrophysiological data in NeuroExplorer, using the same windowing methodology described in Section 5.5.3 (no window pre-processing before FFT, Hann windowing function, Gaussian smoothing).

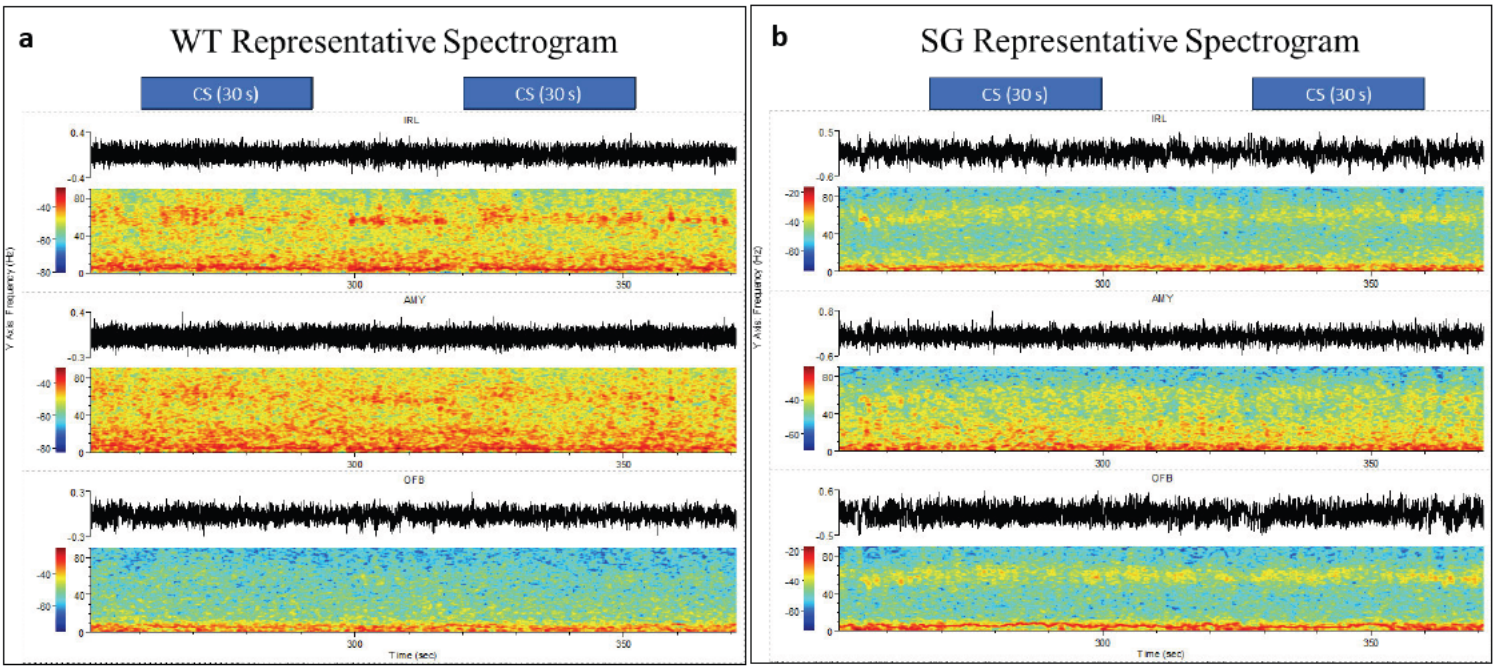

Figure 11 – Representative Spectrograms and Traces for a WT and SG Rat:

(a) WT Representative Spectrogram. *A spectrogram generated by NeuroExplorer for Rat 1021 (WT). The raw neural traces are aligned above the respective spectrogram. The CS presentations shown are CS 6 and 7.*

(b) SG Representative Spectrogram. *A spectrogram generated by NeuroExplorer for Rat 1020 (SG). The raw neural traces are aligned above the respective spectrogram. The CS presentations shown are CS 6 and 7.*

As shown in the spectrograms above, most rats displayed increased frequency within the range of approximately 40 to 60 Hz. These findings are justified in the subsequent power and coherence analysis, but first we had to verify that the increase in activity was not due to mains interference (in Europe, the standard voltage is 220V and the electrical grid runs at 50

Hz, so noise generally presents as a spike in the power spectra around 50 Hz.) In the following section, the continuous power spectra and coherence spectra for the representative rats are compared to their outputs from the MATLAB electrophysiological pipeline; this serves two purposes, both to verify that noise from mains interference is not interfering with the signal, and to confirm that the MATLAB scripts are calculating the power and coherence correctly.

6.2.2 Verification of MATLAB Electrophysiological Pipeline

Figure 12 compares the raw power spectra generated by NeuroExplorer with the MATLAB-plotted power spectra. No noise spikes are present around 50 Hz for either the representative wildtype or *Syngap*$^{+/\Delta GAP}$ rat, and the output of both methodologies are the same. This shows that the MATLAB electrophysiological pipeline is reading, sorting, scoring, and calculating the correct power values for the raw electrophysiological input. Further, it shows that the electrode alignment script is working, and the correct channels are assigned to the appropriate corresponding brain regions.

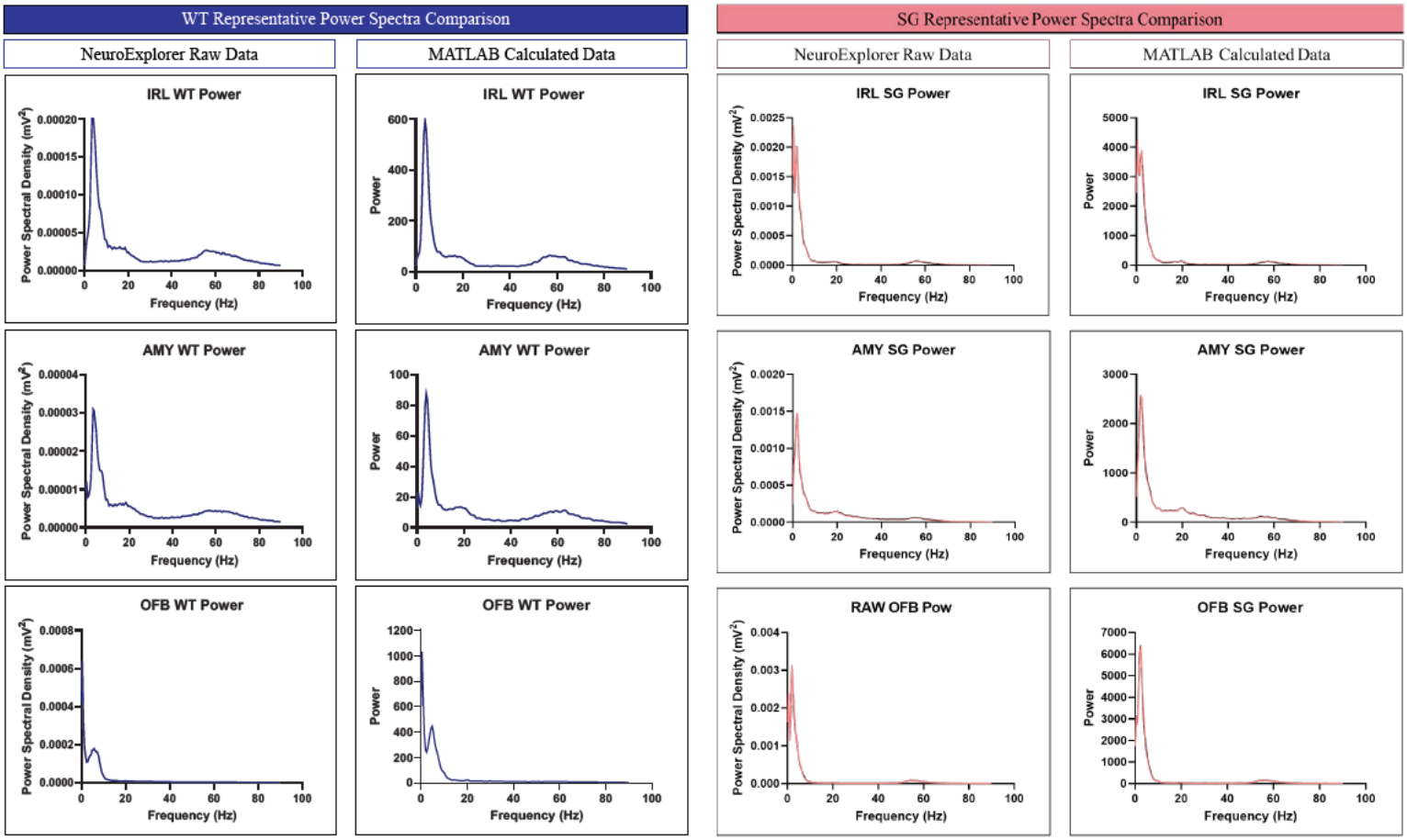

Figure 12 – Comparison of Power Spectra: NeuroExplorer Raw Data and MATLAB Electrphysiology Pipeline Generated Data

(a) WT Representative Power Data Comparison. *The left column displays raw traces for the three regions of interest (IRL, AMY, and OFB) generated by NeuroExplorer, and the right column displays the same trace generated by the MATLAB electrphysiology pipeline. Traces are equivalent from both programmes.*

(b) SG Representative Power Data Comparison. *The left column displays raw traces for the three regions of interest (IRL, AMY, and OFB) generated by NeuroExplorer, and the right column displays the same trace generated by the MATLAB electrphysiology pipeline. Traces are equivalent from both programmes.*

For consistency, this verification test was replicated for the continuous coherence spectra. As illustrated in **Figure 13**, the NeuroExplorer raw coherence spectra and MATLAB coherence spectra are roughly equivalent. This ensures that the coherence calculation scripts are calculating values correctly, and verifies that the subsequent analysis (all carried out via MATLAB) is correct.

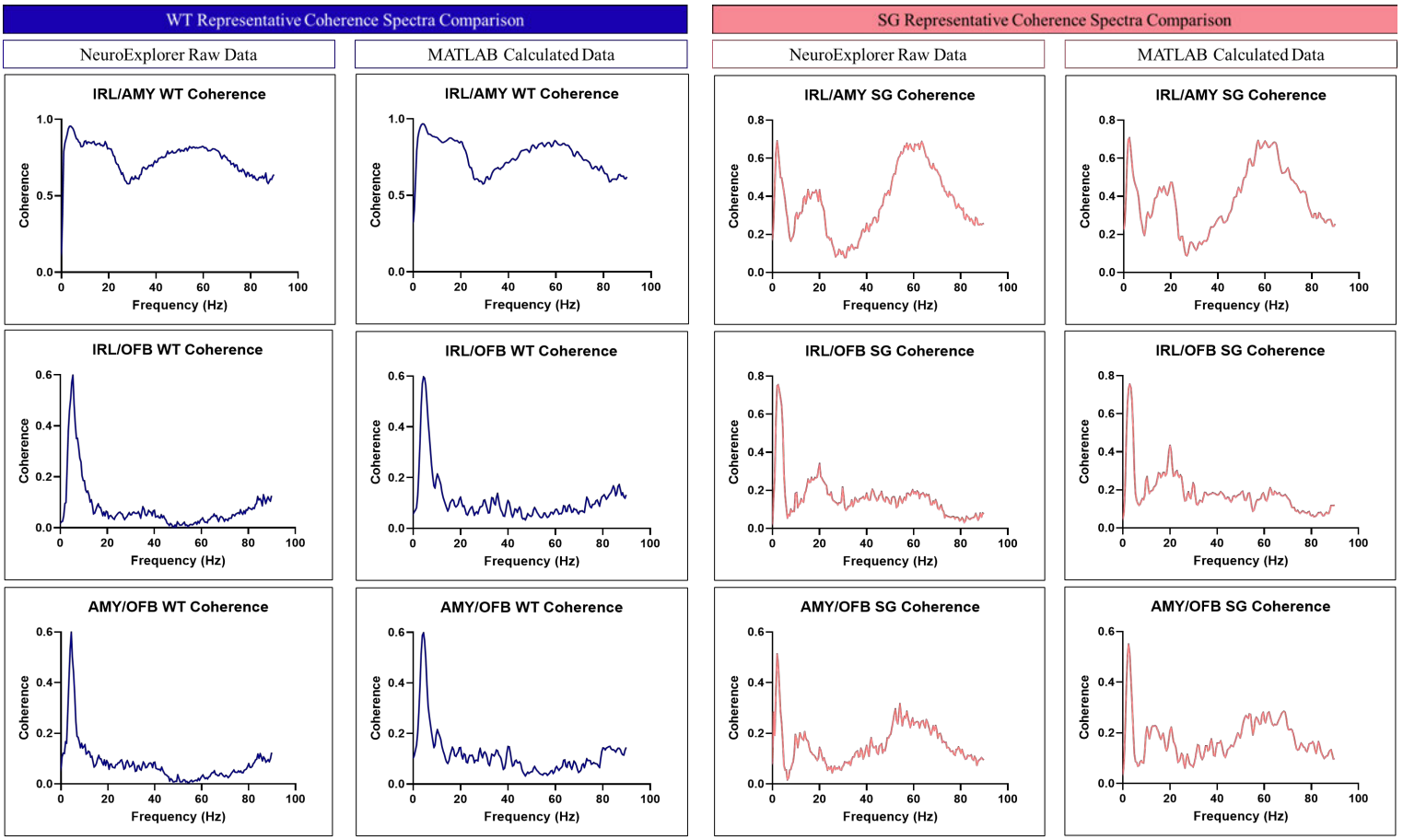

Figure 13 - Comparison of Coherence Spectra: NeuroExplorer Raw Data and MATLAB Electrphysiology Pipeline Generated Data

(a) WT Representative Coherence Data Comparison. *The left column displays raw traces for the three regions of interest (IRL, AMY, and OFB) generated by NeuroExplorer, and the right column displays the same trace generated by the MATLAB electrphysiology pipeline. Traces are equivalent from both programmes.*

(b) SG Representative Coherence Data Comparison. *The left column displays raw traces for the three regions of interest (IRL, AMY, and OFB) generated by NeuroExplorer, and the right column displays the same trace generated by the MATLAB electrphysiology pipeline. Traces are equivalent from both programmes.*

6.3 Power Variances Between Groups

6.3.1 Using Power to Verify Processing of CS

Prior to attempting to explain the behavioural variances between the wildtype and *Syngap*$^{+/\Delta GAP}$ rats, I had to validate that the behavioural difference could not be explained by a visual processing error that prevented either genotype from properly processing the visual CS (a flashing blue LED). This was validated using an LFP electrode implanted in the superior colliculus, which is well-documented as having higher power during the presentation of visual stimuli [45-46].

Figure 14 outlines the results of this control. Both the SG and WT rats displayed a significant difference in superior colliculus power during versus between the CS presentations, with a significantly higher amount of power during the CS presentations. This verifies that both genotypes can visually process and understand the visual stimulus used in this study.

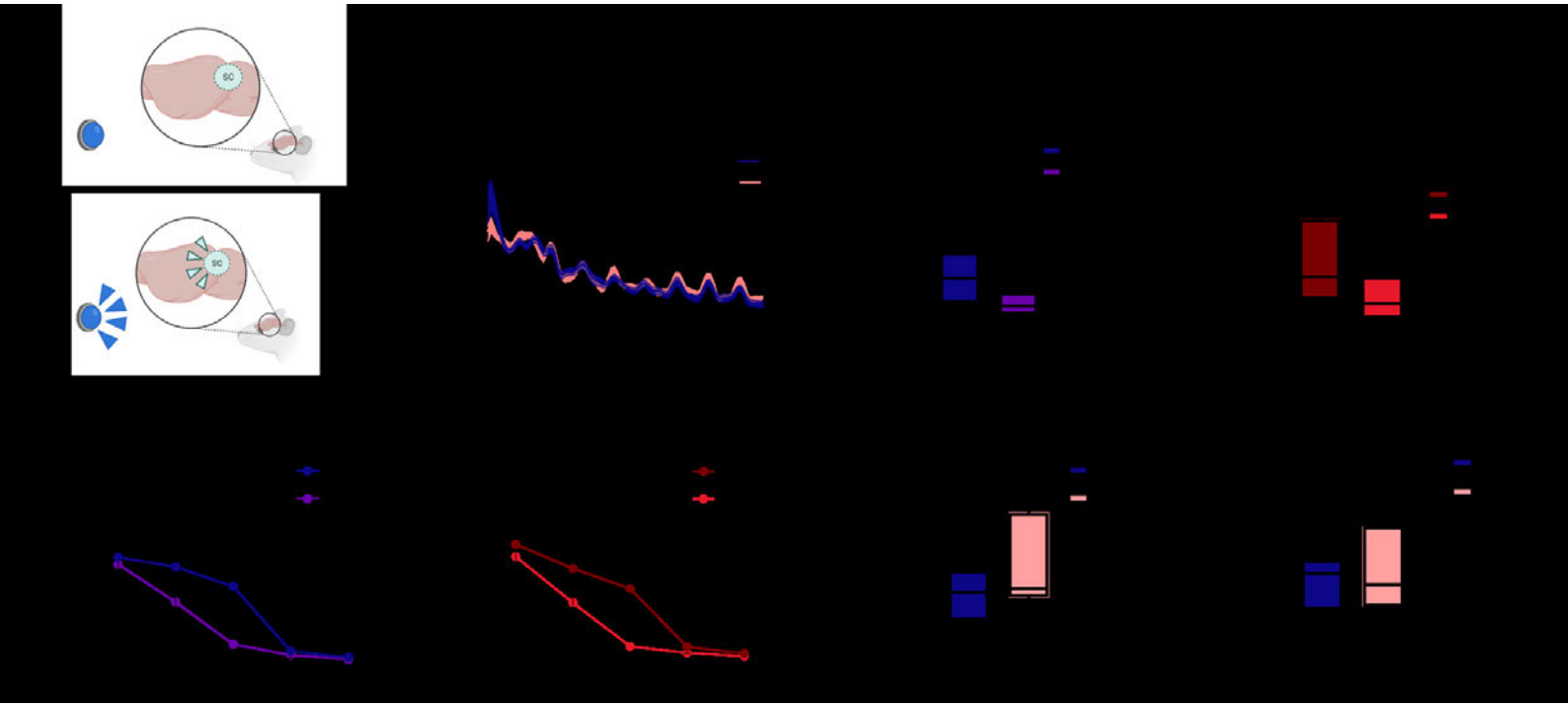

Figure 14 – Superior Colliculus Control for Verification of Visual Processing:

An overview of WT (n = 10) and SG (n = 8) superior colliculus power throughout the recall protocol, used here as a verification measure of the genotype's ability to process the visual conditioned stimulus. ***Detailed statistical analysis, including tests for normality and full ANOVA results, can be found in Appendix I: Supplementary Statistics.***

(a) Superior Colliculus Control Schematic. *Visual representation of how superior colliculus control functions. When the blue LED light flashes (the "CS"), the superior colliculus has an increase in power.*

(b) Superior Colliculus Power Spectra. *A two-way ANOVA (WT, n = 10; SG, n = 8) examined the impact of genotype and frequency on power. No significant genotype differences were found.*

(c) WT Superior Colliculus Theta Power. *Significant differences in WT power during versus between CS presentations indicate visual CS processing ability (p = 0.0067**, t = 3.498, df = 9).*

(d) SG Superior Colliculus Theta Power. *Significant differences in SG power during versus between CS presentations indicate visual CS processing ability ($p = 0.0320$*, $t = 2.592$, $df = 7$).*

(e) Overview of Superior Colliculus Power Across All Frequencies, WT and SG. *Error bars: mean ± SEM.*

(f) Superior Colliculus Theta Power During CS. *There was no significant difference between the genotypes' power during CS presentation, indicating both genotypes were able to process the visual CS to the same degree. The data did not have a normal distribution following a Shapiro-Wilk test (WT, $p = 0.0871$, $W = 0.8649$; SG, $p = 0.0464$*, $W = 0.8198$). A Mann-Whitney test was performed ($p = 0.6334$), and no significant difference was found.*

(g) Superior Colliculus Theta Power Between CS. *There was no significant difference between the genotypes' power between CS presentation, indicating both genotypes were able to process the visual CS to the same degree. The data had a normal distribution following a Shapiro-Wilk test (WT, $p = 0.1860$, $W = 0.4740$; SG, $p = 0.1309$, $W = 0.5145$). An unpaired, two-tailed T test was performed ($p = 0.4865$, $t = 0.7124$, $df = 16$), and no significant difference was found.*

See 'Appendix I: Supplementary Statistics' for the full statistical analysis of this figure.

6.3.2 Power Variances Defined by Global CS Presentations

Aim 2 sought to analyse power across the target structures, namely the infralimbic cortex (IRL), the amygdala (AMY) and the olfactory bulb (OFB). Ultimately, I was investigating whether any attributes of power could be used as a biomarker to explain the mechanism behind the SG and WT rats' behavioural differences during extinction learning.

Figure 15 provides an overview of the power spectra between SG and WT rats during global CS presentations – that is, all CS presentations averaged together. As shown in **Figure 15**, power is difficult to view on a linear scale due to its exponential nature. Therefore, power will be displayed on a logarithmic scale throughout the results of this thesis; it is important to note, however, that all analyses were conducted on the raw power values and not the transformed values displayed on the following graphs, as is common convention.

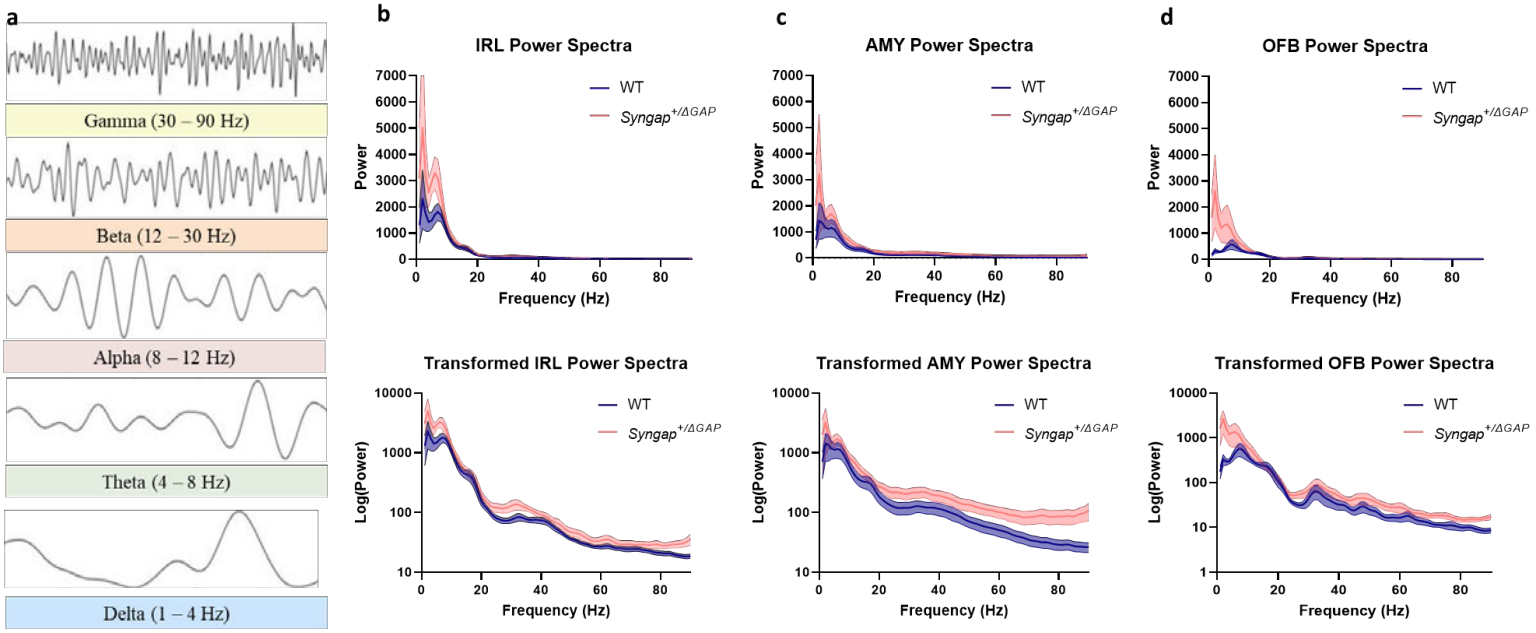

Figure 15 – Overview of Global Power across Recall Protocol:

Power spectra for WT (n = 10) and SG (n = 8) rats across recall protocol. The conversion of the power spectra from a numeric to a logarithmic scale is shown for clarity. For all presented spectra, a two-way ANOVA was performed to analyse the effect of genotype and frequency on power, and Bonferroni's multiple comparisons tests was used to test for significant differences between the genotypes. Across all three regions of interest, Bonferroni's multiple comparisons test found no differences between WT and SG rats.

(a) Illustration and range of frequency bands. *The custom software package developed for coherence and power analysis allowed the user to define the frequencies for each band. This analysis was conducted using common values from the literature: Delta (1 – 4 Hz), Theta (4 – 8 Hz), Alpha (8 – 12 Hz), Beta (12 – 30 Hz), and Gamma (30 – 90 Hz). Example brain waves were created in Biorender.*

(b) IRL power spectra and transformed power spectra. *An interaction between genotype and frequency was found to be statistically significant (F(DFn, DFd) = 1.356, p = 0.0178*). Frequency had a highly significant effect on power (p = 0.0007***), while genotype did not (p = 0.0704).*

(c) AMY power spectra and transformed power spectra. *An interaction between genotype and frequency was found to not have statistical significance (F(DFn, DFd) = 0.5652, p = 0.9996). Frequency had a significant effect on power (p = 0.0102*), but genotype did not (p = 0.0755).*

(d) OFB power spectra and transformed power spectra. *An interaction between genotype and frequency was found to be highly significant (F(DFn, DFd) = 2.653, p < 0.0001****). Both frequency (p = 0.0037**) and genotype (p = 0.0369*) had significant effects on power.*

See 'Appendix I: Supplementary Statistics' for the full statistical analysis of this figure.

Across all three brain regions, no significant difference was found between the genotypes after statistical corrections for multiple comparisons (Bonferroni's multiple comparisons test). However, it is important to remember that these spectra display power across the entire recall protocol. **Figure 16** repeats this analysis for each brain region by comparing power during versus between CS presentations, and by conducting the two-way ANOVA across the literature-defined frequency bands rather than counting each individual frequency as its own group. With this analysis approach, significant differences are found in the gamma frequency band of both the IRL and the OFB. Comparisons are displayed in Figure 16 as box and whisker plots rather than power spectra to better represent the significant differences visually.

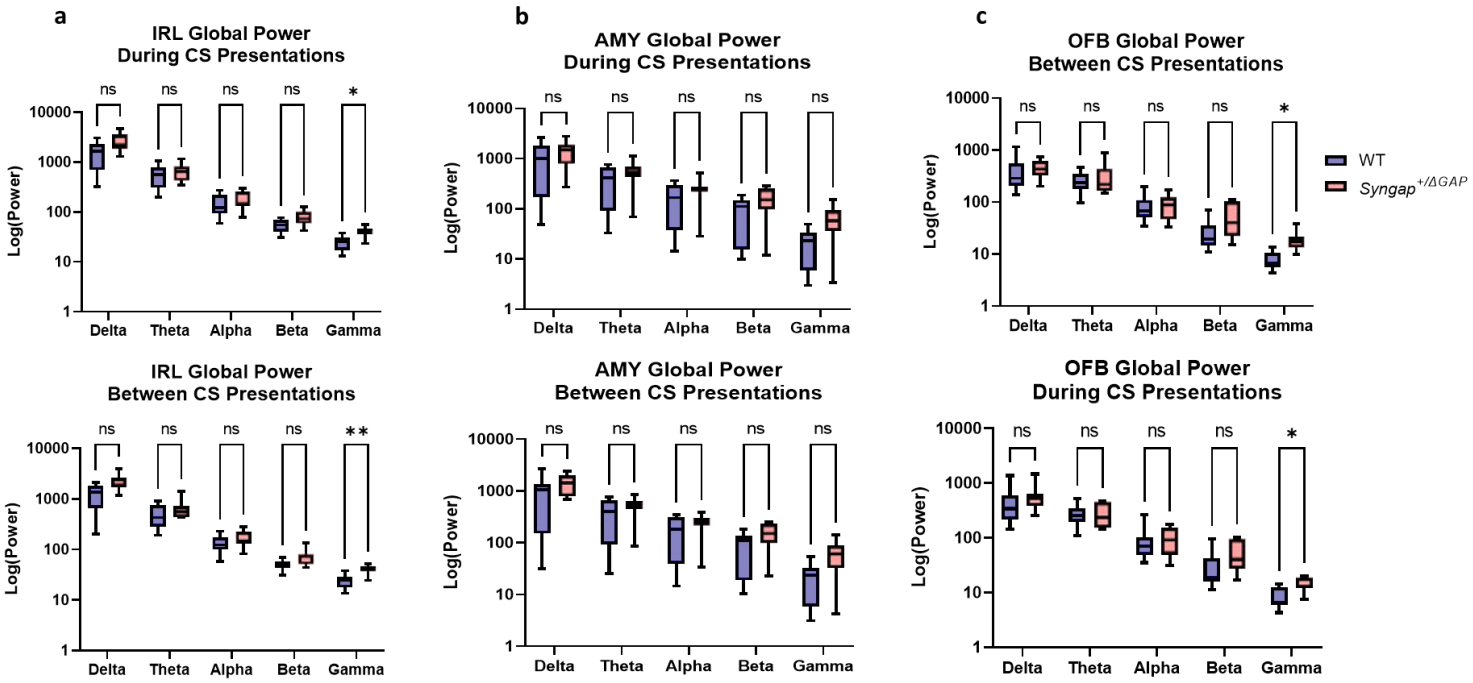

Figure 16 – Overview of Global Power Across Recall Protocol, During versus Between CS Presentations:

Power for WT (n = 10) and SG (n = 8) rats during versus between CS presentations, calculated by frequency band. For all presented graphs, a two-way ANOVA was performed to analyse the effect of genotype and frequency on power, and Bonferroni's multiple comparisons test was used to test for significant differences between the genotypes. Differences between the WT and SG rats were found in the gamma band of the IRL and OFB.

(a) IRL global power, during versus between CS presentations. *During CS: An interaction between genotype and frequency was found to be statistically significant (F(DFn, DFd) = 4.677, p = 0.0024**). Frequency had a highly significant effect on power (p < 0.0001****), while genotype did not (p = 0.0696). Bonferroni's multiple comparisons test revealed a significant difference between the genotypes in the gamma band (p = 0.0180*, t = 3.644, DF = 11.43). Between CS: An interaction between genotype and frequency was found to be statistically significant (F(DFn, DFd) = 5.403, p = 0.0009***). Both frequency (p < 0.0001****) and genotype (p = 0.0450*) had significant effects on power. Bonferroni's multiple comparisons test revealed a significant difference between the genotypes in the gamma band (p = 0.0094**, t = 3.958, DF = 12.02).*

(b) AMY global power, during versus between CS presentations. *During CS: An interaction between genotype and frequency was found to not have statistical significance (F(DFn, DFd) = 0.6933, p = 0.5994). Frequency had a highly significant effect on power (p < 0.0001****), while genotype did not (p = 0.2512). Bonferroni's multiple comparisons test revealed no significant differences between genotypes. Between CS: An interaction between genotype and frequency was found to not have statistical significance (F(DFn, DFd) = 1.452, p = 0.2272). Frequency had a highly significant effect on power (p < 0.0001****), while genotype did not (p = 0.1778). Bonferroni's multiple comparisons test revealed no significant differences between genotypes.*

(c) OFB global power, during versus between CS presentations. *During CS: An interaction between genotype and frequency was found to not have statistical significance (F(DFn, DFd) = 0.5772, p = 0.6802). Frequency had a highly significant effect on power (p < 0.0001****), while genotype did not (p = 0.4300). Bonferroni's multiple comparisons test revealed a significant difference between the genotypes in the gamma band (p = 0.0344*, t = 3.325, DF = 10.86). Between CS: An interaction between genotype and frequency was found to not have statistical significance (F(DFn, DFd) = 1.437, p = 0.2320). Frequency had a significant effect on power (p = 0.0145*), while genotype did not (p = 0.2289). Bonferroni's multiple comparisons test revealed a significant difference between the genotypes in the gamma band (p = 0.0350*, t = 3.508, DF = 8.627).*

As illustrated in Figure 16, significant differences between the genotypes are only found in the gamma frequency band of the IRL and OFB. These significant differences persist across the protocol (both during and between CS presentations), although it is worthwhile to note that the significant difference between wildtype and *Syngap*$^{+/\Delta GAP}$ rats is greater between CS presentations than during CS presentations. This is important because behaviour between the genotypes varies more during the inter-CS intervals than the CS presentations.

The significant differences in Figure 16 are shown in greater detail in **Figure 17**, along with their associated power spectra.

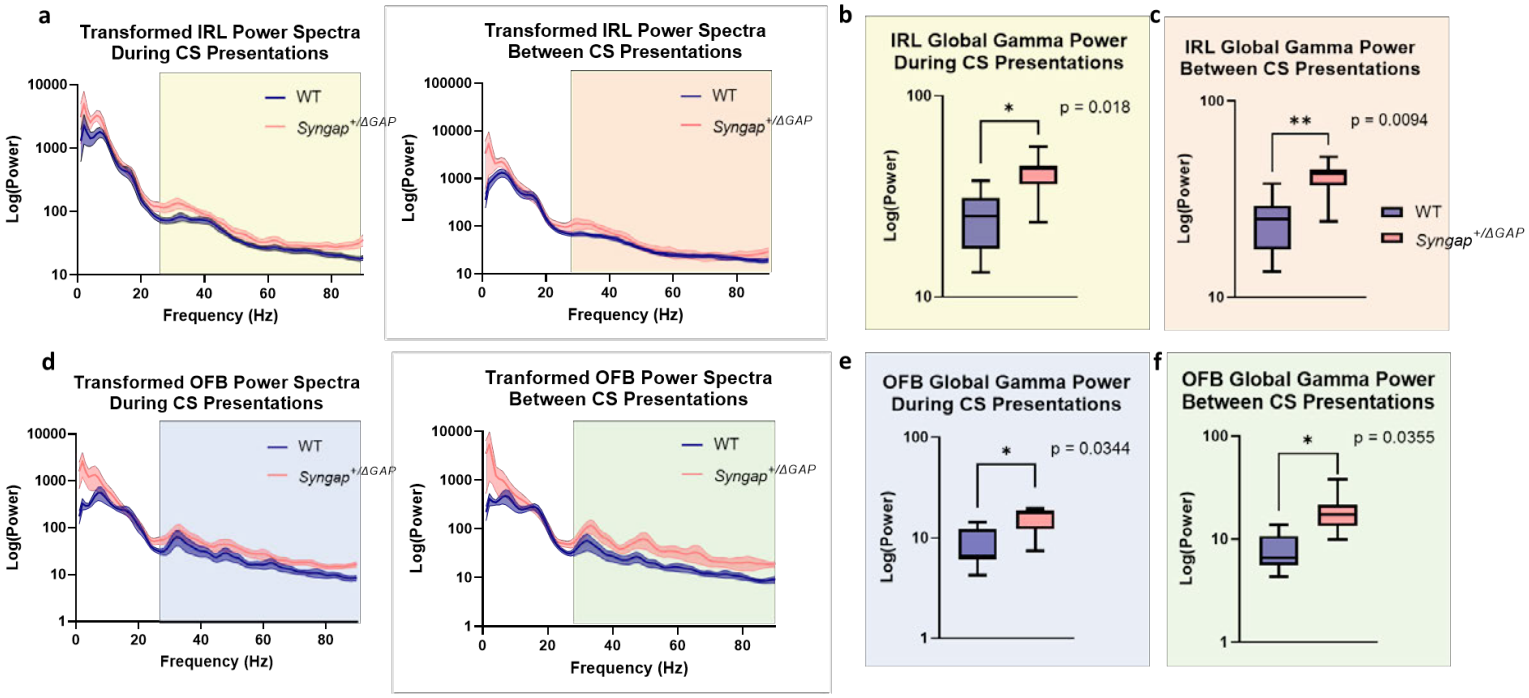

Figure 17 – Overview of Significant Differences in Global Power Across Recall Protocol, During versus Between CS Presentations:

(a) IRL global power spectra during versus between CS presentations. *Power spectra for IRL during versus between CS presentations. ANOVA results can be found in Figure 16 (a).*

(b-c) IRL global gamma power comparisons during and between CS presentations. *Magnified view of genotypic differences in the gamma frequency band. Results from Bonferroni's multiple comparisons test can be found in Figure 16 (a).*

dc) OFB global power spectra during versus between CS presentations. *Power spectra for OFB during versus between CS presentations. ANOVA results can be found in Figure 16 (c).*

(e-f) OFB global gamma power comparisons during versus between CS presentations. *Magnified view of genotypic differences in the gamma frequency band. Results from Bonferroni's multiple comparisons test can be found in Figure 16 (c).*

While these significant genotypic differences may begin to explain some of the behavioural variances between the wildtype and *Syngap*$^{+/\Delta GAP}$ rats, it is important to note that the above

analyses were computed on a global scale; that is, all power across the entire recall paradigm was used in the calculation. Because behaviour varies on a temporal scale, it is important to repeat this analysis where behaviour deviates (early CS presentations 1-3) and eventually realigns (late CS presentations 8-10). The results of this temporal analysis are outlined in Section 6.3.3.

6.3.3 Power Variances defined by Temporal CS Presentations

As exhibited in Figure 8, rat freezing behaviour changes throughout the CS presentations. Extinction learning happens more quickly in the wildtype rats, who quickly unlearn the association of the CS and US; therefore, they stop freezing behaviour (CR) fairly early in the fear recall protocol. By contrast, the *Syngap*$^{+/\Delta GAP}$ rats struggle to unlearn this association; this causes an extinction learning deficit and deviates their behaviour from their WT counterparts. Therefore, to better understand changes in behaviour throughout the recall paradigm (and to try to determine if power could be an underlying mechanism of this deficit), the power analysis described in Section 6.3.2 was repeated by analysing early (CS presentations 1-3) versus late (CS presentations 8-10) bouts of power.

To begin, power in each region and freezing times were calculated and scored across eight distinct groups: WT (During CS 1-3), WT (During CS 8-10), *Syngap*$^{+/\Delta GAP}$ (During CS 1-3), *Syngap*$^{+/\Delta GAP}$ (During CS 8-10), WT (Between CS 1-3), WT (Between CS 8-10), *Syngap*$^{+/\Delta GAP}$ (Between CS 1-3), and *Syngap*$^{+/\Delta GAP}$ (Between CS 8-10). A two-way ANOVA was conducted across all these groups and all frequency bands, although the results are difficult to depict graphically. Therefore, the analysis was completed with a more reader-friendly approach, which is outlined below. It is important to note that the results were consistent with both statistical testing methodologies. To simplify this analysis, I first tested whether either genotype displayed a significant difference in power during versus between CS presentations; if no significant differences were observed, then these timepoints could be collapsed and later compared in early versus late timepoints of the recall protocol. **Figure 18** outlines this initial comparison; for both WT and SG rats, there were no significant differences in power during versus between early and late CS presentations.

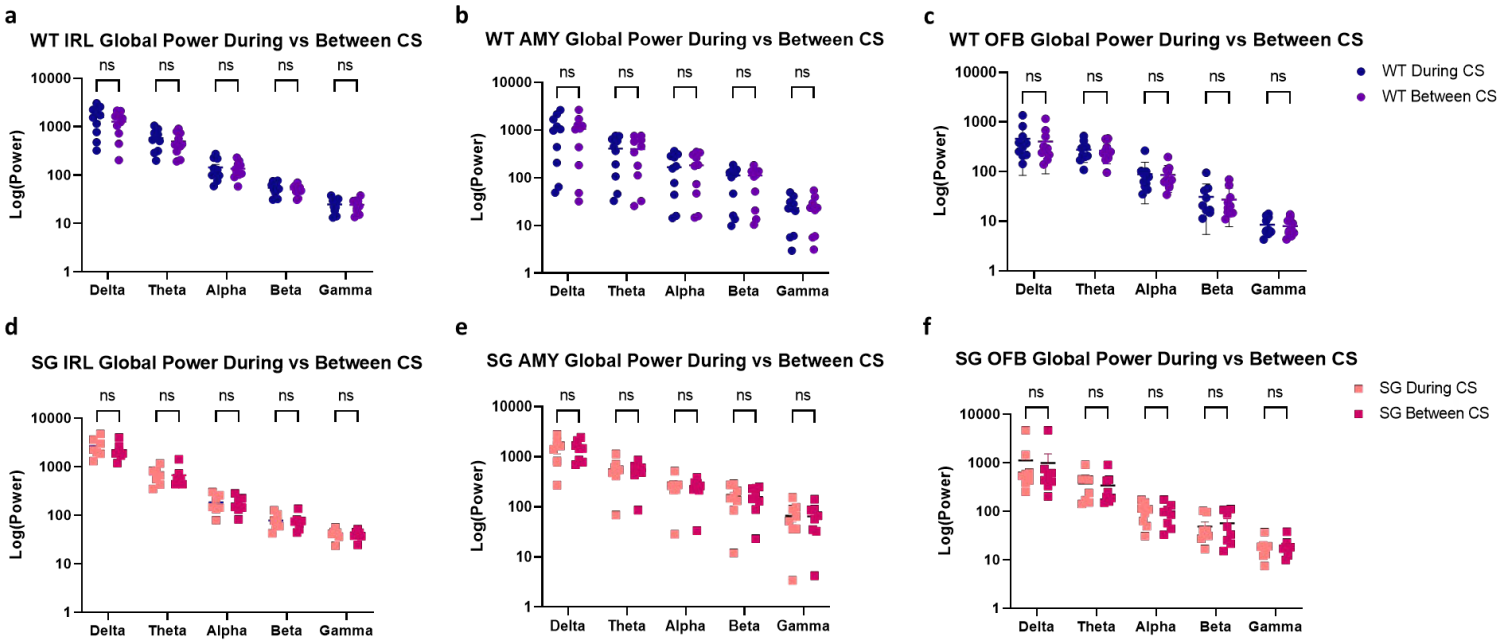

Figure 18 – Overview of Global Power Across Recall, During versus Between Combined Early and Late CS presentations, per Genotype:

Interleaved scatter plots, mean with SEM, for power during versus between CS by genotype. A two-way ANOVA was performed across all plots, and Bonferroni's multiple comparisons test was used to identify significant differences during versus between CS presentations. No significant differences were found for WT (n = 10) or SG (n = 8) rats. ***Detailed statistical analysis, including full ANOVA results, can be found in Appendix I: Supplementary Statistics.***

(a – f) All groupings. *Bonferroni's multiple comparisons test revealed no significant differences during versus between CS presentation power in any frequency bands.*

As no significant differences were found depending on CS presence, power was recalculated for CS presentations by collapsing these two timepoints. Therefore, in the subsequent analysis, the notation "CS 1" includes both the 30s duration of the CS presentation and the following 30s inter-CS interval.

Figure 19 investigates whether either genotype displays a significant difference in power between early (CS 1-3) and late (CS 8-10) CS presentations. As with all presented figures, each dataset underwent a Shapiro-Wilk test for normality, and appropriate subsequent statistical analysis was applied. Neither genotype displayed significant differences in early versus late power, except for the WT rats in the alpha band of the amygdala.

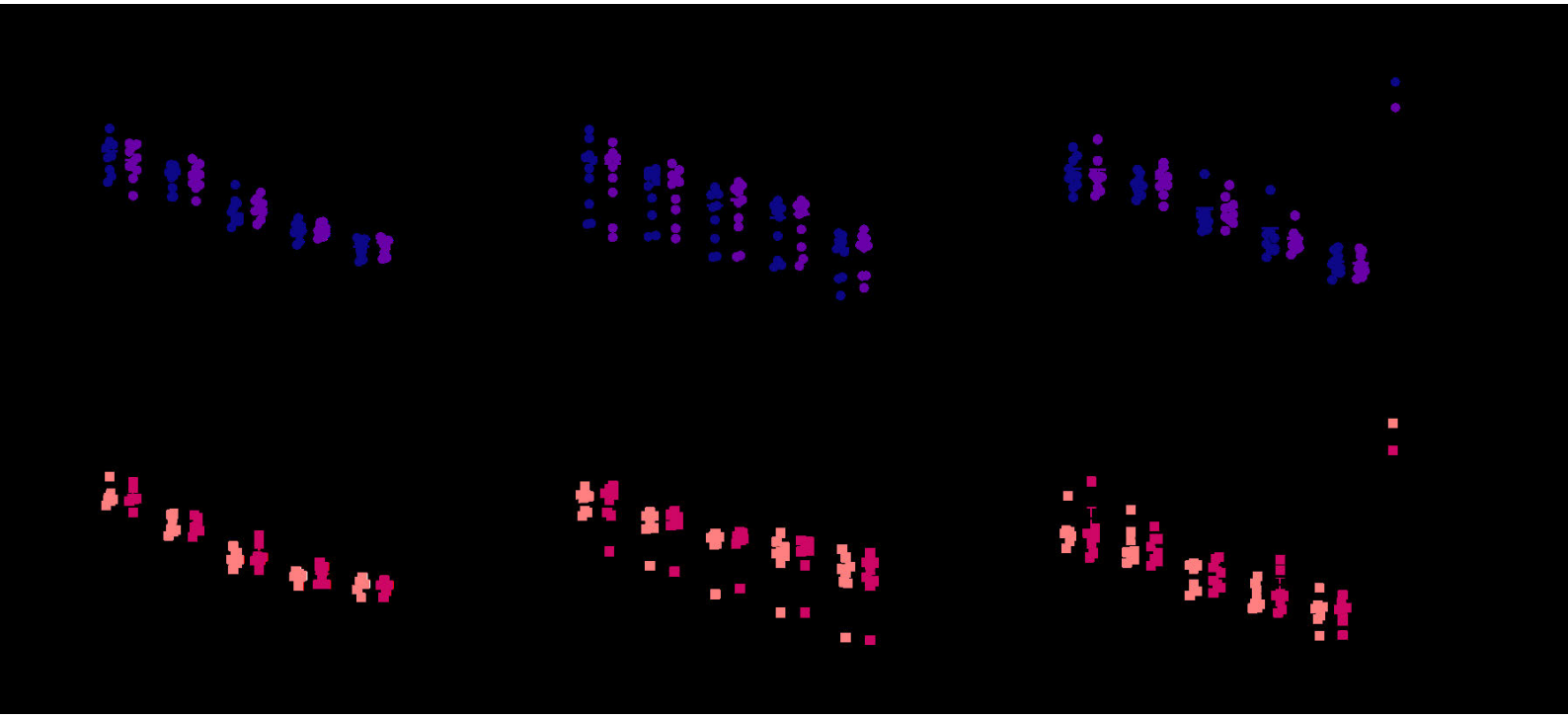

Figure 19 – Overview of Early versus Late Recall Power, per Genotype:

Interleaved scatter plots, mean with SEM, for power during early (CS 1-3) versus late (CS 8-10) CS presentations by genotype. A two-way ANOVA was performed across all plots, and Bonferroni's multiple comparisons test was used to identify significant differences during versus between CS presentations. No significant differences were found for WT (n = 10) or SG (n = 8) rats, except in the alpha band of the WT AMY. ***Detailed statistical analysis, including full ANOVA results, can be found in Appendix I: Supplementary Statistics.***

(b) WT AMY Power, early versus late CS presentations. *Bonferroni's multiple comparisons test revealed significant differences between early versus late power in the alpha frequency band (p = 0.0195*).*

(a, c – f) All other groupings. *Bonferroni's multiple comparisons test revealed no significant differences between early versus late CS coherence in any frequency bands.*

Finally, early vs late power was compared across genotypes. **Figure 20** shows the results of this comparison; significant differences between the power of the genotypes was only found in the gamma frequency band of the IRL after statistical corrections for multiple comparisons.

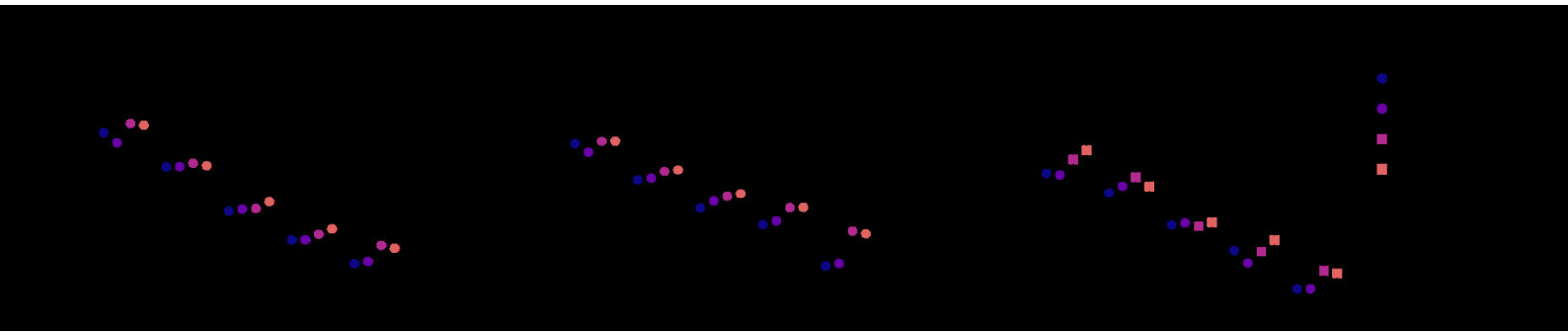

Figure 20 - Overview of Power Epochs (Early versus Late CS Presentations):

A two-way ANOVA was performed for each region, and Bonferroni's multiple comparisons test was used to identify significant differences between the groups. Significant differences were only found after corrections for multiple comparisons in the gamma band of the IRL. ***Detailed statistical analysis, including full ANOVA results, can be found in Appendix I: Supplementary Statistics.***

(a) IRL Power Epoch Comparison. *Bonferroni's multiple comparisons test revealed the following significant differences in the gamma band: WT Early vs SG Early (p = 0.0127*), WT Early vs SG Late (p = 0.0132*), WT Late vs SG Early (p = 0.0226), and WT Late vs SG Late (p = 0.0275*).*

(b-c) AMY and OFB Power Epoch Comparison. *Bonferroni's multiple comparisons test revealed no significant differences between any of the epoch groups.*

For validity testing, these results are consistent with the large ANOVA performed across all eight groups, when the timepoints during versus between CS presentations were kept separate instead of combined. The simplified ANOVA was shown here for ease of visualisation, although the full ANOVA produced the same significant results after corrections for multiple comparisons.

6.3.4 Power and Behaviour Correlations

While some significant differences were found in the prior analysis, no clear power biomarkers of freezing behaviour emerged. To investigate this further, power was correlated with freezing behaviour for both genotypes; it is important to note that correlation does not equate with causation, but some interesting results emerged, which are worth reporting in the main body of text. Additional correlation graphs not presented here will be included in Appendix II: Additional Figures.

Figure 21 outlines the correlation between behaviour and global gamma power for each genotype and brain region of interest. Gamma power was chosen due to being the frequency band with the most significant activity in the preceding power analysis. Pearson's correlation coefficient (r) was calculated for each graph, and p-values were calculated to test for significance. A significant positive correlation was only found in the WT OFB.

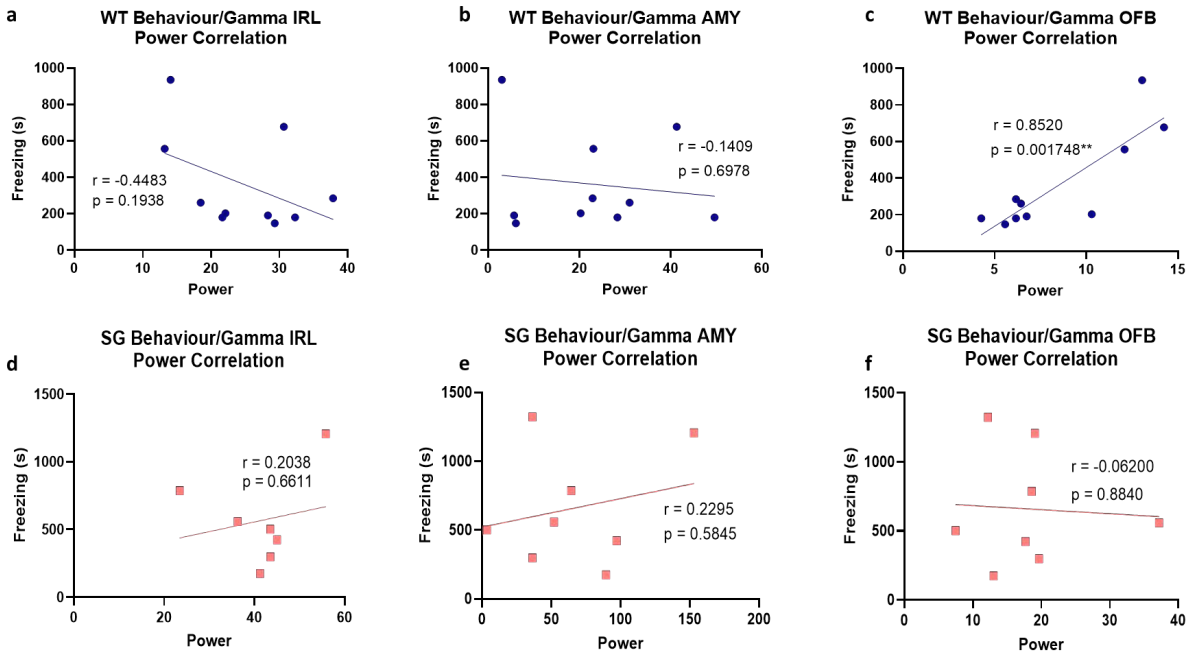

Figure 21 – Correlation between Freezing Behaviour and Gamma Power, across the Recall Protocol:

Correlation coefficients (Pearson's r) and p-values were calculated for each graph, representing the correlation between freezing times and gamma power in the brain regions for each genotype. The p-value indicates the statistical significance of the correlation coefficient (two-tailed test), and the coefficient of determination (R squared) represents the proportion of variability in freezing behaviour explained by gamma power.

(a-c) WT Behaviour and Gamma Power Correlations. *The only statistically significant correlation is illustrated in (c) OFB Power Correlation (p = 0.001748**, r = 0.8520).*

(d – f) SG Behaviour and Gamma Power Correlations. *There were no statistically significant correlations amongst any of the SG coherence pairs and behaviour.*

Figure 22 analyses the gamma frequency band of the OFB in more detail; for both WT and SG rats, power and behaviour are correlated for early and late timepoints, both during and between CS presentations. The WT rats always display a positive, statistically significant correlation, but the SG rats differ drastically. During CS 1-3, the SG rats have a statistically significant, negative correlation between behaviour and power. This negative correlation persists between CS 1-3, although it loses its significance during the inter-CS intervals. However, SG rats have a non-significant positive correlation between behaviour and OFB power during and between CS 8-10. This is an interesting observation as correlations align when the extinction deficit is no longer present, but causality cannot be assumed.

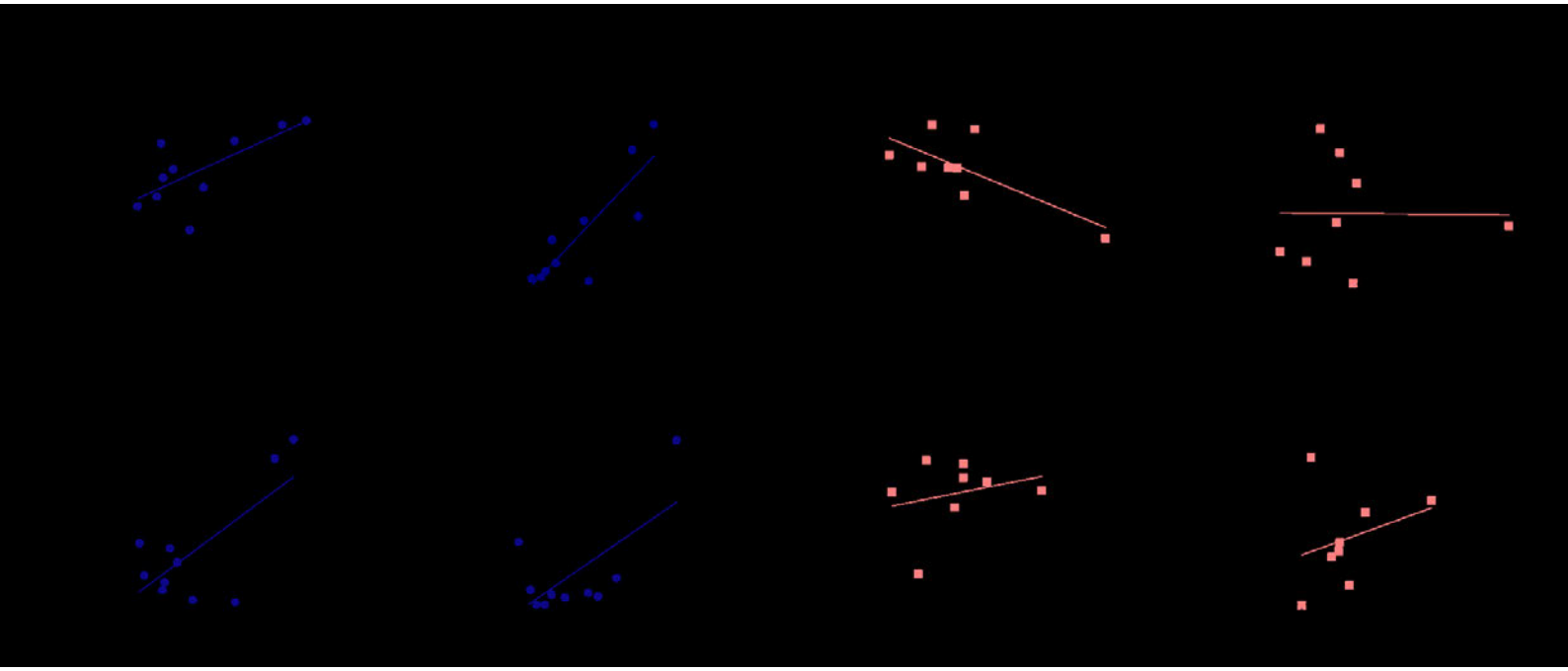

Figure 22 – Correlation between Freezing Behaviour and OFB Gamma Power, During Early versus Late CS Presentations:

Correlation coefficients (Pearson's r) and p-values were calculated for each graph, representing the correlation between freezing times and gamma power in the OFB for each genotype. The p-value indicates the statistical significance of the correlation coefficient (two-tailed test), and the coefficient of determination (R squared) represents the proportion of variability in freezing behaviour explained by gamma power.

(a) WT Behaviour and Gamma Power Correlations, During and Between Early CS 1-3. *A positive, statistically significant correlation between behaviour and gamma power is illustrated both during (p = 0.0220*, r = 0.7078) and between (p = 0.0017**, r = 0.8525) early CS presentations (CS 1-3).*

(b) SG Behaviour and Gamma Power Correlations, During and Between Early CS 1-3. *A negative, statistically significant correlation between behaviour and gamma power is illustrated during (p = 0.0392*, r = - 0.7315) but not between early CS presentations (CS 1-3).*

(c) WT Behaviour and Gamma Power Correlations, During and Between Late CS 8-10. *A positive, statistically significant correlation between behaviour and gamma power is illustrated both during (p = 0.0226*, r = 0.7058) and between (p = 0.0385*, r = 0.6583) late CS presentations (CS 8-10).*

(d) SG Behaviour and Gamma Power Correlations, During and Between Late CS 1-3. *A positive, non-significant correlation between behaviour and gamma power is illustrated both during and between late CS presentations (CS 8-10).*

In the next section, the above analysis will be replicated for coherence in the IRL, AMY, and OFB.

6.4 Coherence Variances Between Groups

6.4.1 Coherence Variances defined by Global CS Presentations

Aim 3 sought to analyse coherence across the target structures, namely the infralimbic cortex (IRL), the amygdala (AMY) and the olfactory bulb (OFB). As with power, I was investigating whether any attributes of coherence could be used as a biomarker to explain the mechanism behind the *Syngap*$^{+/\Delta GAP}$ and wildtype rats' behavioural difference during the recall stage of the fear conditioning paradigm.

Figure 23 provides an overview of the coherence spectra between SG and WT rats during global CS presentations – that is, all CS presentations averaged together. It is important to note that coherence is the synchrony in brain activity in two different brain areas and requires input from two brain regions to calculate. The pairings analysed here are as follows: IRL/AMY (infralimbic cortex and amygdala), IRL/OFB (infralimbic cortex and olfactory bulb) and AMY/OFB (amygdala and olfactory bulb). A two-way ANOVA was conducted on the coherence spectra below, and no significant differences between the genotypes were found.

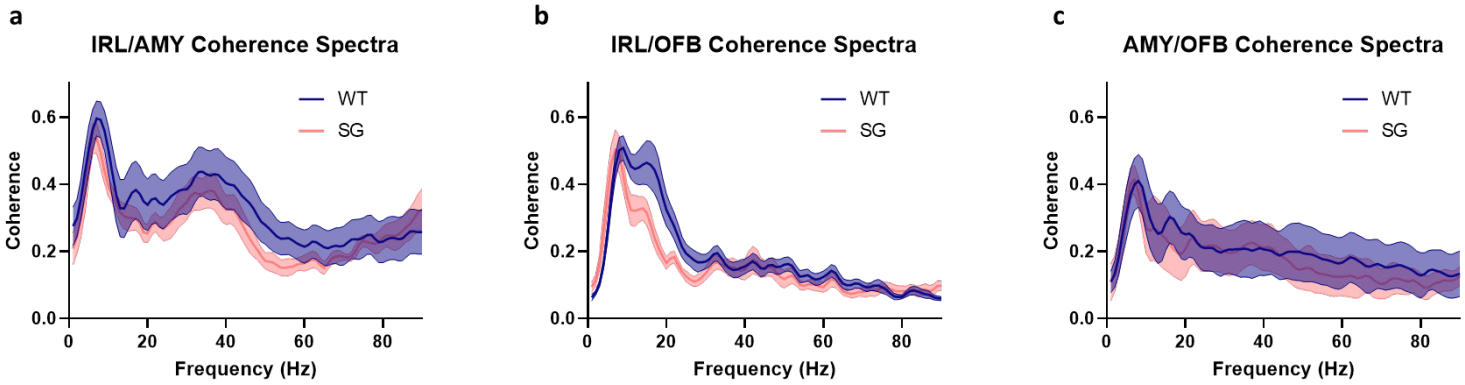

Figure 23 – Overview of Global Coherence across Recall Protocol:

Coherence spectra for WT (n = 10) and SG (n = 8) rats across recall protocol. For all presented spectra, a two-way ANOVA was performed to analyse the effect of genotype and frequency on coherence, and Bonferroni's multiple comparisons tests was used to test for significant differences between the genotypes. Across all three coherence pairings, no differences between WT and SG rats were found.

(a) IRL/AMY coherence spectra. *An interaction between genotype and frequency was found not to have statistical significance (F(DFn, DFd) = 0.9304, p = 0.6611). Frequency had a highly significant effect on coherence (p < 0.0001****), while genotype did not (p =0.4609).*

(b) IRL/OFB coherence spectra. *An interaction between genotype and frequency was found to have statistical significance (F(DFn, DFd) = 3.886, p < 0.0001****). Frequency had a highly significant effect on coherence (p < 0.0001****), while genotype did not (p =0.2406).*

(c) AMY/OFB coherence spectra. *An interaction between genotype and frequency was found not to have statistical significance (F(DFn, DFd) = 0.7705, p = 0.9424). Frequency had a highly significant effect on coherence (p < 0.0001****), while genotype did not (p =0.7959).*

As with the power analysis in Section 6.3, performing a two-way ANOVA across 90 Hz of frequency with a relatively small sample size (WT n = 10, SG n = 8) diminishes the power of the statistical coherence analysis. Put simply, using Bonferroni's multiple comparisons test to correct for ninety comparisons reduces power, and even with a low alpha ($\alpha = 0.05$), significance is often lost. Therefore, the two-way ANOVA was repeated across the same five frequency bands, and each group was compared against one another. Those results, both during and between CS presentations, are outlined in **Figure 24**. Unlike power, no significant differences were found between the genotypes across any of the frequency bands.

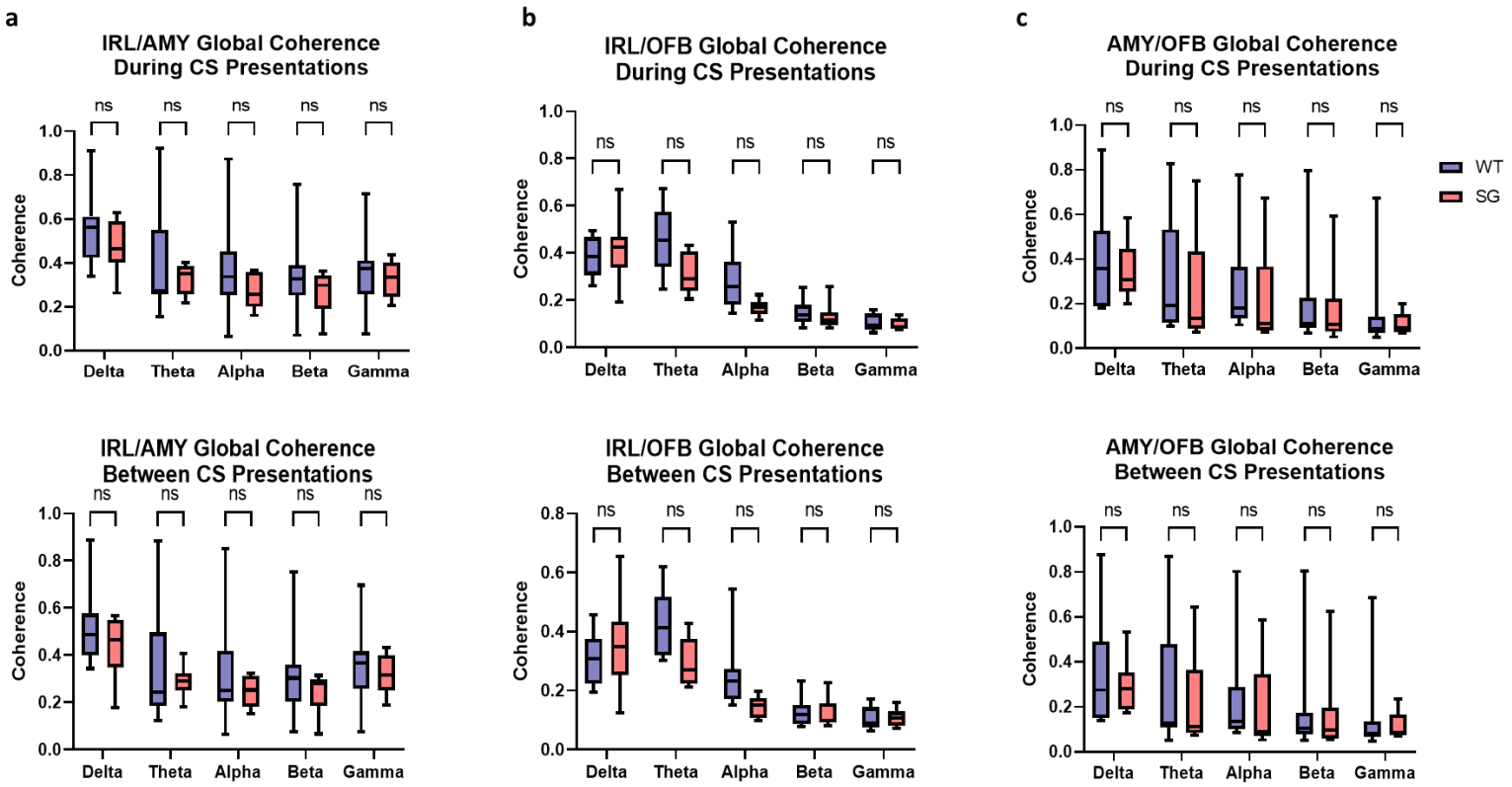

Figure 24 – Overview of Global Coherence during Recall, During versus Between CS Presentations:

Coherence for WT (n = 10) and SG (n = 8) rats during versus between CS presentations, calculated by frequency band. For all presented graphs, a two-way ANOVA was performed to analyse the effect of genotype and frequency on coherence, and Bonferroni's multiple comparisons test was used to test for significant differences between the genotypes. Across all three coherence pairings, no differences between WT and SG rats were found.

(a) IRL/AMY coherence spectra, during versus between CS. *<u>During CS:</u> An interaction between genotype and frequency was found not to have statistical significance (F(DFn, DFd) = 0.08812, p = 0.9859). Frequency (p = 0.0011**) and genotype (p = 0.0395*) had a highly significant effect on coherence. <u>Between CS:</u> An interaction between genotype and frequency was found not to have statistical significance (F(DFn, DFd) = 0.2384, p = 0.9156). Frequency had a highly significant effect on coherence (p < 0.0001****), while genotype did not (p =0.3513).*

(b) IRL/OFB coherence spectra, during versus between CS. *<u>During CS:</u> An interaction between genotype and frequency was found to have statistical significance (F(DFn, DFd) = 4.302, p = 0.0038**). Frequency had a highly significant effect on coherence (p < 0.0001****), while genotype did not (p =0.0870). <u>Between CS:</u> An interaction between genotype and frequency was found to have statistical significance (F(DFn, DFd) = 4.460, p*

*= 0.0031**). Frequency had a highly significant effect on coherence (p < 0.0001****), while genotype did not (p =0.1466).*

(c) AMY/OFB coherence spectra, during versus between CS. *<u>During CS:</u> An interaction between genotype and frequency was found not to have statistical significance (F(DFn, DFd) = 0.03394, p = 0.9977). Frequency had a significant effect on coherence (p = 0.0089**), while genotype did not (p =0.2950). <u>Between CS:</u> An interaction between genotype and frequency was found not to have statistical significance (F(DFn, DFd) = 0.3088, p = 0.8711). Frequency had a highly significant effect on coherence (p < 0.0001****), while genotype did not (p =0.6650).*

6.4.2 Global Coherence Variances defined by Temporal CS Presentations

Like with power, coherence was calculated between eight different groups for temporal comparisons. These groups were WT (During CS 1-3), WT (During CS 8-10), SG (During CS 1-3), SG (During CS 8-10), WT (Between CS 1-3), WT (Between CS 8-10), SG (Between CS 1-3), and SG (Between CS 8-10). These groups were calculated for all three comparisons: IRL/AMY, IRL/OFB, and AMY/OFB.

Firstly, global coherence was compared within each genotype, during versus between CS presentations. The purpose of this was two-fold; first, differences in WT coherence during versus between CS presentations could have biological relevance, as WT rats freeze much less during the inter-CS intervals, and second, if no differences are found, then CS presentations and intervals can be collapsed for subsequent temporal analysis, as demonstrated above with power.

Unlike power, significant differences were found during versus between CS presentations in both the WT and SG rats. Significantly more differences were found between the WT rats, which signifies that higher coherence may be a mediator or biological marker of freezing behaviour. **Figure 25** outlines these differences, which are especially prevalent in the delta band of the WT rats.

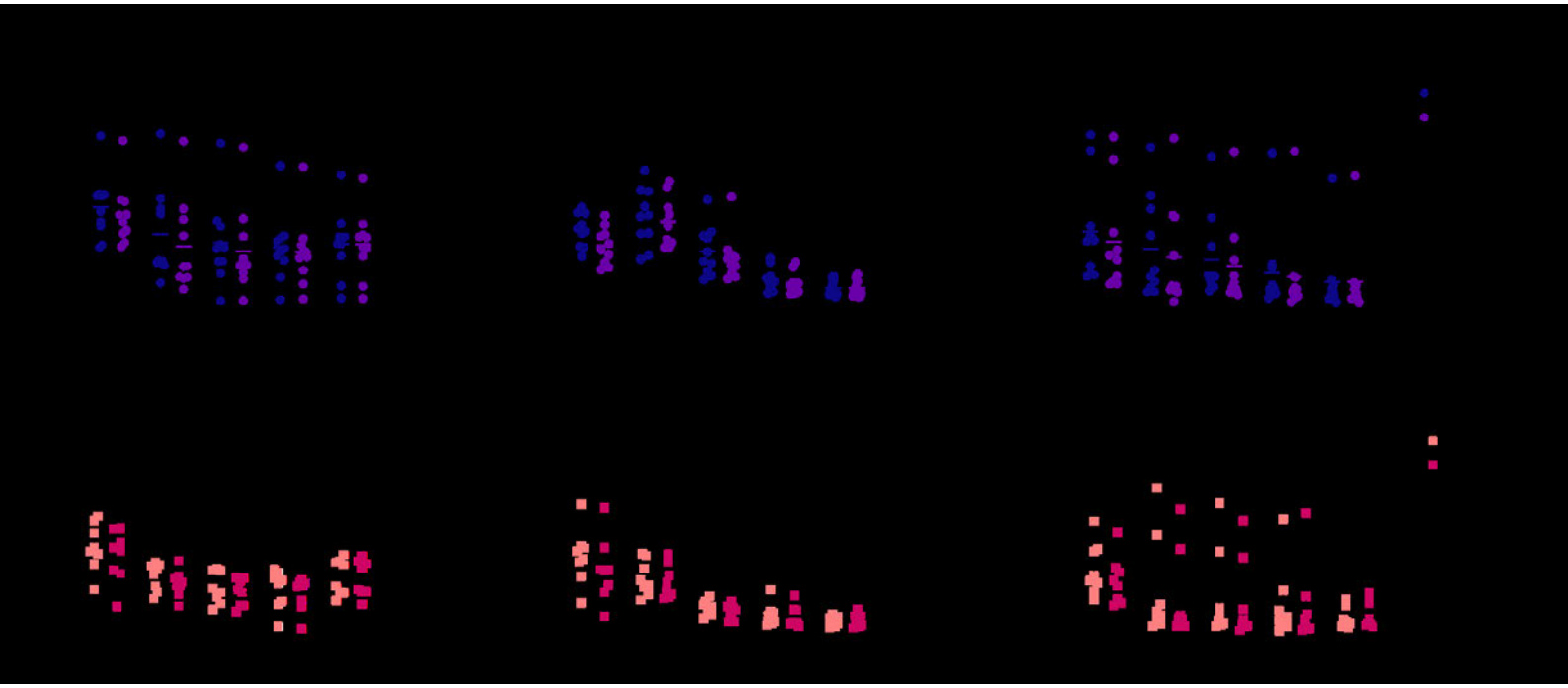

Figure 25 – Overview of Global Coherence, During versus Between Combined Early and Late CS Presentations, per Genotype:

Interleaved scatter plots, mean with SEM, for coherence during versus between CS by genotype. A two-way ANOVA was performed across all plots, and Bonferroni's multiple comparisons test was used to identify significant differences during versus between CS presentations. For WT (n = 10) rats, significant differences were found in the delta, theta, and alpha frequency bands for IRL/AMY, the delta and beta frequency bands for IRL/OFB, and the delta band for AMY/OFB coherence. For SG (n = 8) rats, significant differences were found in the delta band for IRL/OFB and AMY/OFB coherence. ***Detailed statistical analysis, including full ANOVA results, can be found in Appendix I: Supplementary Statistics.***

(a) WT IRL/AMY Coherence, during versus between CS. *Bonferroni's multiple comparisons test revealed significant differences during versus between CS coherence in the delta (p = 0.0004***), theta (p < 0.0001****), and alpha (p = 0.0004***) frequency bands.*

(b) WT IRL/OFB Coherence, during versus between CS. *Bonferroni's multiple comparisons test revealed significant differences during versus between CS coherence in the delta (p = 0.0010***) and beta (p = 0.0232*) frequency bands.*

(c) WT AMY/OFB Coherence, during versus between CS. *Bonferroni's multiple comparisons test revealed significant differences during versus between CS coherence in the delta (p = 0.0005***) frequency band.*

(d) SG IRL/AMY Coherence, during versus between CS. *Bonferroni's multiple comparisons test revealed no significant differences during versus between CS coherence in any frequency bands.*

(e) SG IRL/OFB Coherence, during versus between CS. *Bonferroni's multiple comparisons test revealed significant differences during versus between CS coherence in the delta (p = 0.0242*) frequency band.*

(f) SG AMY/OFB Coherence, during versus between CS. *Bonferroni's multiple comparisons test revealed significant differences during versus between CS coherence in the delta (p = 0.0269*) frequency band.*

As the behavioural observations in Section 6.1 revealed, SG rats are more likely to freeze throughout the inter-CS interval, after the offset of the CS presentation. Therefore, if coherence is playing a role in either mediating or predicting freezing behaviour, we would expect to see less of an effect in the SG rats than the WT rats. This is especially prevalent in the IRL/AMY pairing, where the WT rats display strong significant differences in coherence during versus between CS presentations across the delta, theta, and alpha bands, whereas the SG rats display no significant differences at all. Increased IRL/AMY coherence, therefore, may be a strong indicator of freezing behaviour in these animals.

Because there are significant differences within the genotypes (unlike power), the eight-group analysis will not be able to be collapsed into four groups, as the during and between CS groups cannot be assumed to be equal. However, for consistency, each genotype's CS presentations and inter-CS intervals were collapsed and compared for early versus late CS presentations, as was done with power. **Figure 26** shows the results of this analysis, where a significant difference between coherence in early versus late CS presentations was only identified in the alpha band of WT IRL/AMY coherence.

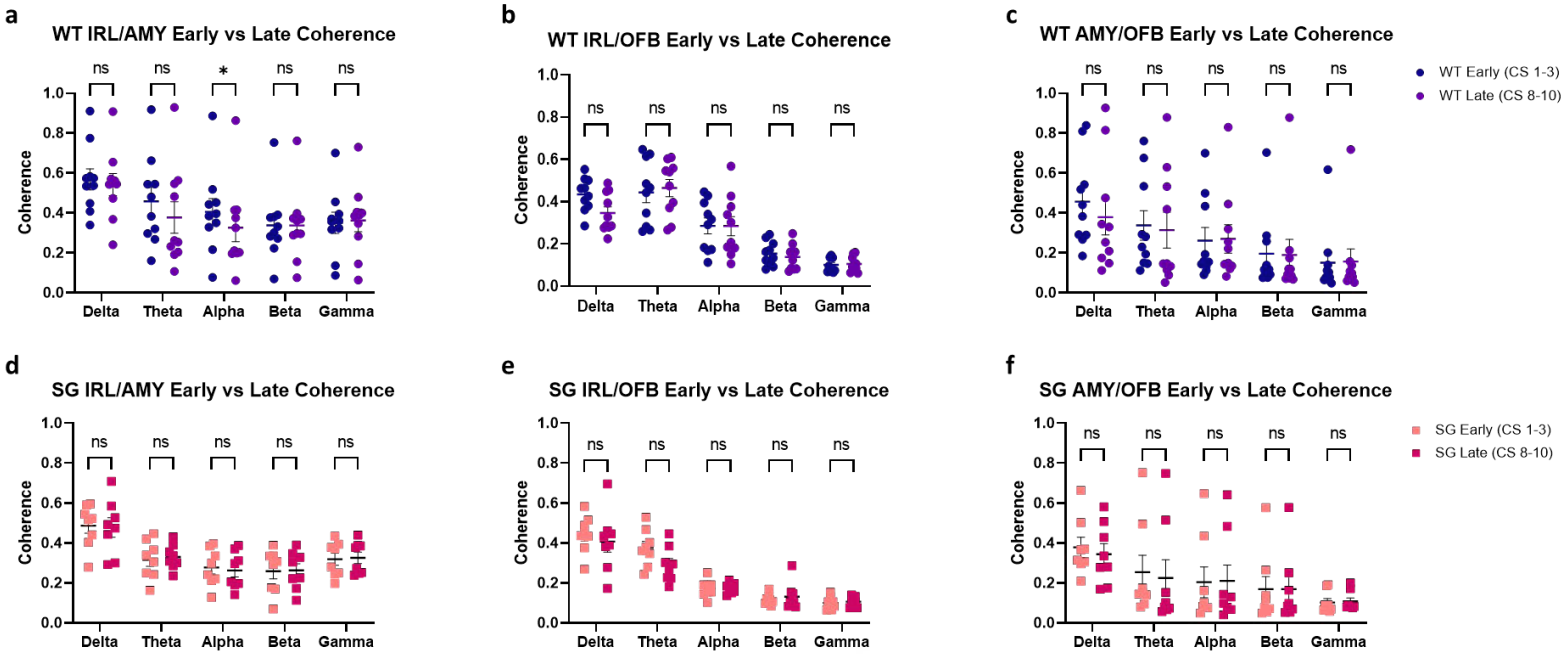

Figure 26 – Overview of Early versus Late Recall Coherence, per Genotype:

Interleaved scatter plots, mean with SEM, for coherence during early versus late CS presentations per genotype. A two-way ANOVA was performed across all plots, and Bonferroni's multiple comparisons test was used to identify significant differences during versus between CS presentations. For WT (n = 10) rats, a significant difference was found in the alpha frequency band for IRL/AMY coherence. For SG (n = 8) rats, no significant differences were found between early and late CS presentations. ***Detailed statistical analysis, including full ANOVA results, can be found in Appendix I: Supplementary Statistics.***

(a) WT IRL/AMY Coherence, early versus late CS. *Bonferroni's multiple comparisons test revealed significant differences between early versus late CS coherence in the alpha frequency band (p = 0.0457*).*

(b - f) All other groupings. *Bonferroni's multiple comparisons test revealed no significant differences between early versus late CS coherence in any frequency bands.*

For the full analysis, all eight groups were calculated for each coherence pairing, and a two-way ANOVA was conducted across all eight groups. No significant differences between any groups of biological relevance were found, but the interleaved scatter plots will be shown below in **Figure 27** for visualization.

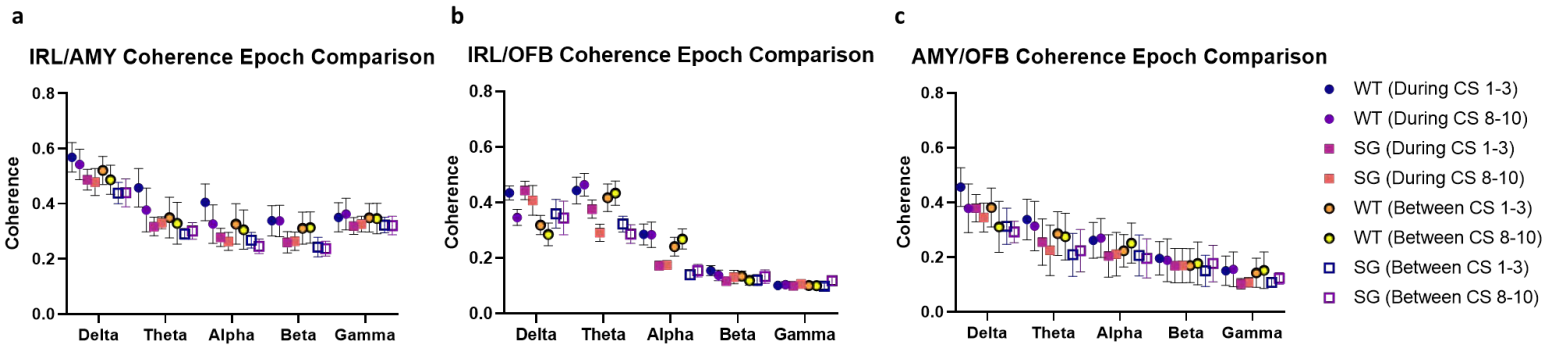

Figure 27 – Overview of Coherence Epochs (Early versus Late, and During versus Between CS Presentations):

Interleaved scatter plots, mean with SEM, for all eight coherence calculation groups. A two-way ANOVA was performed for each plot, and Bonferroni's multiple comparisons test was used to identify significant differences between the groups. For all three coherence pairings, no significant differences were found after corrections for multiple comparisons. ***Detailed statistical analysis, including full ANOVA results, can be found in Appendix I: Supplementary Statistics.***

The lack of significant differences is not surprising, given the small power after adjusting for so many comparisons. Bonferroni's multiple comparisons test was used as a more conservative estimate of significance, but it is worth noting that no significant differences emerge with Šidák's corrections, which gives the statistical test more power, either.

6.4.3 Coherence and Behaviour Correlations

As with power, coherence was correlated with freezing behaviour to look for possible patterns that may contribute to or result from this genotypic difference. As the most significant differences were found in the delta frequency range, correlations between delta coherence and freezing behaviour are illustrated in **Figure 28**.

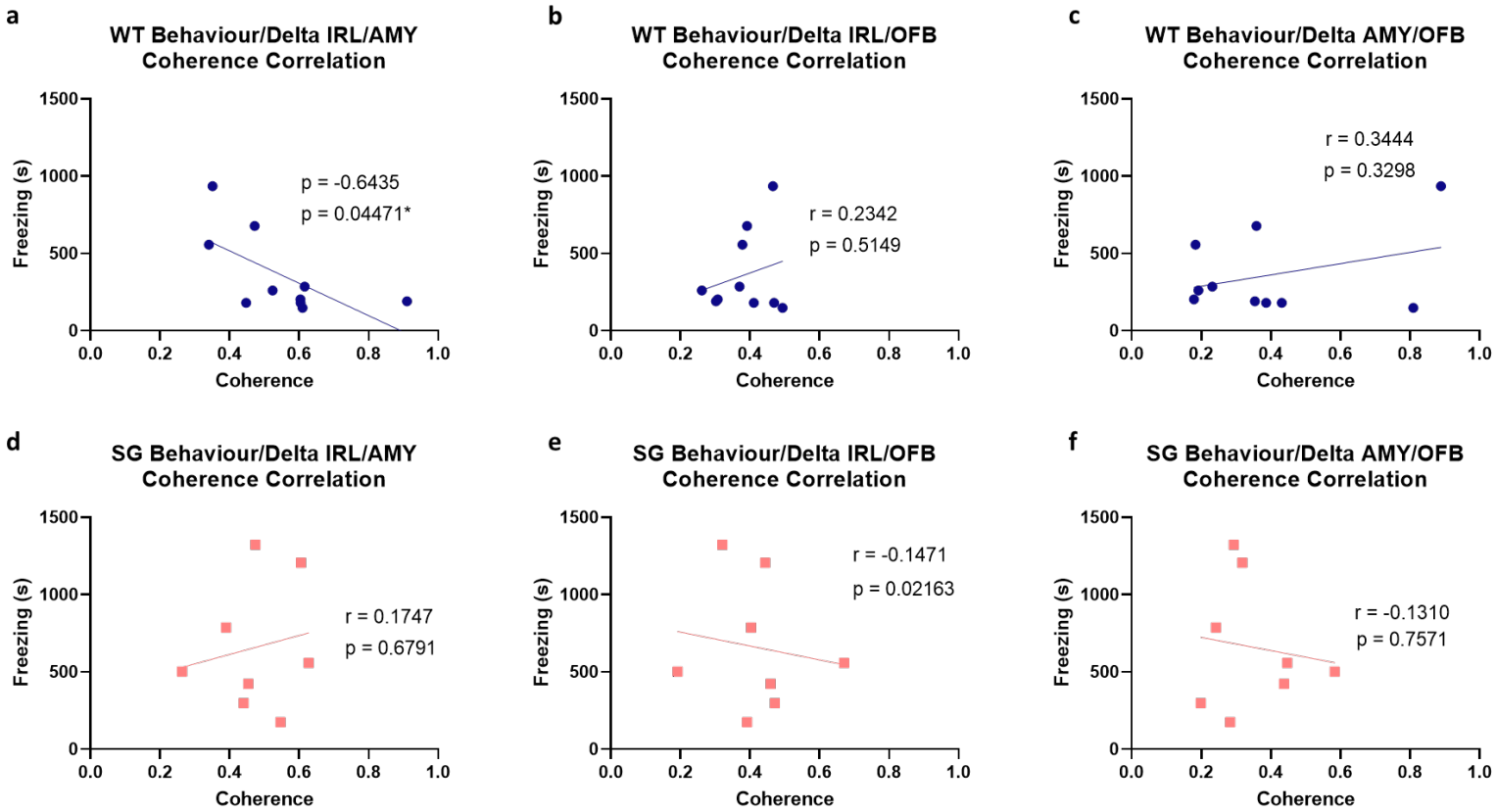

Figure 28 – Correlation between Freezing Behaviour and Delta Coherence during Recall:

Correlation coefficients (Pearson's r) and p-values were calculated for each graph, representing the correlation between freezing times and delta coherence in the brain regions for each genotype. The p-value indicates the statistical significance of the correlation coefficient (two-tailed test), and the coefficient of determination (R squared) represents the proportion of variability in freezing behaviour explained by gamma power.

(a-c) WT Behaviour and Delta Coherence Correlations. *The only statistically significant correlation is illustrated in (a) IRL/AMY Coherence Correlation (p = 0.04471*, r = -0.6435).*

(d – f) SG Behaviour and Delta Coherence Correlations. *There were no statistically significant correlations amongst any of the SG coherence pairs and behaviour.*

A statistically significant correlation was only observed in the WT IRL/AMY pair, although it is interesting to note that the correlations are always in opposite directions for each genotype. No conclusions can be drawn from this analysis (as with the power correlations), although significant correlations may provide insights into regions of interest for further research.

As with power, a negative control of this analysis (this time in the gamma band) is included in Appendix II, where significant correlations were found in the WT IRL/AMY pair and the WT AMY/OFB pair.

7 Discussion

7.1 Summary

Syngap1 disorder is often associated with deficits in learning and memory [17, 19], but our understanding of the underlying neuropathology remains limited. Therefore, the overarching aim of this discovery thesis was to investigate whether an electrophysiological biomarker could be identified between three brain structures of interest (the infralimbic cortex, the amygdala, and the olfactory bulb) to explain the neural mechanism behind the difference in SG and WT fear extinction learning.

At the behavioural level, I verified that the electrode implantation surgery and variant conditions of this experiment had no effect on the previously reported extinction deficit [41] between SG and WT rats. While this does not confirm our hypothesis regarding underlying neural variances causing the difference in behaviour, it does signify that a mechanism other than extraneous factors such as housing, diet, or socialization is driving the disparity. In addition, significant differences were identified between SG and WT rats for freezing prior to CS 1, total freezing duration during recall, average freezing bout length, and the extinction and modulation indexes. This aligns with previous lab findings [41] and further confirms the existence of a significant disparity in fear learning and memory between SG and WT rats.

Similarly, I verified the accuracy of our electrophysiological recordings from the three brain regions of interest, and I validated the accuracy of the custom MATLAB electrophysiology pipeline by comparing raw traces from the NeuroExplorer viewing software with the calculated traces by the MATLAB scripts. All subsequent analysis was carried out via the custom MATLAB software package, so this validates the accuracy of the overall findings.

Spectral power was used to both verify the processing of the visual CS and investigate the three brain regions for electrophysiological biomarkers. An electrode implanted in the superior colliculus, a brain region with known increased power during the presentation of visual stimuli [45-46], was used to verify that the CS (a blue flashing LED) was processed visually by both genotypes. This confirms that the behavioural difference was driven by a deficit in learning rather than the inability to process the conditioned stimulus.

Power was analysed across all three brain regions in varying conditions: during versus between CS presentation, early (CS 1-3) versus late (CS 8-10) CS presentations, and the combination of these two conditions (early during CS, early between CS, etc.). Globally (across the total recall paradigm), significant differences in power between the genotypes were identified in the gamma band of the infralimbic cortex and the olfactory bulb. When comparing all groups, these differences on persisted in the gamma band of the infralimbic cortex, indicating that this may be a brain region and frequency band where power is either a driver of or impacted by the behavioural difference. Further, a significant positive correlation was identified between freezing time and power in the olfactory bulb of WT rats during both early and late CS presentations. Interestingly, a significant negative correlation was found in SG rats during early CS presentations, and a positive correlation was found during late CS presentations. This indicates correlation between the olfactory bulb and power could be a potential driver of extinction learning, as the behaviour of the two genotypes differs in early CS presentations (during the SG extinction learning deficit) and matches during late CS

presentations, when the SG rats unlearn the CS-US association and stop freezing during recall.

Similarly, coherence was used to investigate the three brain regions of interest for potential electrophysiological drivers or results of the extinction learning deficit in SG rats. As with power, coherence was calculated between each pair of brain regions for the aforementioned conditions. No significant differences in coherence were found between the genotypes for any pairs during or between CS presentations, but very strong significant differences were found when comparing coherence during versus between CS presentation within each genotype. In WT rats, significant differences were found in the delta, theta, and alpha bands during versus between IRL/AMY coherence, the delta and beta bands of the IRL/OFB coherence, and the delta band of the AMY/OFB coherence. Comparing coherence in the SG rats during versus between CS presentations, significant differences were only found in the delta frequency band of the IRL/OFB and AMY/OFB pairings. This indicates a possible driver of freezing behaviour in the lower frequency bands – WT rats are more likely to freeze during the CS presentation, while SG rats freeze for longer periods of time without regard to the presence of the CS. Therefore, the strong significant difference between coherence in the WT rats during versus between CS presentations may be related to extinction learning. No clear patterns were observed in the correlations between freezing times and coherence.

Overall, we satisfied **Aim 1** and found promising avenues for further investigation regarding **Aim 2** and **Aim 3**. These further investigations and future work will be discussed in the following sections. Because this was a "discovery" project with a large sample size and millions of neural data points for analysis, the scope and limitations of this project will also be discussed.

7.2 Implications for *SYNGAP1* Research

The findings of this study contribute to the expanding body of literature on *SYNGAP1* haploinsufficiency by shedding light on the neural underpinnings of fear extinction learning deficits associated with this disorder. Previous research has consistently identified deficits in learning and memory in individuals with SYNGAP1 haploinsufficiency [17, 19], aligning with the behavioural disparities observed in our study between the SG and WT rats. By investigating the neural mechanisms underlying these behaviours, our study delves deeper into the neuropathology of *SYNGAP1* haploinsufficiency, providing novel insights into the specific brain regions involved. These findings support and extend the current understanding of *SYNGAP1*-ID in the literature, specifically relating to gamma-band metrics and previously indicated electrophysiological biomarkers.

Existing research on *SYNGAP1* haploinsufficiency has primarily focused on cognitive problems and epilepsy [17, 19, 47]. However, our investigation reveals novel insights into the neural processes linked to *SYNGAP1* mutations. Consistent with previous studies, we observed significant differences in gamma oscillation power [47] between SG and WT rodents; further, we localized these power differences to the infralimbic cortex and olfactory bulb. Our findings especially indicate the olfactory bulb as a region for further investigation; this aligns with additional findings in the literature, which provide compelling evidence for sensory-processing alterations in both rodent models and human patients with *SYNGAP1*

haploinsufficiency [17, 47]. Previous studies indicate that these increases in baseline gamma oscillation power could provide a compelling translational biomarker of sensory-processing alterations associated with *SYNGAP1* haploinsufficiency [47-48], and our findings further support that claim.

While the literature on *SYNGAP1* haploinsufficiency, specifically with regards to rat models, is somewhat limited [41], our findings also support those of the broader findings in autism spectrum disorder research. Gamma band abnormalities have been reported in many studies of ASD [2, 49], further supporting the use of these electrophysiological signals and potential biomarkers and endophenotypes [49]. The reported gamma band metrics in ASD and their heritability suggest shared neural mechanisms with *SYNGAP1* haploinsufficiency, emphasizing the broader relevance of our study in advancing the understanding of neurodevelopmental disorders associated with electrophysiological dysfunction.

Moreover, our study identified differences between SG and WT coherence that possibly describes the identified behaviour difference between the two genotypes. Interestingly, differences in low range frequency bands have been investigated before, with research from another lab at our university identifying reduced EEG connectivity in the sleep spindle frequency band [50]. This finding further supports our hypothesis that differences in connectivity could be a driver of differences in behaviour, a finding which may hold clinical relevance and is worthy of further investigation. We hypothesize that sleep during the consolidation phase between fear extinction learning and recall may be important to understanding this mechanism, and I have already begun implementing the equipment necessary to collect neural recordings during this period for future studies (Section 7.4).

These collective findings not only validate and extend the current understanding of *SYNGAP1*-related behavioural phenotypes, but also underscore the potential translational impact of our study on the identification of electrophysiological biomarkers for disorders involving neural dysfunction.

7.3 Study Limitations

As with all scientific studies, there are limitations with regards to the methods and subsequent applicability of the results of this study. The primary limitations can be categorized into design limitations, subject limitations, and data analysis limitations, and all three categories will be discussed at length in the following section.

Design Limitations

The experimental design of this study involved the implantation of electrodes in multiple brain regions for the purpose of capturing local field potentials (LFP) and electroencephalogram (EEG) data. While this approach allowed for comprehensive exploration of neural activity, several design limitations should be acknowledged.

First, due to time constraints and the intricate nature of the data analysis, not all implanted brain regions could be thoroughly addressed in this thesis. This restriction highlights the vast complexity of neural interactions and the need for future investigations to delve into the

remaining brain regions, potentially unveiling additional electrophysiological markers of interest.

Another limitation of the experimental design pertains to the consistency of electrode placement across all animals. Although efforts were made to standardize electrode coordinates, it is important to acknowledge that subtle variations in electrode positioning might have occurred, possibly influencing the recorded neural signals. To refine this methodology, future studies will employ histological imaging techniques to ensure more accurate and consistent electrode placements.

Additionally, it is important to note that other *in vivo* recording techniques could present a more refined view of neural activity compared to LFP or EEG data, such as single-cell or ensemble recordings. LFP and EEG signals reflect synchronized activity of a population or neurons within a certain vicinity of the electrode; consequently, the spatial resolution of LFP and EEG data is limited, and these measurements might not fully capture the intricacies of individual neuron firing patterns or the precise coordination between specific neuronal ensembles. The complex interactions occurring at the cellular level might be smoothed or obscured in the aggregate signals captured by LFP and EEG.

Further, the temporal resolution of LFP and EEG data presents inherent limitations. While these methods are excellent for capturing oscillatory patterns and broad-scale neural synchronization, they might not adequately capture rapid and transient neural events that could play a critical role in information processing. Single-cell recordings allow for the detection of millisecond-level neuronal firing dynamics, whereas LFP and EEG measurements, due to their inherent integration over larger populations, might miss these fine-grained temporal dynamics.

Therefore, while LFP and EEG data provide valuable insights into network-level neural dynamics, their limitations in spatial and temporal resolution, as well as their inability to capture single-cell activities, should be acknowledged. Future studies aiming to analyse the finer details of neural mechanisms might consider integrating multiple recording modalities to achieve a more comprehensive understanding of the underlying neural processes.

Finally, electrical interference from the arena shock grid prevented real-time data recording during the conditioning phase of the experiment, hence why the analysis here was restricted to the recall phase. Corrective measures were taken to mitigate this interference, and the author's electrical grid correction can be found in the 'Future Work' section. While this will aid future experiments, the absence of data during conditioning presents a limitation of the data analysis presented here.

Subject Limitations

The subjects utilized in this study were living organisms and, as such, certain limitations arose in relation to their well-being and participation. A notable consideration is the variance in recovery times following the surgery for electrode implantation; all subjects were given at least two weeks to recover prior to the start of the experiment, but this interval was not consistent for all rodents as some had much more time to recover. Therefore, the interval between surgery and the commencement of the experimental phase introduced variability in

neural baseline conditions, which may have influenced the observed neural patterns during subsequent fear conditioning tasks. This discrepancy emphasises the importance of carefully managing post-surgery recover periods in future studies.

Additionally, housing constraints imposed certain limitations on the subjects' environment. These constraints inadvertently led to heightened anxiety levels (due to periods of single housing), which could have affected neural activity and behavioural responses during fear conditioning. While efforts were made to minimize environmental stressors, the impact of housing-induced anxiety on the neural measures cannot be definitively dismissed.

Data Analysis Limitations

The development of the data analysis pipeline was the focus of this thesis, but specific limits that it presents still deserve further discussion. Although Gaussian filtering was employed as a pre-processing step to enhance signal-to-noise ratios, it's essential to acknowledge that this method might not fully capture all relevant neural oscillatory patterns. There are limitations of Gaussian filtering, such as inefficiency in capturing rapid and transient neural events; this should be emphasised here, as it could influence the interpretation of the study's findings.

Moreover, while the current analysis focused on coherence and power measures, it's important to recognize that neural dynamics encompass a broader spectrum of interactions and phenomena. The selection of these particular measures reflect the study's scope and objectives, yet other dimensions of neural communication, such as phase-amplitude coupling and spike-field coherence, warrant investigation for a more comprehensive understanding of neural network dynamics.

In conclusion, while this study represents a valuable exploration into the electrophysiological markers of fear conditioning and memory, the aforementioned limitations necessitate cautious interpretation of the results. Acknowledging these limitations not only emphasizes the rigor of the scientific process but also guides future researchers towards addressing these constraints in subsequent studies. Through continued refinement and expansion of methodologies, the field can move closer to a nuanced comprehension of the neural processes behind behaviour and cognition in the fear conditioning paradigm.

7.4 Future Work

As with all discovery studies, perhaps one of the most compelling results to emerge from this master's thesis is the identification of avenues for further experimentation. This study has located brain regions which may carry electrophysiological markers or by-products of fear learning and extinction in *SYNGAP1* disorder, and those regions can now be studied in further detail and more refined conditions. In addition, I have already undertaken the initial circuitry work to expand our recording capabilities, and these improvements to the arena and recording technology will be discussed in the following section.

The most logical next steps in this project are to repeat the experiment with both a) less implanted brain regions for improved accuracy in surgical targeting and easier analysis, and b) implanted electrodes in novel brain regions for further exploration and discovery. The

software package developed in this thesis is fully customizable, so it can be employed with any quantity and placement of implanted electrodes. In addition, frequency bands are input by the user, so activity in frequency bands beyond those explored in this thesis can be analysed.

Time constraints limited this analysis to power and coherence between brain regions, but future work should consider additional electrophysiological measures such as phase-amplitude coupling and spike-field coherence. This would give a more complete view of neural network dynamics, while further identifying potential brain structures driving or impacted by the behavioural disparity.

Another future improvement to this study is to expand the times of the fear conditioning paradigm during which we can make neural recordings. Figure 2 shows the standard fear conditioning paradigm, as well as the associated stages of fear learning: acquisition, consolidation, and recall. Currently, we can only record during the recall stage; the shock floor in the fear conditioning chamber produces electrical interference that distorts the neural recordings beyond recovery, and consolidation happens when the rats are returned to their home cages in between conditioning and recall.

As a part of my project, I have made the necessary engineering and technical improvements to overcome these obstacles and record throughout the entire fear learning paradigm. To address the electrical interference during fear conditioning, I worked with Dr Elizabeth Schultze from Harvard Bioscience, Inc. to develop a grounding relay that suppresses the electrical grid until the moment of the foot shock. This results in usable neural recordings for the entire paradigm, except during the 1 second that the foot shock is delivered. The schematic we developed and implemented is displayed in **Figure 29**.

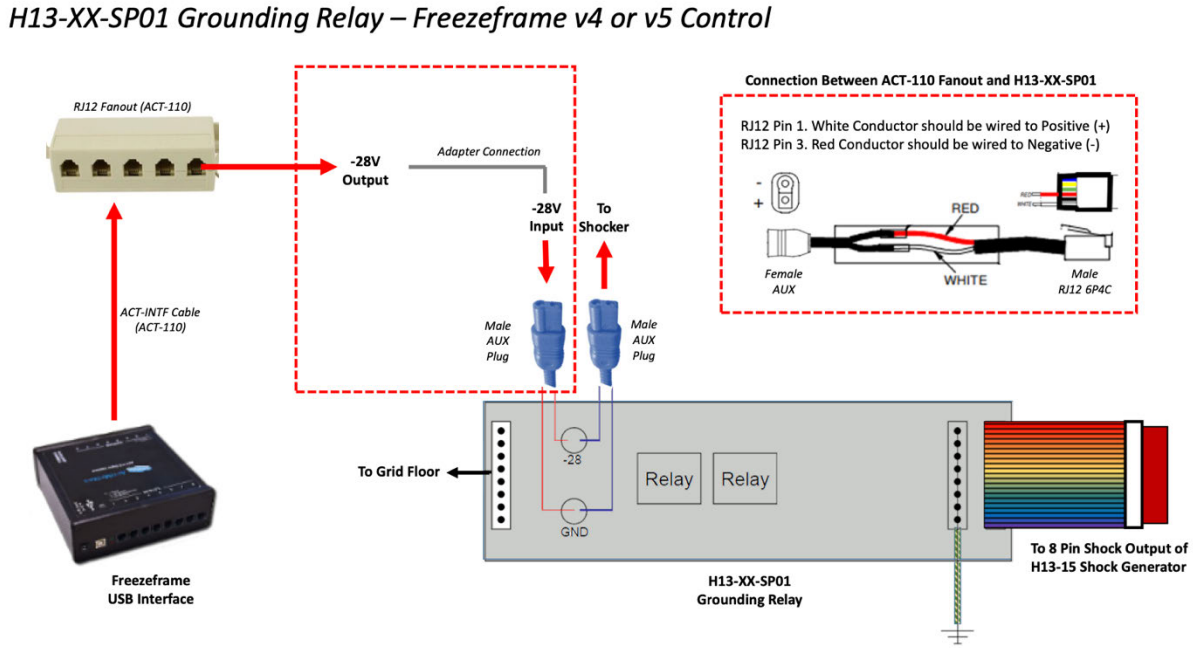

Figure 29 – Circuitry Schematic of Modification to Electrical Foot Shock Grid:

A simple schematic showing the circuitry modifications that suppress the electrical foot shock grid and enable recoding during the fear conditioning stage of the paradigm. ***Figure graphics and images courtesy of Harvard Bioscience, Inc.***

In addition, I began the process of setting up and employing a wireless neural recording device, called a Neurologger (Evolocus LLC, Zurich, Switzerland), that can record continuously up to 24 hours. The Neurologgers are plugged into the implants and protected by a 3D printed cap while the rat is in their home cage. Theoretically, these devices can be used to record during the entire consolidation period, although the longest recordings I made were 2 hours. This was due to previous user error, and the Neurologgers had to be recalibrated and repaired before being returned to the lab. While I never got to use them, in future studies the Neurologgers and 3D printed caps can be used to record throughout the entire consolidation period. This would enable the acquisition of neural recordings throughout the entire fear conditioning paradigm, thus giving a more comprehensive picture of the neural signals driving the behaviour discrepancy between WT and SG rats.

Finally, future studies would be improved by more refined seizure screening and identification. While I manually removed seizures from the data presented here using NeuroExplorer, future iterations of the electrophysiology pipeline could be improved by automated seizure screening scripts. In addition, more formal analysis of the quantity and duration of seizures could inform another component of this neural story; I found that seizures were more common in SG than WT rats, although more refined analysis would be required for any definitive conclusions. **Figure 30** shows an example of a seizure that I removed in NeuroExplorer.

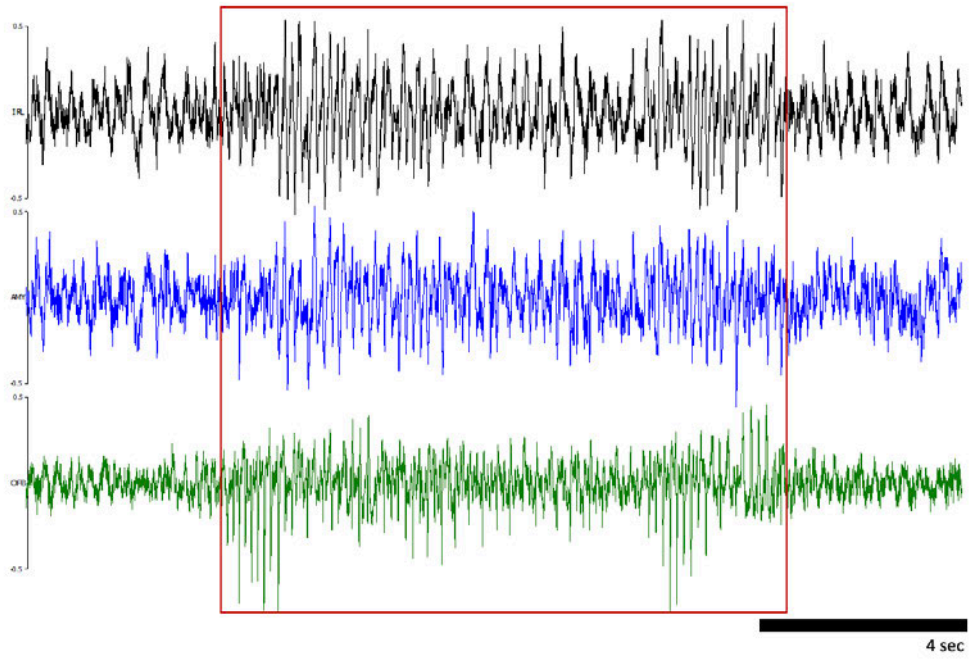

Figure 30 – Example of a Seizure:

This figure shows a raw trace of the IRL, AMY, and OFB neural signals in NeuroExplorer. The seizure, which was later removed, is indicated by the red box.

8 Conclusion

In pursuit of uncovering the intricate neural mechanisms that underly fear extinction learning in *SYNGAP1* disorder, this discovery thesis embarked on a comprehensive exploration of electrophysiological biomarkers across key brain regions. The central aim of identifying an electrophysiological basis for disparity in fear extinction learning between *Syngap*$^{+/\Delta GAP}$ mutant (SG) and wildtype (WT) rats has yielded valuable insights, paving the way for further investigations and a deeper understanding of this complex disorder.

Through meticulous analysis of behavioural assessments, this study confirmed that the observed difference in fear extinction learning between the SG and WT rats is not merely a product of extraneous factors but is rooted in distinct neural mechanisms. Notably, significant differences in freezing behaviour, both prior to and during recall, reinforced the presence of a substantial gap in fear learning and memory between the two genotypes. These findings prove a solid foundation for the subsequent electrophysiological analyses.

The validation of electrophysiological recordings across the infralimbic cortex, amygdala, and olfactory bulb lent credibility to the subsequent analyses. The establishment of a reliable MATLAB electrophysiology pipeline further fortified the accuracy of the study's overarching findings. Notably, power and coherence emerged as critical tools in dissecting the neurophysiological basis of fear extinction learning.

Power analysis, strategically employed to validate the processing of the conditioned stimulus (CS) and to identify potential electrophysiological biomarkers, revealed intriguing results. The gamma band activity in the infralimbic cortex and olfactory bulb emerged as significant differentiators between the genotypes, hinting at their potential roles as neural drivers or responders to the observed behavioural differences. Additionally, correlations between freezing behaviour and power in the olfactory bulb unveiled compelling associations that warrant deeper exploration, particularly concerning the role of the olfactory bulb in rodent extinction learning.

Coherence analysis, while not revealing genotype-specific differences, shed light on the dynamics of neural communication within and between the brain regions of interest. The pronounced differences in coherence during versus between CS presentations within each genotype raised questions about the role of frequency bands, particularly in lower frequencies, in driving freezing behaviour. This phenomenon provides a potential link to the intricate processes underlying extinction learning.

In light of the achieved objectives, this thesis marks the fulfilment of **Aim 1**, offering a solid foundation for the subsequent pursuits of **Aim 2** and **Aim 3**. The results of this study merely scratch the surface of the intricate neural underpinnings of fear extinction learning in *SYNGAP1* haploinsufficiency. The promising avenues illuminated by this research call for further investigations, potentially involving advanced methodologies such as optogenetics and more refined electrophysiological analyses.

As with any scientific endeavour, this study comes with certain limitations and considerations. The sheer scale of data collected and analysed complicates the neural dynamics under investigation. Future endeavours might benefit from integrating more refined

behavioural and electrophysiological approaches to offer a more comprehensive understanding of these dynamics.

In summation, this discovery thesis offers a significant stride toward unravelling the enigma of fear extinction learning in *SYNGAP1* haploinsufficiency. The amalgamation of behavioural assessments, electrophysiological analyses, and novel insights into neural dynamics lays the groundwork for future explorations, driving us closer to unveiling the intricacies of this disorder's neural basis.

9 References

[1] Ismail, F.Y. & Shapiro, B.K. “What are neurodevelopmental disorders?” In: *Current Opinion in Neurology*, 32.4 (2019), pp. 611-616. DOI: 10.1097/WCO.0000000000000710

[2] Lord, C., Brugha, T.S., Charman, T. et al. “Autism spectrum disorder.” In: *Nature Reviews Disease Primers* 6.5 (2020). DOI: 10.1038/s41572-019-0138-4

[3] Reiersen, A.M. “How should we classify complex neurodevelopmental disorders?” In: *Scandinavian Journal of Child and Adolescent Psychiatry and Psychology*, 5.1 (2017), pp. 1-2. DOI: 10.21307/sjcapp-2017-005

[4] American Psychiatric Association. *Diagnostic and Statistical Manual of Mental Disorders.* 5th ed. Arlington, VA (2013).

[5] Centers for Disease Control and Prevention. *Diagnostic criteria for 299.00 Autism Spectrum Disorder*. 2022, November 2. URL: https://www.cdc.gov/ncbddd/autism/hcp-dsm.html

[6] Loomes, R., Hull, L. & Mandy, W. P. L. “What is the male-to-female ratio in autism spectrum disorder? A systematic review and meta-analysis.” In: *Journal of the American Academy of Child and Adolescent Psychiatry*, 56.6 (2017), pp. 466–474. DOI: 10.1016/j.jaac.2017.03.013

[7] Brugha, T., Spiers, N., Bankart, J., Cooper, S., McManus, S., Scott, F., Smith J., & Tyrer, F. “Epidemiology of autism in adults across age groups and ability levels.” In: *The British Journal of Psychiatry*, 209.6 (2016), pp. 498-503. DOI: 10.1192/bjp.bp.115.174649

[8] Baxter, A., Brugha, T., Erskine, H., Scheurer, R., Vos, T., & Scott, J. “The epidemiology and global burden of autism spectrum disorders.” In: *Psychological Medicine*, 45.3 (2015), pp. 601-613. DOI: 10.1017/S003329171400172X

[9] Wu, S., Wu, F., Ding, Y., Hou, J., Bi, J., Zhang, Z. “Advanced parental age and autism risk in children: a systematic review and meta-analysis.” In: *Acta Psychiatrica Scandinavia*, 135.1 (2016), pp. 29-41. DOI: 10.1111/acps.12666

[10] Modabbernia, A., Velthorst, E. & Reichenberg, A. “Environmental risk factors for autism: an evidence-based review of systematic reviews and meta-analyses.” In: *Molecular Autism* 8.13 (2017). DOI: 10.1186/s13229-017-0121-4

[11] Taylor, L. E., Swerdfeger, A. L. & Eslick, G. D. “Vaccines are not associated with autism: an evidence-based meta-analysis of case-control and cohort studies.” In: *Vaccine,* 32.29 (2014), pp. 3623–3629. DOI: 10.1016/j.vaccine.2014.04.085

[12] Cross-Disorder Group of the Psychiatric Genomics Consortium et al. “Genetic relationship between five psychiatric disorders estimated from genome-wide SNPs.” In: *Nature Genetics*, 45 (2013), pp. 984–994. DOI: 10.1038/ng.2711

[13] Gaugler, T., Klei, L., Sanders, S. et al. “Most genetic risk for autism resides with common variation.” In: *Nature Genetics*, 46 (2014), pp. 881-885. DOI: 10.1038/ng.3039

[14] Sanders, S. J. et al. “Insights into autism spectrum disorder genomic architecture and biology from 71 risk loci.” In: *Neuron*, 87 (2015), pp. 1215–1233.

[15] Satterstrom, F. K. et al. “Large-scale exome sequencing study implicates both developmental and functional changes in the neurobiology of autism.” In: *Cell*, 180.3 (2020), pp. 568-584. DOI: 10.1016/j.cell.2019.12.036

[16] Devlin, B. & Scherer, S. W. “Genetic architecture in autism spectrum disorder.” In: *Current Opinion in Genetics & Development*, 22.3 (2012), pp. 229–237. DOI: 10.1016/j.gde.2012.03.002

[17] Holder, J.L., Hamdan, F.F., & Michaud, J.L. *SYNGAP1-Related Intellectual Disability*. In: *GeneReviews [Internet]*. Seattle (WA): University of Washington, Seattle (1993 – 2023).

[18] Cleary, M.A. *Haploinsufficiency*. In: *Encyclopedia of Genetics* (2001), pp. 911. DOI: 10.1006/rwgn.2001.0582

[19] Berryer M.H. et al. “Mutations in SYNGAP1 cause intellectual disability, autism, and a specific form of epilepsy by inducing haploinsufficiency.” In: *Human Mutations*, 34.2 (2013), pp. 385-94. DOI: 10.1002/humu.22248.

[20] Hamdan F.F. et al. “Mutations in SYNGAP1 in autosomal nonsyndromic mental retardation.” In: *New England Journal of Medicine*, 360 (2009), pp. 599-605. DOI: 10.1056/NEJMoa0805392

[21] Prchalova, D., Havlovicova, M., Sterbova, K. et al. “Analysis of 31-year-old patient with SYNGAP1 gene defect points to importance of variants in broader splice regions and reveals developmental trajectory of SYNGAP1-associated phenotype: case report.” In: *BMC Medical Genetics*, 18.62 (2017). DOI: 10.1186/s12881-017-0425-4

[22] American Psychological Association. *APA Dictionary of Psychology*. 2023. URL: https://dictionary.apa.org/fear

[23] Kim, J. J., & Jung, M. W. “Neural circuits and mechanisms involved in Pavlovian fear conditioning: a critical review.” In: *Neuroscience and Biobehavioral Reviews*, 30.2 (2005), pp. 188–202. DOI: 10.1016/j.neubiorev.2005.06.005

[24] Watson, J. B., & Rayner, R. “Conditioned emotional reactions.” In: *Journal of Experimental Psychology*, 3.1 (1920), pp. 1–14. DOI: 10.1037/h0069608

[25] Blanchard, R. J., & Blanchard, D. C. “Crouching as an index of fear.” In: *Journal of Comparative and Physiological Psychology*, 67.3 (1969), pp. 370–375. DOI: 10.1037/h0026779

[26] Blanchard, D. C., & Blanchard, R. J. “Innate and conditioned reactions to threat in rats with amygdaloid lesions.” In: *Journal of Comparative and Physiological Psychology*, 81.2 (1972), pp. 281–290. DOI: 10.1037/h0033521

[27] Bolles, R. C. “Species-specific defense reactions and avoidance learning.” In: *Psychological Review*, 77.1 (1970), pp. 32–48. DOI: 10.1037/h0028589

[28] Fanselow M.S. “What is conditioned fear?” In: *Trends in Neurosciences*, 7.12 (1984), pp. 460-462. DOI: 10.1016/S0166-2236(84)80253-2

[29] Pavlov, I.P. *The Work of the Digestive Glands*. (1897/1902).

[30] Davis M. “Neurobiology of fear responses: the role of the amygdala.” In: *Journal of Neuropsychiatry and Clinical Neuroscience*, 9 (1997), pp. 382–402. DOI: 10.1176/jnp.9.3.382

[31] Davis M., Walker D.L., Mayers K.M. “Role of the amygdala in fear extinction measured with potentiated startle.” In: *Annals of the New York Academy of Sciences*, 985 (2003), pp. 218-232. DOI: 10.1111/J.1749-6632.2003.Tb07084.X

[32] Milad M.R., Quirk G.J. “Neurons in medial prefrontal cortex signal memory for fear extinction.” In: *Nature*, 420 (2002), pp. 70-74. DOI: 10.1038/nature01138

[33] Quirk G.J., Russo G.K., Barron J.L., Lebron K. “The role of ventromedial prefrontal cortex in the recovery of extinguished fear.” In: *Journal of Neuroscience*, 20 (2000), pp. 6225–6231. DOI: 10.1523/JNEUROSCI.20-16-06225.2000

[34] Korshunov, K. S., Blakemore, L. J., Bertram, R., & Trombley, P. Q. “Spiking and Membrane Properties of Rat Olfactory Bulb Dopamine Neurons.” In: *Frontiers in Cellular Neuroscience*, 14.60 (2020). DOI: 10.3389/fncel.2020.00060

[35] Valley, M.T., Mullen, T.R., Schultz, L.C., Sagdullaev, B.T., & Firestein, S. “Ablation of mouse adult neurogenesis alters olfactory bulb structure and olfactory fear conditioning.” In: *Frontiers in Neuroscience,* 3 (2009). DOI: 10.3389/neuro.22.003.2009

[36] Pulvermüller, F., Garagnani, M., & Wennekers, T. “Thinking in circuits: toward neurobiological explanation in cognitive neuroscience.” In: Biological Cybernetics, 108.5 (2014), pp. 573–593. DOI: 10.1007/s00422-014-0603-9

[37] Bowyer, S.M. “Coherence a measure of the brain networks: past and present.” In: *Neuropsychiatry and Electrophysiology*, 2.1 (2016). DOI: 10.1186/s40810-015-0015-7

[38] Velazquez, J.L.P, Mateos, D.M, & Erra, R.G. “On a Simple General Principle of Brain Organization.” In: *Frontiers in Neuroscience,* 13 (2019). DOI: 10.3389/fnins.2019.01106

[39] P. Welch, "The use of fast Fourier transform for the estimation of power spectra: A method based on time averaging over short, modified periodograms." In: *IEEE Transactions on Audio and Electroacoustics*, 15.2 (1967), pp. 70-73. Doi: 10.1109/TAU.1967.1161901.

[40] Harley, J.B. *Continuous-Time and Discrete-Time Signals.* 2022. URL: http://smartdata.ece.ufl.edu/eee5502/lecture.html?lecture=02

[41] Katsanevaki, D. et al. “Heterozygous deletion of SYNGAP enzymatic domains in rats causes elective learning, social and seizure phenotypes.” Preprint in: *bioRxiv,* (2020). DOI: 10.1101/2020.10.12339192

[42] Wittenburg, P., Brugman, H., Russel, A., Klassmann, A., Sloetjes, H. “ELAN: a Professional Framework for Multimodality Research.” In: *Proceedings of LREC 2006, Fifth International Conference on Language Resources and Evaluation* (2006).

[43] Siegle JH, Cuevas López A, Patel YA, Abramov K, Ohayon S, Voigts J. “Open Ephys: an open-source, plugin-based platform for multichannel electrophysiology.” In: *Journal of Neural Engineering*, 14.45 (2017).

[44] Mishra, P., Pandey, C. M., Singh, U., Gupta, A., Sahu, C., & Keshri, A. “Descriptive statistics and normality tests for statistical data.” In: *Annals of Cardiac Anaesthesia*, 22.1 (2019), pp. 67–72. DOI: 10.4103/aca.ACA_157_18

[45] Lee, K. H., Tran, A., Turan, Z., & Meister, M. “The sifting of visual information in the superior colliculus.” In: *eLife*, 9 (2020). DOI: 10.7554/eLife.50678

[46] Bytautiene, J., & Baranauskas, G. “Rat superior colliculus neurons respond to large visual stimuli flashed outside the classical receptive field.” In: *PLoS One*, 12.4 (2017). DOI: 10.1371/journal.pone.0174409

[47] Carreño-Muñoz, M.I. et al. “Sensory processing dysregulations as reliable translational biomarkers in SYNGAP1 haploinsufficiency.” In: *Brain*, 145.2 (2022), pp. 754–769. DOI: 10.1093/brain/awab329

[48] Côté, V. et al. “Differential auditory brain response abnormalities in two intellectual disability conditions: *SYNGAP1* mutations and Down syndrome.” In: *Clinical Neurophysiology,* 132.8 (2021), pp. 1802-1812. DOI: 10.1016/j.clinph.2021.03.054

[49] Rojas, D. & Wilson, L. “γ-band abnormalities as markers of autism spectrum disorders.” In: *Biomarkers in Medicine*, 8.3 (2014). DOI: 10.2217/bmm.14.15

[50] Buller-Peralta, I. et al. “Abnormal brain state distribution and network connectivity in a *SYNGAP1* rat model.” In: *Brain Communications*, 4.6 (2022). DOI: 10.1093/braincomms/fcac263

Appendix I: Supplementary Statistics

The following figures are from **Section 6: Results**. These figures include the expanded statistical analyses, including full ANOVA results that were not reported in Section 6. Please note that, unless otherwise stated, the following data meet the conditions for normality defined by the Shapiro-Wilk Normality Test.

Figure 9 - Overview of Differences in Freezing Behaviour between SG and WT Rats during the Recall Stage of Fear Conditioning:

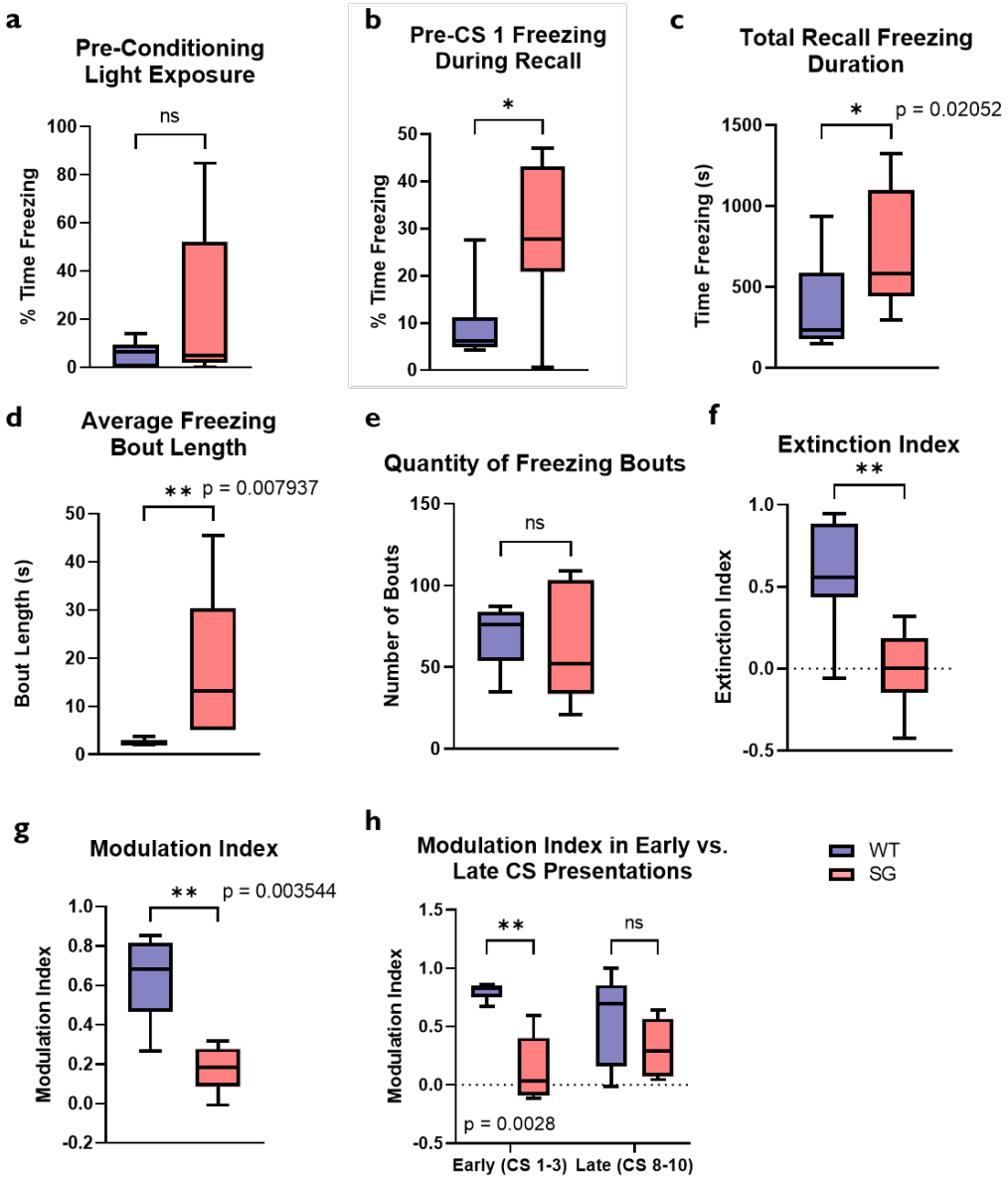

Detailed behaviour comparison for implanted (WT, n = 10, SG, n = 8) rats during the recall stage of the fear conditioning protocol.

(a) Pre-Conditioning Exposure Baseline. *% of total time freezing during CS exposure prior to conditioning. The data did not meet the conditions for normality following a Shapiro-Wilk test (WT, p = 0.3855, W = 0.9019;*

SG, p = 0.0136, W = 0.7150). An unpaired, two-tailed Mann-Whitney test was performed (p = 0.7944), and no significant difference in freezing was found between the genotypes during the pre-exposure baseline study.*

(b) Pre-CS 1 Freezing. *The SG rats (n = 8) exhibited significantly greater freezing than the WT littermates (n = 10) before the first CS presentation. The data did not meet the conditions for normality following a Shapiro-Wilk test (WT, p = 0.0020**, W = 0.6964; SG, p = 0.7610, W = 0.9535). An unpaired, two-tailed Mann-Whitney test was performed (p = 0.0401*), and a significant difference (p < 0.05) was found between the pre-CS 1 freezing times of the genotypes.*

(c) Total Freezing Duration. *The SG rats (n = 8) exhibited significantly greater total freezing time than the WT littermates (n = 10). The data did not meet the conditions for normality following a Shapiro-Wilk test (WT, p = 0.0075**, W = 0.7766; SG, p = 0.0010**, W = 0.6671). An unpaired, two-tailed Mann-Whitney test was performed (p = 0.0205*), and a significant difference (p < 0.05) was found between the total freezing time of the WT and SG rats.*

(d) Average freezing bout duration. *The SG rats has a significantly greater average freezing bout duration than the WT littermates. The data did not meet the conditions for normality following a Shapiro-Wilk test (WT, p = 0.0020, W = 0.6399; SG, p = 0.0450, W = 0.7699). An unpaired, two-tailed Mann-Whitney test was performed (p = 0.0079**), and a significant difference was found between the average freezing bout durations of the WT and SG rats.*

(e) Quantity of freezing bouts. *There was no significant difference between the quantity of freezes (freezing bouts) between the WT and SG rats. The data had a normal distribution following a Shapiro-Wilk test (WT, p = 0.0901, W = 0.8057; SG, p = 0.5241, W = 0.9191). An unpaired, two-tailed T test with Welch's correction was performed (p = 0.8002, t = 0.2642, df = 14.232), and no significant difference was found.*

(f) Extinction Index. *The extinction index [(total time freezing during CS 8-10 – total time freezing during CS 1-3)/(total time freezing during CS 8-10 + total time freezing during CS 1-3)] was calculated for each rat. The data met the conditions for normality following a Shapiro-Wilk test (WT, p = 0.3782, W = 0.9133; SG, p = 0.9404, W = 0.9760). An unpaired, two-tailed T test was performed (p = 0.0012**, t = 4.062, df = 16), and a significant difference was found between the WT and SG extinction indexes.*

(g) Overall Modulation Index. *The modulation index [(total time freezing during CS presentations – total time freezing between CS presentations)/(total time freezing)] was calculated for each rat across all CS presentations. The data met the conditions for normality following a Shapiro-Wilk test (WT, p = 0.1653, W = 0.8401; SG, p = 0.5458, W = 0.9224). An unpaired, two-tailed T test was performed (p = 0.0035**, t = 4.078, df = 16), and a significant difference was found between the overall modulation indexes.*

(h) Early vs. Late Modulation Indexes. *The modulation index was calculated for each rat across early (CS 1-3) and late (CS 8-10) CS presentations. A two-way ANOVA was performed to analyse the effect of time and genotype on the modulation index. An interaction between time and genotype was found to not be statistically significant (F(DFn, DFd) = 2.556, p = 0.1485). Genotype had a significant effect on modulation index (p = 0.0030**), but time did not (p = 0.7798). Bonferroni's multiple comparisons test revealed a significant difference in modulation index between the genotypes during early CS presentations (p = 0.0028**).*

Figure 14 – Superior Colliculus Control for Verification of Visual Processing:

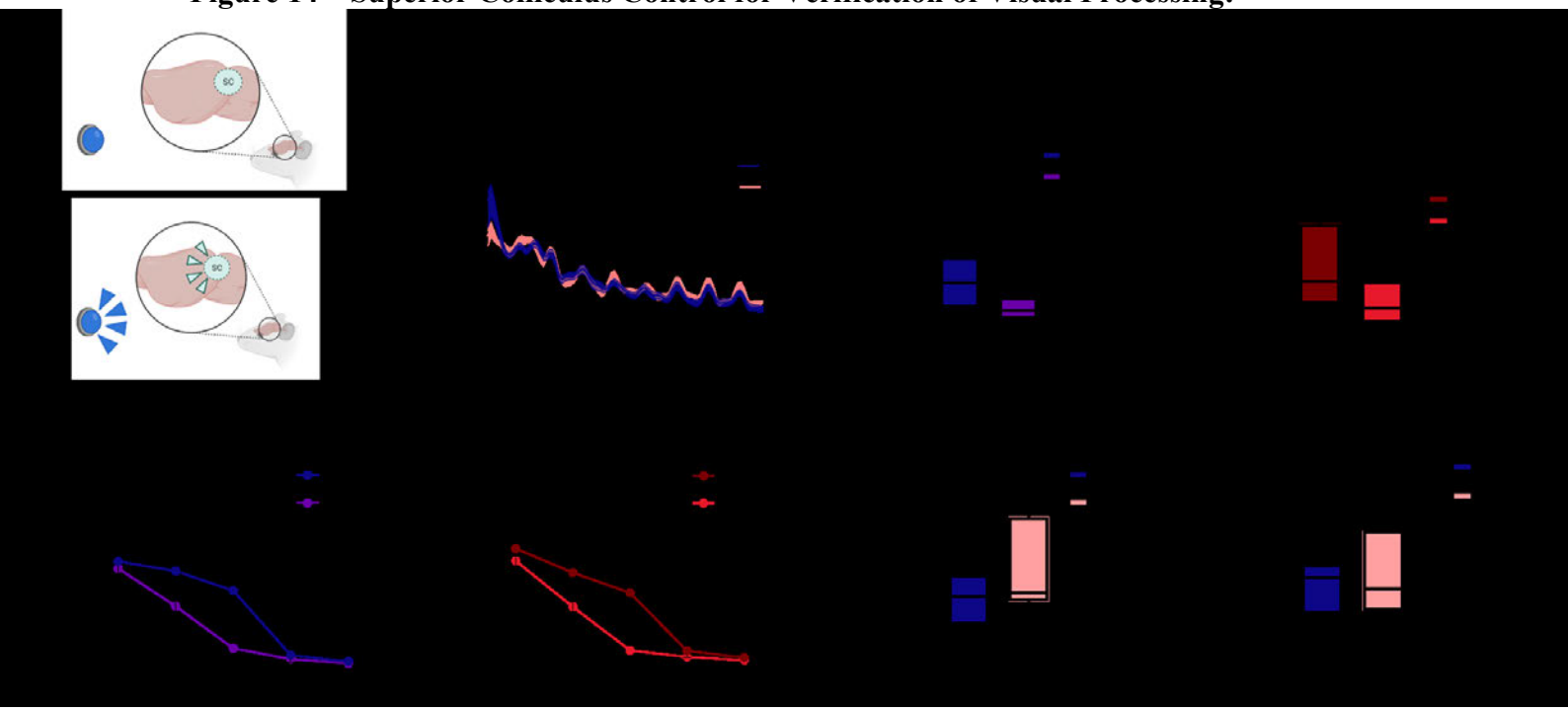

An overview of WT (n = 10) and SG (n = 8) superior colliculus power throughout the recall protocol, used here as a verification measure of the genotype's ability to process the visual conditioned stimulus.

(a) Superior Colliculus Control Schematic. *Visual representation of how superior colliculus control functions. When the blue LED light flashes (the "CS"), the superior colliculus has an increase in power.*

(b) Superior Colliculus Power Spectra. *A two-way ANOVA was performed on WT (n = 10) and SG (n = 8) rats to analyze the effect of genotype and frequency on power. Bonferroni's multiple comparisons test revealed no significant differences between genotypes.*

(c) WT Superior Colliculus Theta Power. *There was a significant difference between the WT power during versus between CS presentation, indicating the WT rats were able to process the visual CS. The data had a normal distribution following a Shapiro-Wilk test (WT During CS, p = 0.0672, W = 0.8553; WT Between CS, p = 0.1526, W = 0.8859). A paired, two-tailed T test was performed (p = 0.0067**, t = 3.498, df = 9), and a significant difference was found.*

(d) SG Superior Colliculus Theta Power. *There was a significant difference between the SG power during versus between CS presentation, indicating the SG rats were able to process the visual CS. The data had a normal distribution following a Shapiro-Wilk test (SG During CS, p = 0.4249, W = 0.9238; SG Between CS, p = 0.8262, W = 0.9627). A paired, two-tailed T test was performed (p = 0.0320*, t = 2.592, df = 7), and a significant difference was found.*

(e) Overview of Superior Colliculus Power Across All Frequencies, WT and SG. *Error bars: mean ± SEM.*

(f) Superior Colliculus Theta Power During CS. *There was no significant difference between the genotypes' power during CS presentation, indicating both genotypes were able to process the visual CS to the same degree. The data did not have a normal distribution following a Shapiro-Wilk test (WT, p = 0.0871, W = 0.8649; SG, p = 0.0464*, W = 0.8198). A Mann-Whitney test was performed (p = 0.6334), and no significant difference was found.*

(g) Superior Colliculus Theta Power Between CS. *There was no significant difference between the genotypes' power between CS presentation, indicating both genotypes were able to process the visual CS to the same degree. The data had a normal distribution following a Shapiro-Wilk test (WT, p = 0.1860, W = 0.4740; SG, p = 0.1309, W = 0.5145). An unpaired, two-tailed T test was performed (p = 0.4865, t = 0.7124, df = 16), and no significant difference was found.*

Figure 15 – Overview of Global Power across Recall Protocol:

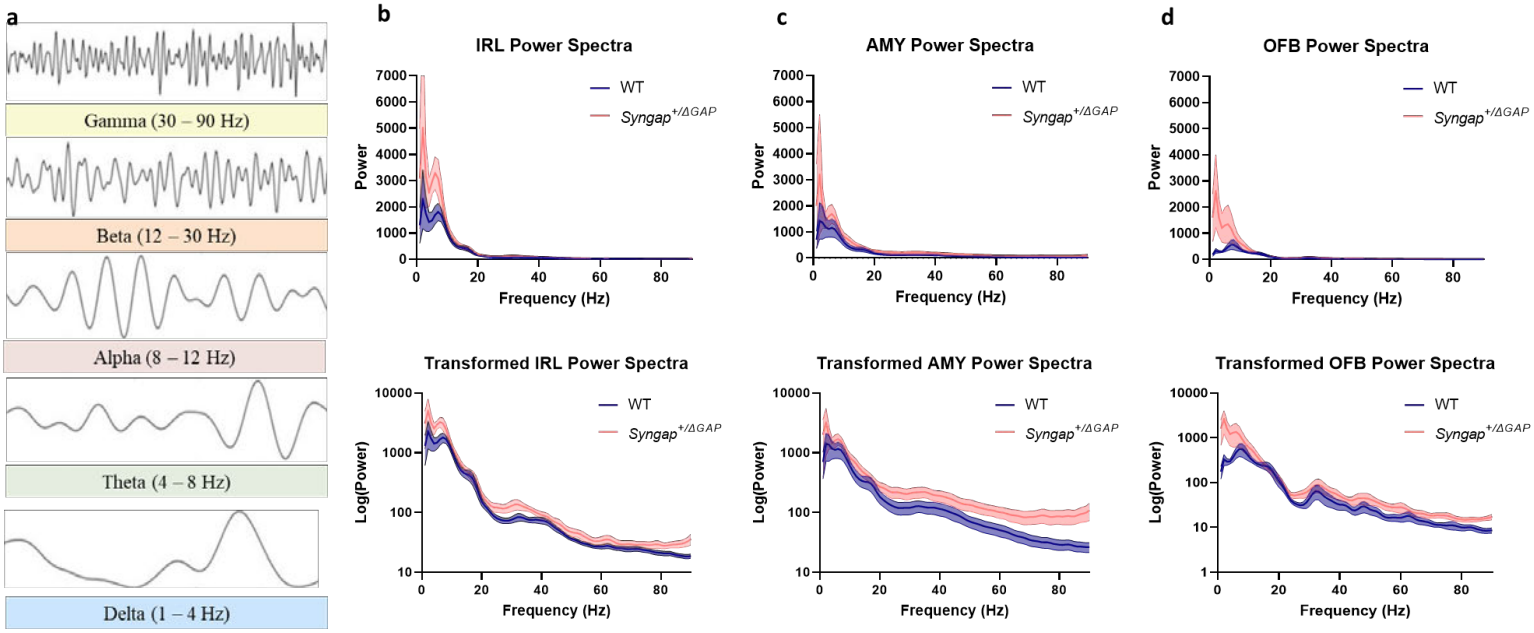

Power spectra for WT (n = 10) and SG (n = 8) rats across recall protocol. The conversion of the power spectra from a numeric to a logarithmic scale is shown for clarity. For all presented spectra, a two-way ANOVA was performed to analyse the effect of genotype and frequency on power, and Bonferroni's multiple comparisons tests was used to test for significant differences between the genotypes. Across all three regions of interest, Bonferroni's multiple comparisons test found no differences between WT and SG rats.

(a) Illustration and range of frequency bands. *The custom software package developed for coherence and power analysis allowed the user to define the frequencies for each band. This analysis was conducted using common values from the literature: Delta (1 – 4 Hz), Theta (4 – 8 Hz), Alpha (8 – 12 Hz), Beta (12 – 30 Hz), and Gamma (30 – 90 Hz). Example brain waves were created in Biorender.*

(b) IRL power spectra and transformed power spectra. *A two-way ANOVA was performed to analyze the effect of genotype and frequency on power. An interaction between genotype and frequency was found to be statistically significant (F(DFn, DFd) = 1.356, p = 0.0178*). Frequency had a highly significant effect on power (p = 0.0007***), while genotype did not (p = 0.0704). Bonferroni's multiple comparisons test revealed no significant differences between genotypes.*

(c) AMY power spectra and transformed power spectra. *A two-way ANOVA was performed to analyze the effect of genotype and frequency on power. No statistically significant interaction was found (F(DFn, DFd) = 0.5652, p = 0.9996). Frequency had a significant effect on power (p = 0.0102*), but genotype did not (p = 0.0755). Bonferroni's multiple comparisons test revealed no significant differences between genotypes.*

(d) OFB power spectra and transformed power spectra. *A two-way ANOVA was performed to analyze the effect of genotype and frequency on power. An interaction between genotype and frequency was found to be highly significant (F(DFn, DFd) = 2.653, p < 0.0001****). Both frequency (p = 0.0037**) and genotype (p = 0.0369*) had significant effects on power. Bonferroni's multiple comparisons test revealed no significant differences between genotypes.*

Figure 18 - Overview of Global Power Across Recall, During versus Between Combined Early and Late CS presentations, per Genotype:

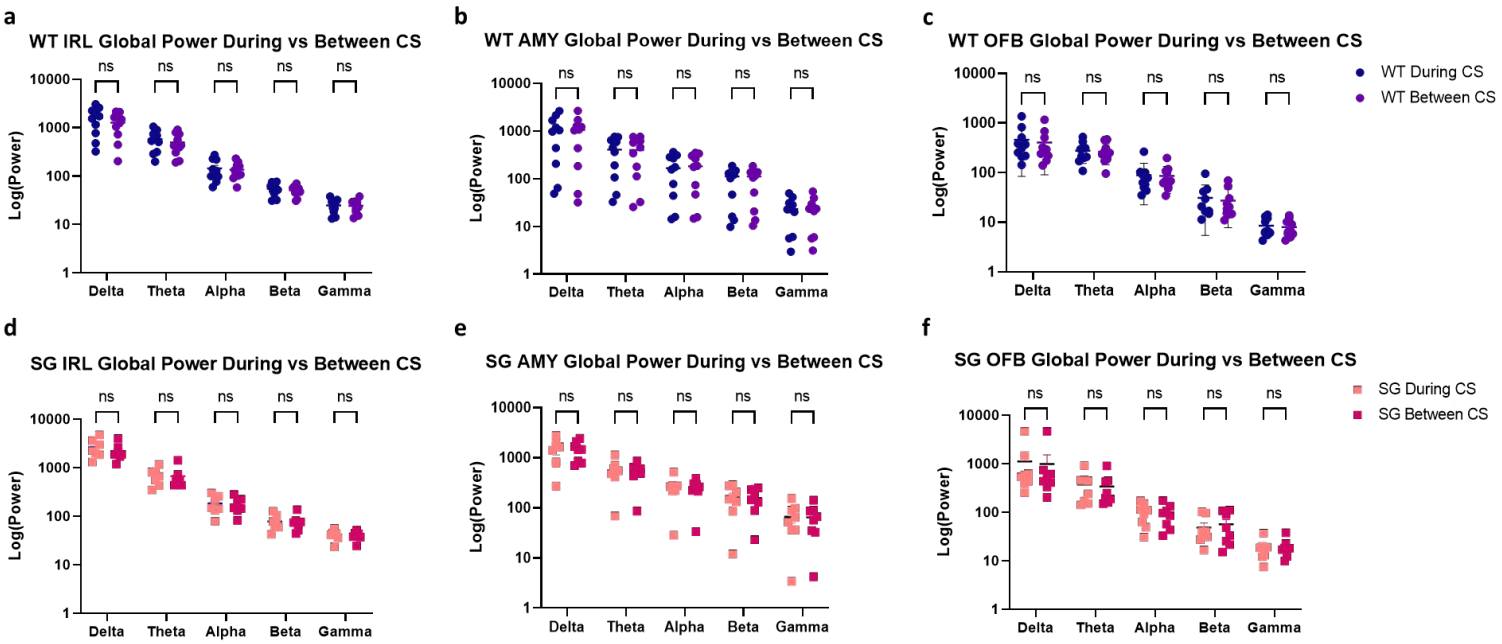

Interleaved scatter plots, mean with SEM, for power during versus between CS by genotype. A two-way ANOVA was performed across all plots, and Bonferroni's multiple comparisons test was used to identify significant differences during versus between CS presentations. No significant differences were found for WT (n = 10) or SG (n = 8) rats. ***Full ANOVA results for each comparison.***

(a) WT IRL Power, during versus between CS presentations. *A two-way ANOVA was performed on WT (n = 10) rats to analyse the effect of CS presence and frequency on power. An interaction between CS presence and frequency was found to not have statistical significance (F(DFn, DFd) = 0.6939, p = 0.5986). Frequency (p < 0.0001****) had a highly significant effect on power. Bonferroni's multiple comparisons test revealed no significant differences during versus between CS presentation power in any frequency bands.*

(b) WT AMY Power, during versus between CS presentations. *A two-way ANOVA was performed on WT (n = 10) rats to analyse the effect of CS presence and frequency on power. An interaction between CS presence and frequency was found to not have statistical significance (F(DFn, DFd) = 0.04505, p = 0.9961). Frequency (p < 0.0001****) had a highly significant effect on power. Bonferroni's multiple comparisons test revealed no significant differences during versus between CS presentation power in any frequency bands.*

(c) WT OFB Power, during versus between CS presentations. *A two-way ANOVA was performed on WT (n = 10) rats to analyse the effect of CS presence and frequency on power. An interaction between CS presence and frequency was found to not have statistical significance (F(DFn, DFd) = 0.1218, p = 0.9742). Frequency (p < 0.0001****) had a highly significant effect on power. Bonferroni's multiple comparisons test revealed no significant differences during versus between CS presentation power in any frequency bands.*

(d) SG IRL Power, during versus between CS presentations. *A two-way ANOVA was performed on SG (n =8) rats to analyse the effect of CS presence and frequency on power. An interaction between CS presence and frequency was found to not have statistical significance (F(DFn, DFd) = 0.8059, p = 0.5275). Frequency (p < 0.0001****) had a highly significant effect on power. Bonferroni's multiple comparisons test revealed no significant differences during versus between CS presentation power in any frequency bands.*

(e) SG AMY Power, during versus between CS presentations. *A two-way ANOVA was performed on SG (n =8) rats to analyse the effect of CS presence and frequency on power. An interaction between CS presence and frequency was found to not have statistical significance (F(DFn, DFd) = 0.01321, p = 0.9996). Frequency (p <*

*0.0001****) had a highly significant effect on power. Bonferroni's multiple comparisons test revealed no significant differences during versus between CS presentation power in any frequency bands.*

(f) SG OFB Power, during versus between CS presentations. *A two-way ANOVA was performed on SG (n =8) rats to analyse the effect of CS presence and frequency on power. An interaction between CS presence and frequency was found to not have statistical significance (F(DFn, DFd) = 0.03047, p = 0.9982). Frequency (p < 0.0001****) had a highly significant effect on power. Bonferroni's multiple comparisons test revealed no significant differences during versus between CS presentation power in any frequency bands.*

Figure 19 – Overview of Early versus Late Recall Power, per Genotype:

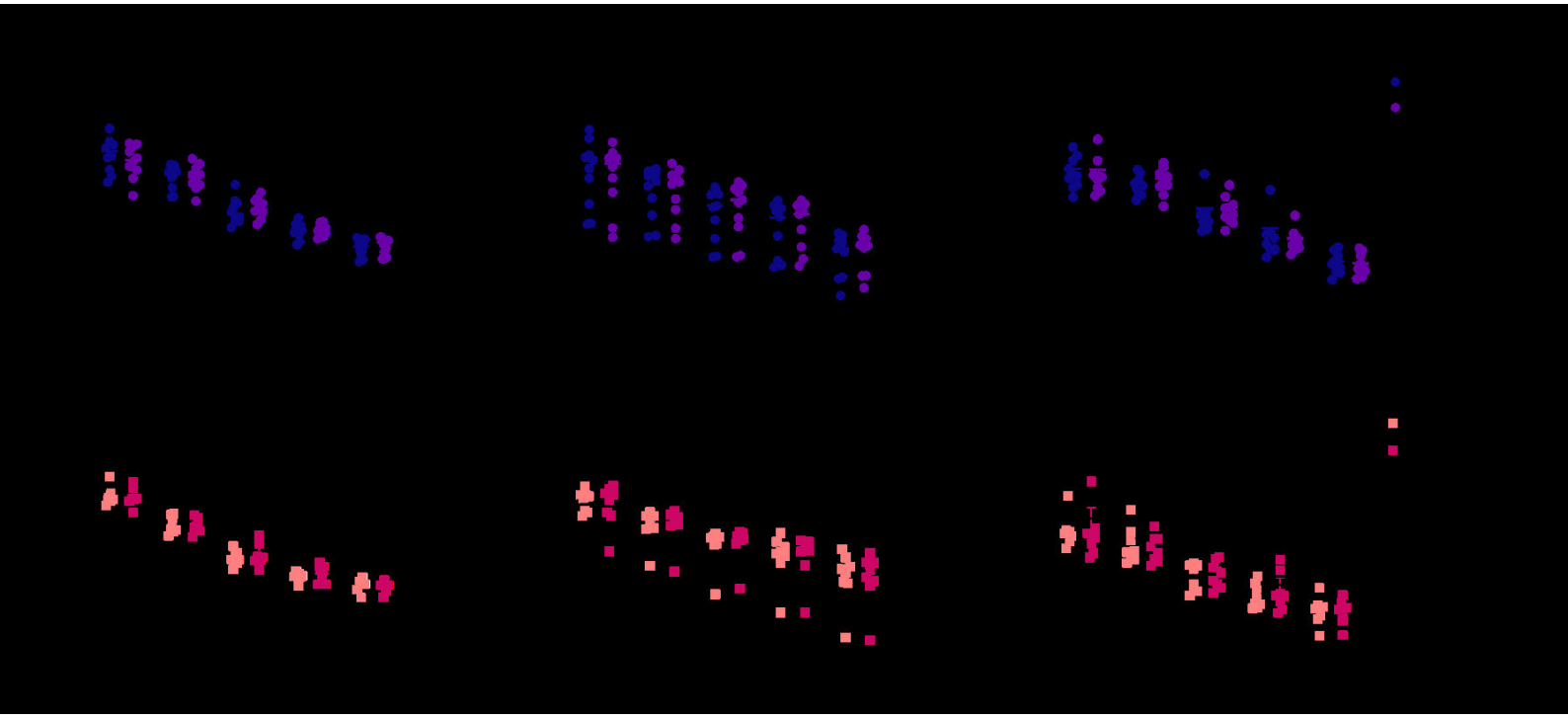

Interleaved scatter plots, mean with SEM, for coherence during early versus late CS presentations per genotype. A two-way ANOVA was performed across all plots, and Bonferroni's multiple comparisons test was used to identify significant differences during versus between CS presentations. For WT (n = 10) rats, a significant difference was found in the alpha frequency band for IRL/AMY coherence. For SG (n = 8) rats, no significant differences were found between early and late CS presentations.

(a) WT IRL Power, early versus late CS. *A two-way ANOVA was performed on WT (n = 10) rats to analyse the effect of protocol timing and frequency on power. An interaction between protocol timing and frequency was found to not have statistical significance (F(DFn, DFd) = 1.336, p = 0.2650). Frequency (p < 0.0001****) had a highly significant effect on power, while CS presentation time (p = 0.3991) did not. Bonferroni's multiple comparisons test revealed no significant differences between early versus late CS coherence in any frequency bands.*

(b) WT AMY Power, early versus late CS. *A two-way ANOVA was performed on WT (n = 10) rats to analyse the effect of protocol timing and frequency on power. An interaction between protocol timing and frequency was found to not have statistical significance (F(DFn, DFd) = 0.5127, p = 0.7265). Frequency (p = 0.0005***) had a highly significant effect on power, while CS presentation time (p = 0.7201) did not. Bonferroni's multiple comparisons test revealed significant differences between early versus late power in the alpha frequency band (p = 0.0195*).*

(c) WT OFB Power, early versus late CS. *A two-way ANOVA was performed on WT (n = 10) rats to analyse the effect of protocol timing and frequency on power. An interaction between protocol timing and frequency was found to not have statistical significance (F(DFn, DFd) = 1.073, p = 0.3812). Frequency (p < 0.0001****) had a highly significant effect on power, while CS presentation time (p = 0.6694) did not. Bonferroni's multiple comparisons test revealed no significant differences between early versus late CS coherence in any frequency bands.*

(d) SG IRL Power, early versus late CS. *The data did not meet the conditions for normality following a Shapiro-Wilk test (Early CS 1-3: W = 0.7208, p = 0.0156*; Late CS 8-10: W = 0.7269, p = 0.0179*). Multiple Wilcoxon matched-pairs signed rank tests were used to compare each frequency group with the Bonferroni-Dunn method (α = 0.05). Multiple Wilcoxon tests revealed no significant differences between early versus late CS coherence in any frequency bands.*

(e) SG AMY Power, early versus late CS. *A two-way ANOVA was performed on SG (n = 8) rats to analyse the effect of protocol timing and frequency on power. An interaction between protocol timing and frequency was found to not have statistical significance (F(DFn, DFd) = 0.05636, p = 0.9938). Frequency (p < 0.0001****) had a highly significant effect on power, while CS presentation time (p = 0.6621) did not. Bonferroni's multiple comparisons test revealed no significant differences between early versus late CS coherence in any frequency bands.*

(f) SG OFB Power, early versus late CS. *The data did not meet the conditions for normality following a Shapiro-Wilk test (Early CS 1-3: W = 0.8235, p = 0.1241; Late CS 8-10: W = 0.7525, p = 0.0314 *). Multiple Wilcoxon matched-pairs signed rank tests were used to compare each frequency group with the Bonferroni-Dunn method ($\alpha = 0.05$). Multiple Wilcoxon tests revealed no significant differences between early versus late CS coherence in any frequency bands.*

Figure 20 – Overview of Power Epochs (Early versus Late CS presentations):

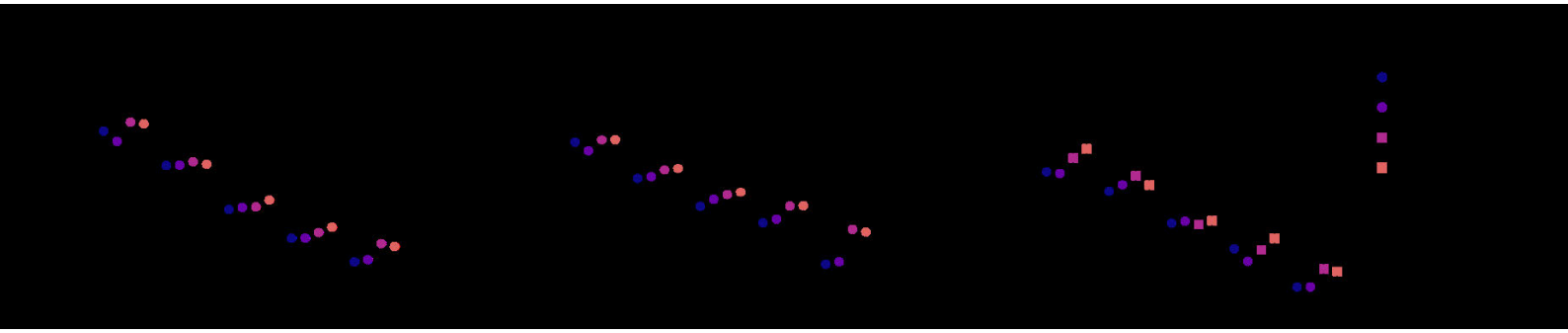

Interleaved scatter plots, mean with SEM, for all four power calculation groups. Power calculations during versus between CS groups were combined, as no significant differences were found based upon CS presence (Figure 18).

A two-way ANOVA was performed for each region, and Bonferroni's multiple comparisons test was used to identify significant differences between the groups. Significant differences were only found after corrections for multiple comparisons in the gamma band of the IRL.

(a) IRL Power Epoch Comparison. *A two-way ANOVA was performed on WT (n = 10) and SG (n = 8) rats to analyse the effect of genotype and protocol timing on coherence. An interaction between epoch group and frequency was found to have statistical significance (F(DFn, DFd) = 1.942, p = 0.0357*). Frequency (p < 0.0001****) had a highly significant effect on power, while genotypic epoch (p = 0.2109) did not. Bonferroni's multiple comparisons test revealed the following significant differences in the gamma band: WT Early vs SG Early (p = 0.0127*), WT Early vs SG Late (p = 0.0132*), WT Late vs SG Early (p = 0.0226), and WT Late vs SG Late (p = 0.0275*).*

(b) AMY Power Epoch Comparison. *A two-way ANOVA was performed on WT (n = 10) and SG (n = 8) rats to analyse the effect of genotype and protocol timing on coherence. An interaction between epoch group and frequency was found to not have statistical significance (F(DFn, DFd) = 0.3905, p = 0.9649). Frequency (p < 0.0001****) had a highly significant effect on power, while genotypic epoch (p = 0.6365) did not. Bonferroni's multiple comparisons test revealed no significant differences between any of the epoch groups.*

(c) OFB Power Epoch Comparison. *A two-way ANOVA was performed on WT (n = 10) and SG (n = 8) rats to analyse the effect of genotype and protocol timing on coherence. An interaction between epoch group and frequency was found to not have statistical significance (F(DFn, DFd) = 0.7175, p = 0.7322). Frequency (p = 0.0003***) had a highly significant effect on power, while genotypic epoch (p = 0.5888) did not. Bonferroni's multiple comparisons test revealed no significant differences between any of the epoch groups.*

Figure 25 – Overview of Global Coherence, During versus Between Combined Early and Late CS Presentations, per Genotype:

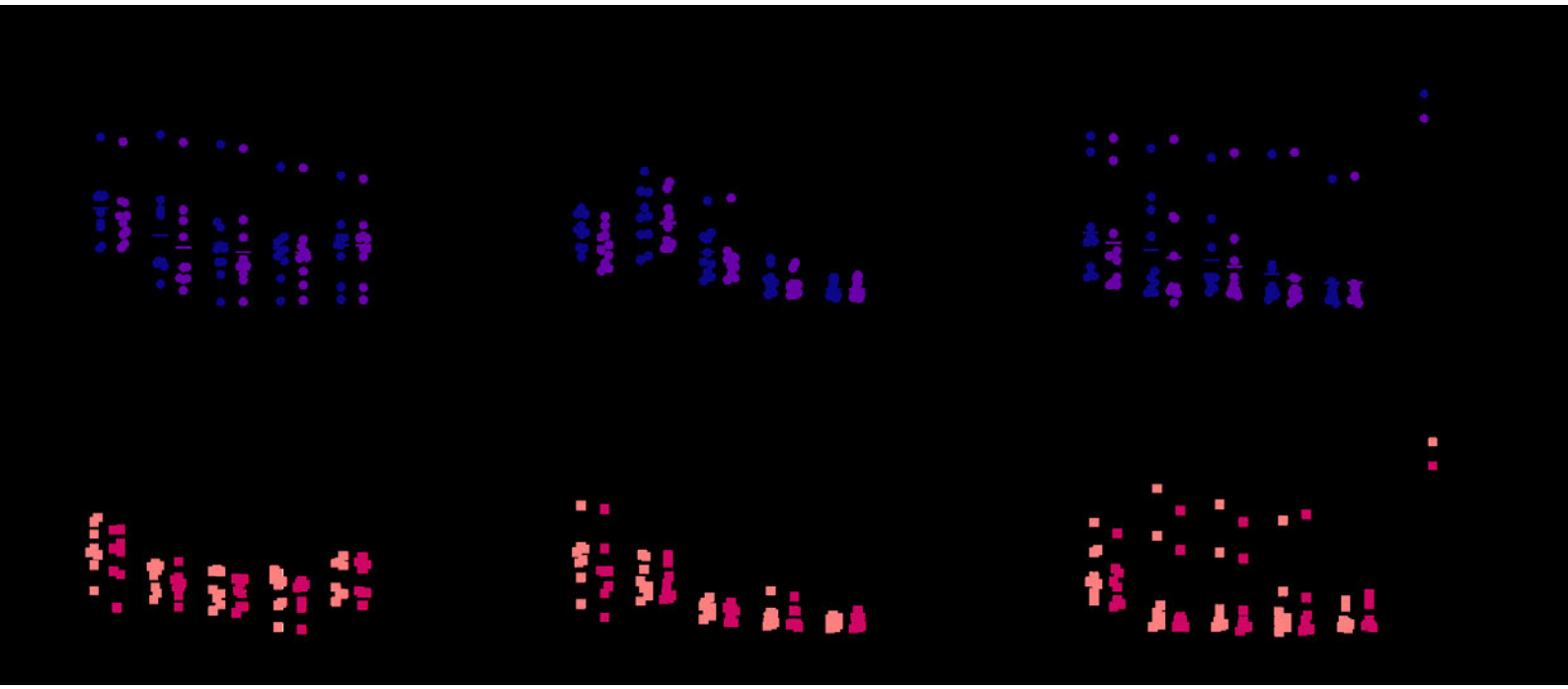

Interleaved scatter plots, mean with SEM, for coherence during versus between CS by genotype. A two-way ANOVA was performed across all plots, and Bonferroni's multiple comparisons test was used to identify significant differences during versus between CS presentations. For WT (n = 10) rats, significant differences were found in the delta, theta, and alpha frequency bands for IRL/AMY, the delta and beta frequency bands for IRL/OFB, and the delta band for AMY/OFB coherence. For SG (n = 8) rats, significant differences were found in the delta band for IRL/OFB and AMY/OFB coherence.

(a) WT IRL/AMY Coherence, during versus between CS presentations. *A two-way ANOVA was performed on WT (n = 10) rats to analyse the effect of CS presence and frequency on coherence. An interaction between CS presence and frequency was found to have statistical significance (F(DFn, DFd) = 4.572, p = 0.0043**). Frequency (p < 0.0001***) had a highly significant effect on coherence. Bonferroni's multiple comparisons test revealed significant differences during versus between CS coherence in the delta (p = 0.0004***), theta (p < 0.0001****), and alpha (p = 0.0004***) frequency bands.*

(b) WT IRL/OFB Coherence, during versus between CS presentations. *A two-way ANOVA was performed on WT (n = 10) rats to analyse the effect of CS presence and frequency on coherence. An interaction between CS presence and frequency was found to have statistical significance (F(DFn, DFd) = 5.559, p = 0.0076**). Frequency (p < 0.0001***) had a highly significant effect on coherence. Bonferroni's multiple comparisons test revealed significant differences during versus between CS coherence in the delta (p = 0.0010***) and beta (p = 0.0232*) frequency bands.*

(c) WT AMY/OFB Coherence, during versus between CS presentations. *A two-way ANOVA was performed on WT (n = 10) rats to analyse the effect of CS presence and frequency on coherence. An interaction between CS presence and frequency was found to have statistical significance (F(DFn, DFd) = 5.677, p = 0.0093**). Frequency (p = 0.0009***) had a highly significant effect on coherence. Bonferroni's multiple comparisons test revealed significant differences during versus between CS coherence in the delta (p = 0.0005***) frequency band.*

(d) SG IRL/OFB Coherence, during versus between CS presentations. *A two-way ANOVA was performed on SG (n = 8) rats to analyse the effect of CS presence and frequency on coherence. An interaction between CS presence and frequency was found to not have statistical significance (F(DFn, DFd) = 2.283, p = 0.1458).*

*Frequency (p = 0.0046**) had a highly significant effect on coherence. Bonferroni's multiple comparisons test revealed no significant differences during versus between CS coherence in any frequency bands.*

(e) SG IRL/OFB Coherence, during versus between CS presentations. *A two-way ANOVA was performed on SG (n = 8) rats to analyse the effect of CS presence and frequency on coherence. An interaction between CS presence and frequency was found to have statistical significance (F(DFn, DFd) = 6.944, p = 0.0046**). Frequency (p = 0.0002***) had a highly significant effect on coherence. Bonferroni's multiple comparisons test revealed significant differences during versus between CS coherence in the delta (p = 0.0242*) frequency band.*

(f) SG AMY/OFB Coherence, during versus between CS presentations. *A two-way ANOVA was performed on SG (n = 8) rats to analyse the effect of CS presence and frequency on coherence. An interaction between CS presence and frequency was found to have statistical significance (F(DFn, DFd) = 4.843, p = 0.0253*). Frequency (p = 0.0334*) had a significant effect on coherence. Bonferroni's multiple comparisons test revealed significant differences during versus between CS coherence in the delta (p = 0.0269*) frequency band.*

Figure 26 – Overview of Early versus Late Recall Coherence, per Genotype:

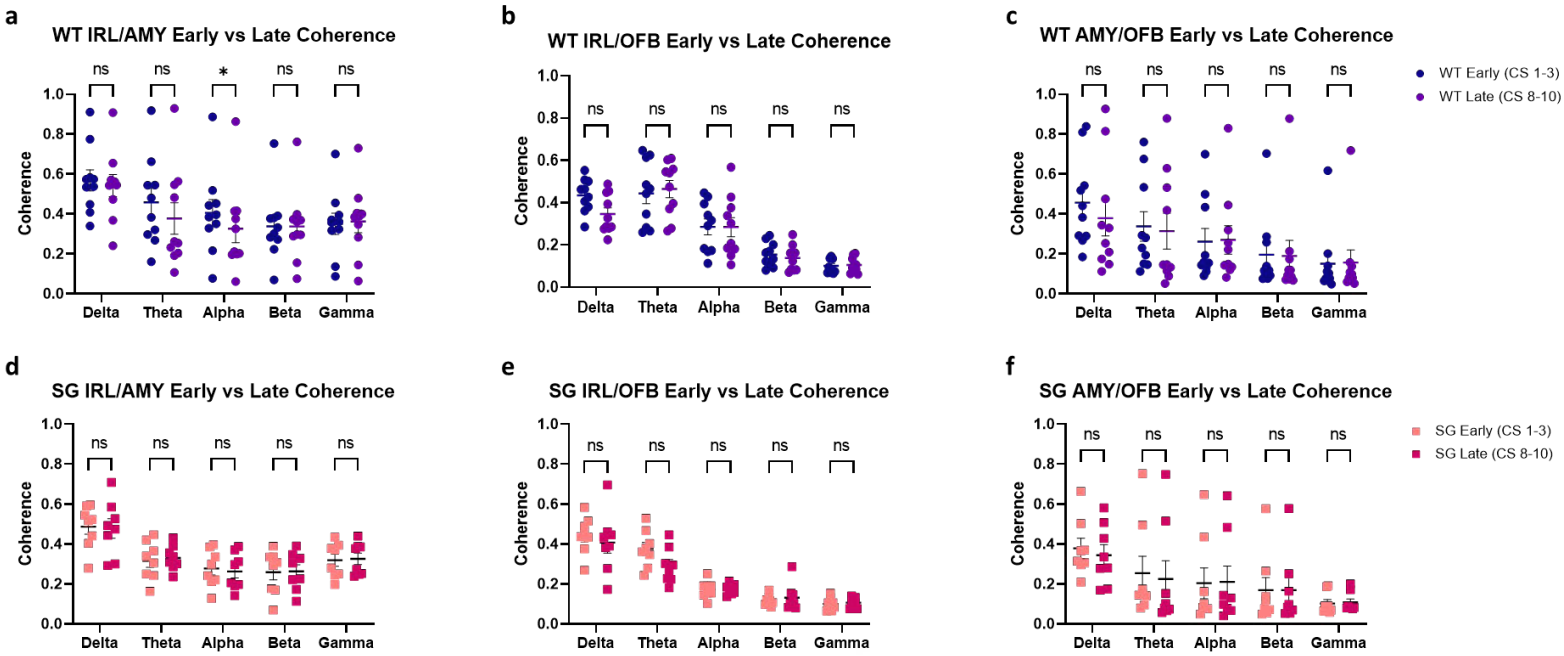

Interleaved scatter plots, mean with SEM, for coherence during early versus late CS presentations per genotype. A two-way ANOVA was performed across all plots, and Bonferroni's multiple comparisons test was used to identify significant differences during versus between CS presentations. For WT (n = 10) rats, a significant difference was found in the alpha frequency band for IRL/AMY coherence. For SG (n = 8) rats, no significant differences were found between early and late CS presentations. ***Detailed statistical analysis, including full ANOVA results, can be found in Appendix I: Supplementary Statistics.***

(a) WT IRL/AMY Coherence, early versus late CS. *A two-way ANOVA was performed on WT (n = 10) rats to analyse the effect of protocol timing and frequency on coherence. An interaction between protocol timing and frequency was found to have statistical significance (F(DFn, DFd) = 4.264, p = 0.0259*). Frequency (p = 0.0015**) had a highly significant effect on coherence, while CS presentation time (p = 0.0794) did not. Bonferroni's multiple comparisons test revealed significant difference between early versus late CS coherence in the alpha frequency band (p = 0.0457*).*

(b) WT IRL/OFB Coherence, early versus late CS. *A two-way ANOVA was performed on WT (n = 10) rats to analyse the effect of protocol timing and frequency on coherence. An interaction between protocol timing and frequency was found to not have statistical significance (F(DFn, DFd) = 1.637, p = 0.2279). Frequency (p < 0.0001****) had a highly significant effect on coherence, while CS presentation time (p = 0.2412) did not. Bonferroni's multiple comparisons test revealed no significant differences between early versus late CS coherence in any frequency bands.*

(c) WT AMY/OFB Coherence, early versus late CS. *A two-way ANOVA was performed on WT (n = 10) rats to analyse the effect of protocol timing and frequency on coherence. An interaction between protocol timing and frequency was found to not have statistical significance (F(DFn, DFd) = 3.123, p = 0.0535). Frequency (p = 0.0004***) had a highly significant effect on coherence, while CS presentation time (p = 0.3203) did not. Bonferroni's multiple comparisons test revealed no significant differences between early versus late CS coherence in any frequency bands.*

(d) SG IRL/AMY Coherence, early versus late CS. *A two-way ANOVA was performed on SG (n =8) rats to analyse the effect of protocol timing and frequency on coherence. An interaction between protocol timing and frequency was found to not have statistical significance (F(DFn, DFd) = 0.2570, p = 0.7562). Frequency (p = 0.0028**) had a highly significant effect on coherence, while CS presentation time (p = 0.9969) did not.*

Bonferroni's multiple comparisons test revealed no significant differences between early versus late CS coherence in any frequency bands.

(e) SG IRL/OFB Coherence, early versus late CS. *A two-way ANOVA was performed on SG (n =8) rats to analyse the effect of protocol timing and frequency on coherence. An interaction between protocol timing and frequency was found to not have statistical significance (F(DFn, DFd) = 0.2.536, p = 0.1089). Frequency (p < 0.0001****) had a highly significant effect on coherence, while CS presentation time (p = 0.1499) did not. Bonferroni's multiple comparisons test revealed no significant differences between early versus late CS coherence in any frequency bands.*

(f) SG AMY/OFB Coherence, early versus late CS. *A two-way ANOVA was performed on SG (n =8) rats to analyse the effect of protocol timing and frequency on coherence. An interaction between protocol timing and frequency was found to not have statistical significance (F(DFn, DFd) = 1.379, p = 0.2844). Frequency (p = 0.0173 *) had a significant effect on coherence, while CS presentation time (p = 0.0654) did not. Bonferroni's multiple comparisons test revealed no significant differences between early versus late CS coherence in any frequency bands.*

Figure 27 – Overview of Coherence Epochs (Early versus Late, and During versus Between CS Presentations):

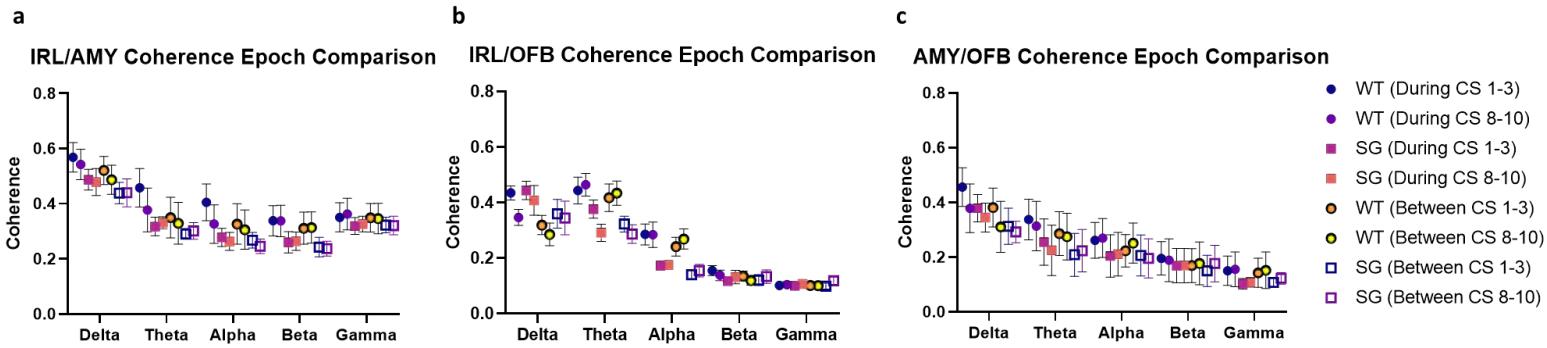

Interleaved scatter plots, mean with SEM, for all eight coherence calculation groups. A two-way ANOVA was performed for each plot, and Bonferroni's multiple comparisons test was used to identify significant differences between the groups. For all three coherence pairings, no significant differences were found after corrections for multiple comparisons.

(a) IRL/AMY Coherence Epoch Comparison. *A two-way ANOVA was performed on WT (n = 10) and SG (n = 8) rats to analyse the effect of CS presentation and protocol timing on coherence. An interaction between epoch group and frequency was found to not have statistical significance (F(DFn, DFd) = 0.4886, p = 0.9872). Frequency (p < 0.0001****) had a highly significant effect on coherence, while epoch (p = 0.6373) did not. Bonferroni's multiple comparisons test revealed no significant differences between any of the epoch groups.*

(b) IRL/OFB Coherence Epoch Comparison. *A two-way ANOVA was performed on WT (n = 10) and SG (n = 8) rats to analyse the effect of CS presentation and protocol timing on coherence. An interaction between epoch group and frequency was found to have statistical significance (F(DFn, DFd) = 2.694, p < 0.0001****). Frequency (p < 0.0001****) had a highly significant effect on coherence, while epoch (p = 0.0633) did not. Bonferroni's multiple comparisons test revealed no significant differences between any of the epoch groups.*

(a) AMY/OFB Coherence Epoch Comparison. *A two-way ANOVA was performed on WT (n = 10) and SG (n = 8) rats to analyse the effect of CS presentation and protocol timing on coherence. An interaction between epoch group and frequency was found to not have statistical significance (F(DFn, DFd) = 0.6547, p = 0.9103). Frequency (p < 0.0001****) had a highly significant effect on coherence, while epoch (p = 0.9833) did not. Bonferroni's multiple comparisons test revealed no significant difference between any of the epoch groups.*

Appendix II: Additional Figures

The following two figures were created so that the same correlations were calculated between both the power and coherence sections. Both figures have their associated p and R-squared values reported.

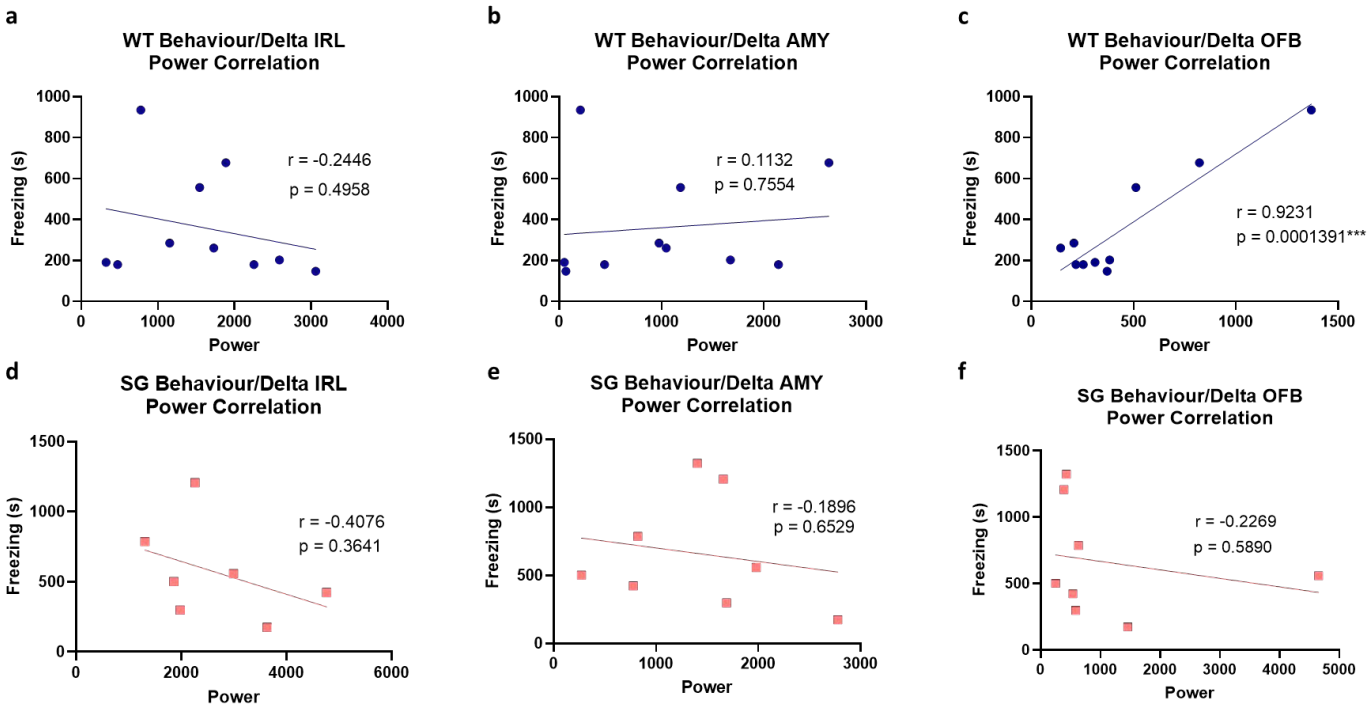

Figure 31 – Correlation between Freezing Behaviour and Delta Power during Recall:

Correlation coefficients (Pearson's r) and p-values were calculated for each graph, representing the correlation between freezing times and delta power in the brain regions for each genotype. The p-value indicates the statistical significance of the correlation coefficient (two-tailed test), and the coefficient of determination (R squared) represents the proportion of variability in freezing behaviour explained by gamma power.

(a-c) WT Behaviour and Delta Power Correlations. *The only statistically significant correlation is illustrated in (c) OFB Power Correlation (p = 0.0001391***, r = 0.9231).*

(d – f) SG Behaviour and Delta Power Correlations. *There were no statistically significant correlations amongst any of the SG regions' power and behaviour.*

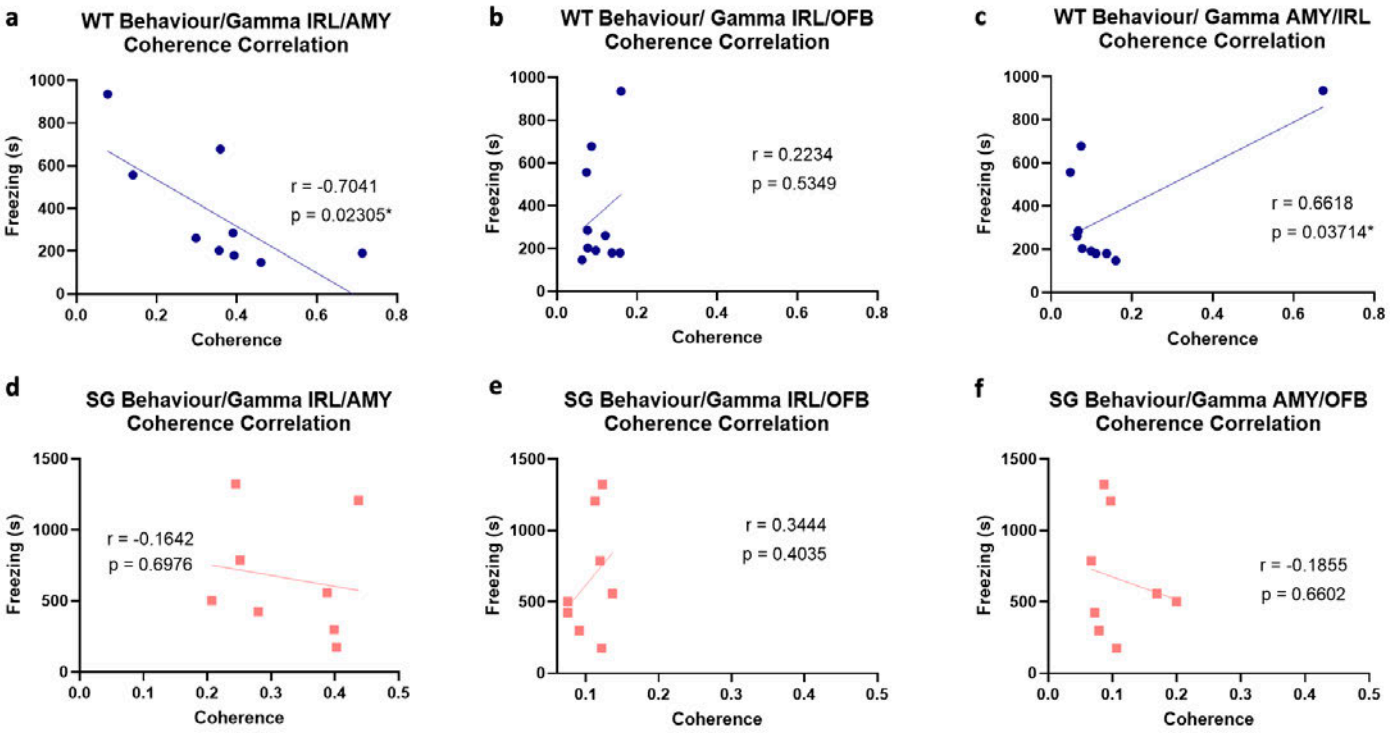

Figure 32 - Correlation between Freezing Behaviour and Gamma Coherence during Recall:

Correlation coefficients (Pearson's r) and p-values were calculated for each graph, representing the correlation between freezing times and gamma coherence in the brain regions for each genotype. The p-value indicates the statistical significance of the correlation coefficient (two-tailed test), and the coefficient of determination (R squared) represents the proportion of variability in freezing behaviour explained by gamma power.

(a-c) WT Behaviour and Gamma Coherence Correlations. *The statistically significant correlations are illustrated in (a) IRL/AMY Coherence Correlation (p = 0.02305*, r = -0.7041) and (c) AMY/IRL Coherence Correlation (p = 0.03714*, r = 0.6618).*

(d – f) SG Behaviour and Delta Coherence Correlations. *There were no statistically significant correlations amongst any of the SG coherence pairs and behaviour.*

Appendix III: Access to the Electrophysiology Analysis Pipeline

Hopefully, in the near future, the Electrophysiology Analysis Pipeline will be made available in full on GitHub. In the meantime, rather than providing tens of pages of typed-out scripts, I will provide access to the Electrophysiology Pipeline through the University of Edinburgh OneDrive: MATLAB Scripts

Here is an alternative link in case the embedded link above fails: https://uoe-my.sharepoint.com/:f:/r/personal/s2264432_ed_ac_uk/Documents/MATLAB%20Scripts?csf=1&web=1&e=wCtUIv)

If any particular scripts are required for review or in a text-only format, please contact myself ( ) or my supervisors (and). Many thanks!